Water quality related to pharmaceutical and nitrogen compounds during infiltration of treated wastewater for Managed Aquifer Recharge

Silver, Matthew

(2020)

TECHNISCHE UNIVERSITÄT DARMSTADT

Water quality related to pharmaceutical and nitrogen compounds during infiltration of treated wastewater for Managed Aquifer Recharge

Dissertation
By Matthew Silver

Submitted in fulfillment of the requirements for the degree of Doctor rerum naturalium (Dr. rer. nat.)

At the Institute of Applied Geosciences, Department of Materials and Earth Sciences, Technische Universität Darmstadt

First assessor: Prof. Dr. Christoph Schüth
Second assessor: Dr. Kay Knöller (Helmholtz Centre for Environmental Research - UFZ)

Darmstadt, Germany; 2019

Silver, Matthew: Water quality related to pharmaceutical and nitrogen compounds during infiltration of treated wastewater for Managed Aquifer Recharge

Dissertation written at the Institute of Applied Geosciences, Department of Materials and Earth Sciences, Technische Universität Darmstadt; Darmstadt, Germany

Viva voce: 17th of December 2019
Available in TUprints: November 2020

This dissertation contains work previously published in two journals articles:

Silver, M., Selke, S., Balsaa, P., Wefer-Roehl, A., Kübeck, C., Schüth, C., 2018. Fate of five pharmaceuticals under different infiltration conditions for Managed Aquifer Recharge. Sci. Total Environ. 642, 914–924. https://doi.org/10.1016/j.scitotenv.2018.06.120

Silver, M., Knöller, K., Schlögl, J., Kübeck, C., Schüth, C., 2018. Nitrogen cycling and origin of ammonium during infiltration of treated wastewater for Managed Aquifer Recharge. Appl. Geochemistry 97, 71–80. https://doi.org/10.1016/j.apgeochem.2018.08.003

Ehrenwörtliche Erklärung (Declaration of authorship)

Ich erkläre hiermit ehrenwörtlich, dass ich die vorliegende Arbeit selbstständig angefertigt habe. Sämtliche aus fremden Quellen direkt oder indirekt übernommenen Gedanken sind als solche kenntlich gemacht.

Die Arbeit wurde bisher keiner anderen Prüfungsbehörde vorgelegt.

Unterschrieben von: Matthew Silver

11 November 2019

Publications and conference presentations

Publications

Silver, M., Selke, S., Balsaa, P., Wefer-Roehl, A., Kübeck, C., Schüth, C., 2018. Fate of five pharmaceuticals under different infiltration conditions for Managed Aquifer Recharge. Sci. Total Environ. 642, 914–924. https://doi.org/10.1016/j.scitotenv.2018.06.120

Silver, M., Knöller, K., Schlögl, J., Kübeck, C., Schüth, C., 2018. Nitrogen cycling and origin of ammonium during infiltration of treated wastewater for Managed Aquifer Recharge. Appl. Geochemistry 97, 71–80. https://doi.org/10.1016/j.apgeochem.2018.08.003

Conference presentations

Silver, M., Selke, S., Balsaa, P., Wefer-Roehl, A., Kübeck, C., and Schüth, C., 2017. Managed Aquifer Recharge: the fate of pharmaceuticals from infiltrated treated wastewater investigated through soil column experiments. Geophysical Research Abstracts Vol. 19 (European Geosciences Union), EGU2017-7437.

Silver, M., Wefer-Roehl, A., Kuebeck, C., and Schüth, C., 2016. Transformations of nitrogen from secondary treated wastewater when infiltrated in Managed Aquifer Recharge schemes. Geophysical Research Abstracts (European Geosciences Union), Vol. 18, EGU2016-4862.

Silver, M., Schueth, C., Wefer-Roehl, A., and Kuebeck, C., 2014. Column experiments investigating wetting and drying of soil and consumption of organic contaminants for Managed Aquifer Recharge. American Geophysical Union 2014 Fall Meeting, Abstract H43C-0973.

Acknowledgements

There are many people I would like to thank for their cooperation and support of my doctoral work. First and foremost, I thank my advisor, Prof. Dr. Christoph Schüth, for giving me the opportunity to work on the EU project *MARSOL: Demonstrating Managed Aquifer Recharge as a Solution to Water Scarcity and Drought* and on this dissertation. I would also like to thank Dr. Kay Knöller of the Helmholtz Centre for Environmental Research - UFZ, Department of Catchment Hydrology, for analyses of stable isotopes in nitrogen and his guidance in evaluating the results.

I am thankful to all MARSOL project partners for illustrating many exciting MAR applications. In particular, I would like to thank the staff of IWW Water Centre, especially Dr. Christine Kübeck, for their support of my doctoral position and the numerous water analyses that were conducted in their laboratories. Furthermore, I thank the National Technical University of Athens and Dr. Andreas Kallioras for supporting collection of the soil used in the experiments. I am also thankful to the University of Tübingen Hydrogeochemistry Workgroup and Dr. Thomas Wendel for conducting an analysis of the elemental composition (C and N) of organic matter in the soil used for the experiments.

At Technische Universität Darmstadt, I would like to thank my fellow doctoral students and post docs at the Institute of Applied Geosciences, and in the Hydrogeology Workgroup in particular, for the interesting and thoughtful discussions we had of scientific topics. I am thankful to Dr. Annette Wefer-Roehl for her support, particularly in the early stages of my experiments. Furthermore, I am grateful to all staff of the Institute. In particular, support from laboratory technicians was essential, from constructing the soil columns to conducting water and soil analyses. I also thank the TU Darmstadt Department of Civil Engineering, Wastewater Technology and Wastewater Engineering Workgroups, especially Prof. Dr. Susanne Lackner, for helpful discussions related to treated wastewater and providing access to the municipal wastewater treatment plant from which water for the experiments was collected.

I would like to give special thanks to three master's students—Patrick Marschall, Rainer Kurdum and Johanna Schlögl—for their collaborative work on the topics presented here. I enjoyed working with each of them, and other thesis students, and seeing how they engaged with the work itself and the scientific world. Finally, I am especially grateful to my family and friends for their support and patience while I have been completing this dissertation.

Abstract

As more regions in the world look to replenish depleted aquifers, treated wastewater (TWW) is increasingly infiltrated in Managed Aquifer Recharge (MAR) schemes. While MAR is a promising emerging technology, water quality issues—including potential contaminants present in the recharge water as well as the possibility of generation of pollutants along the infiltration flow path—should be considered. This dissertation documents and evaluates column experiments in which TWW was infiltrated through soil containing a considerable amount of organic matter (2.57% organic carbon). Three topics were investigated through column experiments: 1) cycling of nitrogen, 2) the fate of non-antibiotic pharmaceuticals and 3) the fate of antibiotic pharmaceuticals.

In the study of nitrogen cycling, soil column experiments were operated with wetting and drying cycles. Ammonium, which was present only in trace concentrations in the TWW, increased in concentration with depth in the column and exceeded the EU Water Framework Directive limit of 0.5 mg/L (0.39 mg(N)/L) for up to a year, depending on the sampling depth. Pore water samples collected at the end of drying periods showed very high nitrate concentrations, indicating nitrification of some of the ammonium. Oxidation reduction potential often exceeded 200 mV during drying periods, showing conditions for nitrification, but dropped to below -100 mV during wetting periods, creating several possible pathways for ammonium production. Potential sources of ammonium are (1) dissolved organic nitrogen in the TWW, (2) nitrate in the TWW, and (3) organic nitrogen in the soil. δ15N in ammonium in pore water samples (mean 4.7 ‰) was slightly higher than δ15N the soil (2.4 ‰), indicating that the soil was likely the major source but also that nitrate (mean 17.2 ‰) may have been the source of some of the ammonium. Fractionation of 15N in nitrate as well as high (often >10 mg(C)/L during the first 50 days of infiltration) concentrations of acetate (a labile form of organic carbon) also indicate that dissimilatory nitrate reduction to ammonium may have formed some of the ammonium.

In the study of pharmaceutical compounds, column experiments were conducted under three different conditions: continuous infiltration, wetting and drying cycles, and wetting and drying cycles with elevated concentrations of antibiotics in the inflow water, which may reduce microbially aided degradation of other compounds. A mass balance comparing pharmaceutical mass in the water phase over the 16-month duration of the experiments to mass sorbed to the soil was used to infer the mass of pharmaceuticals degraded. Results show sorption as the main attenuation mechanism for carbamazepine. About half of the mass of diclofenac was degraded with wetting and drying cycles, but no significant degradation was found for continuous infiltration, while 32% of infiltrated mass sorbed.

Fenoprofen was degraded in the shallow and aerobic part of the soil, but degradation appeared to cease beyond 27 cm depth. Gemfibrozil attenuated through a combination of degradation and sorption, with slight increases in attenuation with depth from both mechanisms. Naproxen degraded progressively with depth, resulting in attenuation of more than 90% of the mass. In the column with elevated concentrations of antibiotics, the antibiotics attenuated to about 50% or less of inflow concentrations by 27 cm depth and within this zone, less degradation of the other compounds was observed. In this same experiment, the mass balance suggests that the antibiotic sulfamethoxazole was degraded during infiltration, while for sulfadimidine, sorption was an important attenuation mechanism.

Table of contents

Ehrenwörtliche Erklärung (Declaration of authorship) I

Publications and conference presentations II

Acknowledgements III

Abstract IV

Table of contents VI

List of figures VIII

List of tables X

Abbreviations and acronyms XI

1 Introduction 1

1.1 Nitrogen cycling and redox conditions 3

1.2 Fate of non-antibiotic pharmaceuticals 5

1.3 Fate of antibiotic pharmaceuticals 7

2 Nitrogen cycling and redox conditions 10

2.1 Materials and methods 10

2.1.1 Soil and inflow water 10

2.1.2 Column experiments and sampling 11

2.1.3 Oxygen and oxidation reduction potential 15

2.1.4 Ions and total bound nitrogen 15

2.1.5 Isotopes 16

2.1.6 Batch sorption experiments 18

2.2 Results and discussion 18

2.2.1 Wetting periods 19

2.2.2 Drying periods 21

2.2.3 Oxygen and oxidation reduction potential 24

2.2.4 Acetate 26

2.2.5 Ammonium 27

2.2.6 Stable isotopes in nitrate 29

2.2.7 Stable isotopes in ammonium and its possible origin 32
2.2.8 Sorption of ammonium 33
3 Fate of non-antibiotic pharmaceuticals 36
3.1 Materials and methods 36
3.1.1 Soil and inflow water 36
3.1.2 Column experiments, sampling and monitoring 37
3.1.3 Pressurized liquid extraction 40
3.1.4 Analysis of pharmaceutical and dissolved ionic compounds 42
3.1.5 Mass balance 44
3.2 Results and discussion 48
3.2.1 Column experiments 48
3.2.2 Sorbed pharmaceutical mass 56
3.2.3 Fate of pharmaceutical mass 58
4 Fate of antibiotic pharmaceuticals 64
4.1 Materials and methods 64
4.1.1 Properties of the antibiotic pharmaceutical compounds 64
4.1.2 Extraction 65
4.2 Results and discussion 65
4.2.1 Column experiment 65
4.2.2 Sorbed mass and overall fate of antibiotic mass 67
5 Environmental implications and conclusions 70
5.1 Nitrogen cycling and redox conditions 70
5.2 Fate of non-antibiotic pharmaceuticals 71
5.3 Fate of antibiotic pharmaceuticals 72
5.4 Conclusions 72
References 74
Appendix A 88
Appendix B 104

List of figures

Figure 2-1. Schematic of the experimental columns. CI = Column I, CII = Column II. 12

Figure 2-2. Photograph of Column II during a drying phase 13

Figure 2-3. Sampling port construction 14

Figure 2-4. Oxygen concentration at three depths in Column I 19

Figure 2-5. Ammonium nitrogen concentrations measured during the long-term experiment relative to the EU drinking water limit 19

Figure 2-6. Nitrate nitrogen concentrations measured during end of wetting and first flush (end of drying periods) sampling during a selected portion of the long-term experiment 22

Figure 2-7. Ammonium nitrogen concentrations measured during end of wetting and first flush (end of drying periods) sampling during a selected portion of the long-term experiment 23

Figure 2-8. Oxygen concentrations decreased with depth in the soil at the end of drying periods in the long-term experiment. 24

Figure 2-9. Oxidation reduction potential in Column II 25

Figure 2-10. Oxygen concentrations measured 15 cm below the soil surface 25

Figure 2-11. Acetate carbon concentrations in inflow and pore water over the course of the short-term experiment 27

Figure 2-12. Ammonium nitrogen concentrations in pore water samples over the course of the short-term experiment 28

Figure 2-13. Dual isotope plot of ^{15}N and ^{18}O in all samples analyzed over the course of the experiment 30

Figure 2-14. ^{18}O:^{15}N fractionation ratios over the course of the experiment 31

Figure 2-15. $\delta^{15}N$ in ammonium in comparison to $\delta^{15}N$ in the soil nitrogen, inflow water nitrate and inflow water DON 33

Figure 2-16. Results of the batch experiments with and without spiked ammonium 34

Figure 2-17. Sorption isotherm for ammonium nitrogen from the batch experiment with post-experiment soil from Column A 34

Figure 3-1. Oxidation reduction potential in Column B during the middle of the experiment 48

Figure 3-2. Measured concentrations of the non-antibiotic pharmaceuticals 51

Figure 3-3. Comparison of the expected spiked mass to the spiked mass calculated from the sampling results 55
Figure 3-4. Measured concentrations of the antibiotic pharmaceuticals in Column C 56
Figure 3-5. Calculated total sorbed mass of the non-antibiotic pharmaceutical compounds extracted from soil samples..... 58
Figure 3-6. Fate of mass infiltrated during the column experiments 60
Figure 4-1. Apparent total sorbed mass in the post-experiment soil samples 68
Figure 4-2. Fate of mass of sulfadimidine and sulfamethoxazole infiltrated during the column experiment 68

List of tables

Table 1-1. Nitrogen transforming reactions based on acetate ($C_2H_3O_2^-$) as the organic carbon source .4

Table 2-1. Composition and variation of the inflow TWW. The summarized data reflect samples collected for the long-term experiment. 11

Table 2-2. Composition of a representative sample of TWW and batch experiment aqueous solutions, in mmol/L. 18

Table 2-3. Ammonium concentration relative to cumulative flow volume in Column I 20

Table 2-4. Ammonium concentration relative to cumulative flow volume in Column II 28

Table 3-1. Properties of the non-antibiotic pharmaceutical compounds investigated in this study 37

Table 3-2. Overview of experimental stages 39

Table 3-3. Detection limits (undiluted samples) and precision 43

Table 3-4. Average nitrate concentrations (mg/L) during the second half of the experiments 49

Table 3-5. Pre-spiking concentrations and mass 50

Table 3-6. Mass passing each sampling location in the water phase during the spiking phase of the experiments. 52

Table 3-7. Concentrations of the pharmaceuticals in unspiked TWW 54

Table 3-8. Pre-spiking mass as a percentage of total mass infiltrated 56

Table 3-9. Relative recovery of spiked mass of the pharmaceutical compounds from three soil samples and the average relative recovery 57

Table 4-1. Chemical properties of sulfamethoxazole and sulfadimidine 64

Table 4-2. Recoveries of the antibiotics sulfadimidine (SDM) and sulfamethoxazole (SMX) from post-experiment soil, reported as mean and standard deviation of duplicate samples (triplicate samples at 12 cm depth) in percent. 67

Abbreviations and acronyms

BDOC	biodegradable organic carbon
DIN	dissolved inorganic nitrogen
DNRA	dissimilatory nitrate reduction to ammonium
DOC	dissolved organic carbon
DON	dissolved organic nitrogen
Eh	Oxidation-reduction potential relative to a standard hydrogen electrode
MAR	Managed Aquifer Recharge
MeOH	Methanol
ORP	oxidation-reduction potential
PTFE	polytetrafluoroethylene
redox	oxidation-reduction
SAT	Soil Aquifer Treatment
SPE	solid phase extraction
tNb	total bound nitrogen
TrOCs	trace organic compounds
TWW	treated wastewater

1 Introduction

In many regions worldwide, increasing demand for usable water is creating water supply challenges. Managed Aquifer Recharge (MAR) is a set of techniques to inexpensively extend water supplies by recharging aquifers with locally available water sources (Dillon, 2005). Recharge techniques used in MAR include injection wells and infiltration basins, while treated wastewater (TWW) and captured rainwater (e.g. stormwater runoff) are examples of recharge water sources (Dillon et al., 2009). When a flowpath through the unsaturated zone exists (e.g. under an infiltration basin), an opportunity for treatment of the recharge water exists.

This dissertation focuses on MAR conducted when TWW enters the subsurface through a constructed infiltration basin, which is also referred to as Soil Aquifer Treatment (SAT). SAT is often conducted with intermittent flooding of the basin, resulting in wetting and drying cycles (Dillon, 2005). In some cases, however, MAR is conducted with continuous infiltration, with the main example being (river) bank filtration, in which surface water containing some fraction of TWW is infiltrated (Tufenkji et al., 2002; Eckert and Irmscher, 2006; Storck et al., 2010; Li et al., 2019). While this dissertation focuses on MAR with undiluted TWW, studies of bank filtration are also considered for certain contaminants.

Trace organic compounds (TrOCs), including antibiotic and non-antibiotic pharmaceuticals, have been found in TWW and surface water bodies worldwide (Wilkinson et al., 2019). MAR presents an opportunity for water quality improvements through (bio)geochemical processes that can occur in the unsaturated zone (Dillon et al., 2009). In several cases, attenuation of emerging anthropogenic contaminants has been observed (Amy and Drewes, 2007; Laws et al., 2011; Valhondo et al., 2015). Improvements in water quality typically occur through sorption and/or biodegradation (Maeng et al., 2011b). Intermittent drying periods reintroduce oxygen into the subsurface (Dutta et al., 2015), allowing for a broad range of (bio)geochemical reactions (Miotlinski et al., 2010). After traveling through the unsaturated zone to groundwater, the infiltrated water can be extracted and then used for irrigation (Dillon, 2005). In this way, potential exists for water quality improvements before TWW is applied to crops.

Infiltration rates are an important topic with implications for both recharged water quantity and quality. While sustained faster infiltration rates would enable greater recharge water quantity, a low-permeability “clogging” layer typically forms, limiting infiltration rates (Miotlinski et al., 2010). Both physical clogging (i.e. accumulation of particulate matter) and microbial clogging (e.g. growth of algae)

exist, with physical clogging found to play a greater role when recharge water containing more particulates (e.g. TWW) is used (Pavelic et al., 2011). Periodic drying periods can help maintain higher hydraulic conductivity (Miotlinski et al., 2010), perhaps due to desiccation of the material. Advanced wastewater treatment, such as sand filtration and ultraviolet light disinfection, can also help reduce clogging (Barry et al., 2017). Infiltration rates of 20 to 1680 cm/d (Powelson et al., 1993; the higher end may not represent sustained infiltration), 10 to 100 cm/d (Barry et al., 2017) and 13 cm/d (Baumgarten et al., 2011; bank filtration study) have been reported.

While higher infiltration rates may result in greater recharged water quantity, slower infiltration may present advantages with respect to water quality. For (bio)degradation of pollutants to occur, longer retention times (i.e. lower infiltration rates) may allow for more degradation. Infiltration rate can be lowered by choosing sites with finer grained soils, or by adding an artificial layer at the basin surface, e.g. a mixture of clay, iron oxide and compost (Valhondo et al., 2015). In some cases, particularly in Australia, MAR is done through sandy sediment, such as calcareous sands, containing very little organic matter (Bekele et al., 2011; Barry et al., 2017). At other MAR sites the soil is reported to contain up to 2% organic carbon, e.g. a bank filtration site in Berlin, Germany (Massmann et al., 2006).

In this dissertation, water quality changes are investigated by column experiments in which TWW was infiltrated through a loamy sand containing a relatively high fraction of organic matter. The research is organized as follows:

1. Cycling of nitrogen compounds and overall oxidation-reduction (redox) conditions present in the soil-TWW system (Chapters 1.1 and 2).
2. The fate of non-antibiotic pharmaceuticals under different infiltration conditions, including one column in which antibiotic pharmaceuticals were spiked in the experiment inflow water (Chapters 1.2 and 3).
3. The fate of antibiotic pharmaceuticals with wetting and drying cycles and spiked concentrations (Chapters 1.3 and 4).

Methods and results are presented in Chapters 2 (nitrogen compounds and redox conditions), 3 (fate of non-antibiotic pharmaceuticals), and 4 (fate of antibiotic pharmaceuticals). Chapter 2 contains the overall methods for the column experiments as well as methods specific to the study of nitrogen compounds. In Chapters 3 and 4, methods specific to the respective topic are described.

This work was completed as part of the European Union FP7 project *MARSOL: Demonstrating Managed Aquifer Recharge as a Solution to Water Scarcity and Drought*, which was intended to advance methods that contribute to the development and use of MAR as a robust and safe technology for recharging depleted aquifers. MARSOL included work at field sites in the Mediterranean region and with different infiltration waters and techniques. The work reported in this dissertation focuses on water quality during SAT by means of column experiments, in which the processes occurring during infiltration just below the soil surface can be readily studied at a scale of decimeters.

1.1 Nitrogen cycling and redox conditions

Nitrogen compounds are present in both TWW and soil. In studies of water quality in MAR, much attention is given to the fate of pollutants (e.g. TrOCs) present in the recharge water, with less focus on pollutants that can be generated along the infiltration flow path. In some MAR applications, dissolved inorganic nitrogen (DIN) in its most oxidized form—nitrate—persists in the recharged water (Bekele et al., 2011), while in others, nitrate has been attenuated by adding a reactive, organic-rich surface layer (Valhondo et al., 2015). While this technique is effective for nitrate and other compounds, it has the potential to generate ammonium, the most reduced form of DIN. Ammonium has a much lower drinking water limit of 0.5 mg/L (0.39 mg(N)/L) compared to nitrate (50 mg/L, i.e. 39 mg(N)/L) (The Council of the European Union, 1998) and both are relevant to the status of surface water and groundwater (The Council of the European Union, 2000). The present study considers the redox conditions when TWW is infiltrated through a soil with considerable organic matter content, and in particular, the effects on nitrogen compounds.

Infiltration in MAR applications is commonly conducted in wetting and drying cycles (Bouwer, 2002; Morugán-Coronado et al., 2011; Goren et al., 2014; Barry et al., 2017), which are effective at re-introducing oxygen to the subsurface, at least at the macro scale (Dutta et al., 2015). Wastewater treatment effluents contain dissolved organic nitrogen (DON), often in concentrations of 1-2 mg/L (Parkin and McCarty, 1981; Czerwionka et al., 2012), as well as DIN. In MAR applications, both nitrified-denitrified (DIN is mostly nitrate) and conventional secondary (DIN is mostly ammonium) effluents have been infiltrated (Kopchynski et al., 1996). Infiltration of conventional secondary effluent can result in elimination of ammonium mass through a combination of retardation resulting in retention in the upper part of the soil, nitrification during drying periods, and denitrification (Table 1-1) and/or anaerobic ammonium oxidation during wetting periods (Miller et al., 2006; Goren et al., 2014; Hernández-Martínez et al., 2016). This combination of processes, however, has resulted in low

(apparent) nitrogen elimination rates in several MAR field applications: around 20% at Alice Springs, Australia (Barry et al., 2017), or up to 42% in one instance (Miotlinski et al., 2010); 0-30% at Flushing Meadows, Arizona, USA, as well as rates close to 50% at Dan Region, Israel and Sweetwater, Arizona, USA (Miller et al., 2006); and temporally and spatially varying elimination as low as 30% at Harkins Slough, California, USA (Schmidt et al., 2012). Although slight increases in ammonium concentrations during infiltration were observed at the Dan Region site by Goren et al. (2014), the possibility of ammonium production within MAR schemes has not been widely studied.

Table 1-1. Nitrogen transforming reactions based on acetate ($C_2H_3O_2^-$) as the organic carbon source

Process name	Chemical reaction
Nitrification	$NH_4^+ + 2O_2 \rightarrow NO_3^- + 2H^+ + H_2O$
Denitrification	$4NO_3^- + 3C_2H_3O_2^- \rightarrow 2N_2 + 6HCO_3^- + 3H^+$
Dissimilatory nitrate reduction to ammonium (DNRA)	$NO_3^- + C_2H_3O_2^- + H^+ + H_2O \rightarrow NH_4^+ + 2HCO_3^-$

The nitrite ion (NO_2^-) is omitted for simplification.

In a system with TWW infiltrated through a soil with organic matter, several sources of nitrogen are present: DON in the TWW, nitrate in the TWW, and organic nitrogen in the soil. Bekele et al. (2011) report nitrification from both ammonium and DON in a calcareous aquifer, but nitrate remained present as oxidizing conditions persisted. Based on the nitrogen mass balance, some DON had to have been ultimately converted to nitrate (Bekele et al., 2011), possibly with DON being mineralized to ammonium in an initial step. In a laboratory study infiltrating artificial wastewater, Essandoh et al. (2011) found that ammonium was produced from DON. Another possible source of ammonium is nitrate. Infiltration of nitrate in soils under reducing conditions often leads to denitrification, but the process dissimilatory nitrate reduction to ammonium (DNRA) can also occur (Buresh and Patrick, 1978). Recent research suggests that some microorganisms are able to perform both nitrate reducing processes (Mania et al., 2014; Yoon et al., 2015), and that the environmental conditions, rather than the specific microbial species, determine the end product (Kraft et al., 2014). Most researchers agree that higher C:N ratios make DNRA more likely, but the exact environmental controls are not known. Finally, the soil organic matter is a possible source for ammonium. Some soils contain a substantial fraction of mineralizable nitrogen (Stanford and Smith, 1972), which can be accessed by soil microbes to form ammonium (Hadas et al., 1992; Murphy et al., 2003). Positive but low $\delta^{15}N\text{-}NH_4^+$ values have indicated formation of ammonium in aquifers from mineralization of soil organic matter (Lingle et al., 2017; Caschetto et al., 2017).

To characterize and evaluate the production of ammonium in a MAR-like system, column experiments were performed in which TWW was infiltrated through a soil with substantial organic matter content. Two experiments were conducted: a long-term experiment (Column I) lasting approximately 615 days, and a short-term experiment (Column II) lasting 140 days to study ammonium-forming processes in more detail. In both experiments, soil pore water samples were collected from sampling ports along the length of the column. In the long-term experiment, only ammonium and nitrate were measured, but the total time of the experiment provides an overview of the occurrence of ammonium that can be expected and the time necessary for ammonium concentrations to fall below the EU drinking water standard. In the short-term experiment, samples were also measured for ions, including acetate (a form of labile organic carbon that could influence nitrate reduction), as well as for stable isotopes in nitrate and ammonium. Since nitrate is a possible source of ammonium, isotopic data related to the fate of nitrate were also collected. Oxygen concentrations were measured to provide information related to nitrification and denitrification. With these data, the overall purpose of this work is to evaluate the source(s) and mode of origin of ammonium produced in a system simulating MAR.

1.2 Fate of non-antibiotic pharmaceuticals

A wide range of pharmaceuticals are generally present in TWW, often in concentrations of up to ca. 20 µg/L (Verlicchi et al., 2012), presenting a pathway for the compounds into environmental waters (Nikolaou et al., 2007), including MAR systems (Maeng et al., 2011b). Many studies have investigated the occurrence of pharmaceuticals and other TrOCs in groundwater receiving infiltrated TWW (Drewes et al., 2003; Amy and Drewes, 2007; Bekele et al., 2011; Patterson et al., 2011). Concentrations generally decrease with distance from the infiltration source, but understanding the attenuation mechanism(s) is critical. Numerous studies have utilized tracer methods combined with monitoring pharmaceutical breakthrough (Matamoros et al., 2008; Rauch-Williams et al., 2010; Hoppe-Jones et al., 2012; Burke et al., 2013; Durán-Álvarez et al., 2015) while other studies have included transport modeling (Greskowiak et al., 2006; Nham et al., 2015; Hamann et al., 2016) or compared biotic with abiotic experiments (Lin et al., 2010; Lin and Gan, 2011; Maeng et al., 2011a; D'Alessio et al., 2015; Martínez-Hernández et al., 2015; Zemann et al., 2016).

However, few studies have quantified the mass of pharmaceuticals into a system and the mass remaining in the soil after some time period. Banzhaf et al. (2012) performed column experiments lasting 71 days and extracted pharmaceuticals from the soil afterwards, finding sorption of almost half of the infiltrated carbamazepine but less than 3% of infiltrated diclofenac. In a field-based study of soils

from several field sites irrigated with TWW, Kinney et al. (2006) found accumulation of carbamazepine in all soils exceeding infiltrated mass monitored over a six-month time period (additional unmonitored irrigation also occurred before the monitored period), suggesting that the compound is recalcitrant. No accumulation was found for other pharmaceutical compounds, including gemfibrozil. Accumulation exceeding the six-month infiltrated mass of the antibiotic sulfamethoxazole was observed by Kinney et al. (2006), while Banzhaf et al. (2012) found degradation of sulfamethoxazole where nitrate reducing conditions are present. In MAR applications, the fate of pharmaceuticals has been studied extensively (Maeng et al., 2011b; Hoppe-Jones et al., 2012; D'Alessio et al., 2015; Nham et al., 2015; Valhondo et al., 2015; Hamann et al., 2016), but mass balance approaches are not common.

The aim of this study is to determine the fate of pharmaceutical compounds by quantifying both the water (dissolved) and solid (sorbed) phase mass, under conditions of continuous infiltration, wetting and drying cycles, and wetting and drying cycles with elevated water-phase concentrations of antibiotics. Continuous infiltration was conducted as a reference (with more consistent redox conditions) to wetting and drying cycles, which are commonly used in the field (Goren et al., 2014). An infiltration water with higher concentrations of antibiotics was used to evaluate the possibility that antibiotics commonly present in the environment might reduce microbial degradation of other compounds, as well as to investigate the fate of the antibiotics themselves (Chapter 1.3). Oxidation-reduction potential (ORP) was measured in the column with wetting and drying cycles to observe changes in redox conditions with this infiltration mode.

Research on the fate of pharmaceuticals in MAR has shown that concentrations of pharmaceuticals generally decrease along the infiltration flowpath, with sorption and degradation playing roles that vary by compound (Maeng et al., 2011b). In soils with low organic matter content, sorption typically plays less of a role than in organic-rich soils (Chefetz et al., 2008). Meanwhile, several studies have shown that some pharmaceuticals (and other TrOCs), including diclofenac, gemfibrozil, and naproxen, are degraded better when biodegradable organic carbon (BDOC) concentrations are low, with bacteria becoming less selective in utilization of carbon sources (Rauch-Williams et al., 2010; Hoppe-Jones et al., 2012; Alidina et al., 2014b). Moreover, some recent studies have found better degradation for certain compounds (e.g. diclofenac and sulfamethoxazole) under oxic conditions (Bertelkamp et al., 2016; Müller et al., 2017). However, with the presence of other contaminants (e.g. nitrate) that are better degraded with high BDOC concentrations, reducing conditions are also important. Valhondo et al. (2015 and 2018) investigated adding an organic carbon-rich layer at the top of infiltration basins, making conditions more reducing. Others have proposed and demonstrated the concept of sequential

MAR technology, in which an aeration step follows initial infiltration with higher BDOC conditions and/or microbial activity, with the aeration step typically resulting in similar or better degradation of TrOCs compared to without aeration (Regnery et al., 2016; Hellauer et al., 2017a; Hellauer et al., 2017b). This sequential technique may be applicable to combining riverbank filtration (step 1), in which wetting and drying cycles are not practical, with extraction, aeration, and reinfiltration in a SAT basin (Regnery et al., 2016). In SAT, infiltration is often conducted in wetting and drying cycles (Drewes et al., 2003; Goren et al., 2014). He et al., (2016) found better degradation of some compounds, such as sulfamethoxazole, with wetting and drying cycles compared to continuous infiltration, but did not find a difference for many other compounds (e.g. diclofenac, fenoprofen, gemfibrozil, and naproxen).

For the current study, an organic-rich natural soil from a possible future MAR site in Greece was used. With this soil, column experiments were conducted and secondary TWW of mostly domestic urban origin was used as inflow water. As sorption is a key process to be quantified, a soil with high organic content was chosen as it is expected to increase sorption and retardation of pharmaceuticals (Chefetz et al., 2008; Hebig et al., 2017). This study focuses on the pharmaceuticals carbamazepine (an anti-epileptic medication), diclofenac (a non-steroidal anti-inflammatory drug), gemfibrozil (a cholesterol-lowering medication), and naproxen (a non-steroidal anti-inflammatory drug), which are each commonly found in TWW at concentrations up to ~5-20 µg/L, as well as fenoprofen (a non-steroidal anti-inflammatory drug) which is found at lower concentrations (up to ~0.04 µg/L) (Verlicchi et al., 2012). Many studies of the environmental fate of carbamazepine have found the compound to be recalcitrant (Maeng et al., 2011b), although one study found some degradation with an organic-rich soil (Banzhaf et al., 2012), while both sorption and degradation of the four remaining compounds have been reported (Maeng et al., 2011a,b; Fang et al., 2012). Sampling of the inflow water and soil pore water at depths of 12, 27, and 72 cm was conducted during the experiments, with the sampling results and measurement of the volume of infiltrated water allowing for calculation of the mass of each pharmaceutical passing each sampling port in the water phase. When the experiments ended, the pharmaceutical compounds were extracted from soil samples to obtain the mass sorbed to the soil. The mass sorbed was then compared to the mass attenuated (i.e., mass that left the water phase) at each sampling point to infer the quantity of mass degraded.

1.3 Fate of antibiotic pharmaceuticals

In addition to considering elevated concentrations of antibiotics in the recharge water as an infiltration condition (Chapter 1.2), the fate of three antibiotics—doxycycline, sulfamethoxazole and

sulfadimidine—spiked in the inflow water is investigated. Sulfamethoxazole and sulfadimidine (also known as sulfamethazine) belong to the sulfonamide class of antibiotics and target a broad range of bacteria. Doxycycline is a tetracycline antibiotic and is used to treat a wide variety of infections in the human body, as well as in veterinary medicine.

Doxycycline has been detected in secondary TWW at concentrations up to 0.1 µg/L (Verlicchi et al., 2012). In a soil environment, Zaranyika et al. (2015) found that doxycycline sorbed to sediment, but also degraded in both the aqueous and sorbed phases.

Each of the two sulfonamide antibiotics has been detected in untreated urban wastewater (Verlicchi et al., 2012) and the aquatic environment (Kümmerer, 2009). Wilkinson et al. (2019) found that sulfamethoxazole had the tenth highest mean concentrations in TWW and the 12th highest mean concentration in surface water worldwide, among the analyzed pharmaceutical compounds. In addition to common usage of sulfamethoxazole in human medicine, both sulfamethoxazole and sulfadimidine are used in veterinary applications, beginning a pathway for them to reach environmental waters (Boxall et al., 2003). In wastewater treatment, both are biodegradable, with the best degradation rates obtained during activated sludge treatment (Pérez et al., 2005). However, antibiotics are generally not sufficiently removed with common wastewater treatment technologies and therefore a need for development of inexpensive technologies exists (Ahmed et al., 2015).

MAR presents opportunities to inexpensively attenuate TrOCs, including antibiotics. Sulfamethoxazole has been studied in MAR, especially in the context of bank filtration. A >99% elimination rate was found under anoxic infiltration conditions, while the elimination rate was only 52% with seasonally oxic conditions (Heberer et al., 2008). However, Baumgarten et al. (2011) determined half-lives of sulfamethoxazole of up to 49 days, indicating that long flowpaths are needed to attenuate the compound. They also found that years of adaptation may be required before peak removal potential is reached. Degradation of the compound appears to be sensitive to redox conditions. Banzhaf et al. (2012) demonstrated that sulfamethoxazole is degraded when nitrate-reducing conditions are present. Some degradation reactions are reversible, dependent on the redox state (Rodriguez-Escales and Sanchez-Vila, 2016). Degradation of sulfamethoxazole has been enhanced in a MAR system by adding a compost (organic-rich) layer to the bottom of the infiltration basin (Valhondo et al., 2014; Schaffer et al., 2015).

Sulfadimidine is a common veterinary antibiotic used in raising livestock (Postigo and Barceló, 2015). In a study of water from wells impacted by agriculture in Idaho, USA, Batt et al. (2006) found sulfadimidine concentrations of up to 0.22 µg/L. In a study with both sulfamethoxazole and sulfadimidine present, the function and diversity of soil microbes was found to be affected (Gutiérrez et al., 2010). Sorption of sulfadimidine was found to be higher in soils with higher organic carbon content (Lertpaitoonpan et al., 2009). This suggests that sorption to the soil used in the present study should occur. Sorption can remove mass from the aqueous phase, but does not eliminate it from the water-soil system, unless degradation also occurs.

Results from the soil column with sulfamethoxazole and sulfadimidine spiked in the inflow TWW and extraction of these antibiotics from the post-experiment soil are evaluated. The approach to evaluating the fate of the compounds (pore water sampling, extraction from post-experiment soil, and mass balance) follows the approach used for the non-antibiotic pharmaceuticals.

2 Nitrogen cycling and redox conditions

The following sections present the methods for and results of the study of nitrogen cycling and redox conditions. Appendix A contains additional figures.

2.1 Materials and methods

2.1.1 Soil and inflow water

The experimental soil is classified as a rendzina soil (Zvorykin and Saul, 1948) and was obtained from non-agricultural grassland approximately 12 km northeast of Athens, Greece, immediately west of the Dimosio Dasos Rapentosas wildlife refuge, at a possible future MAR site. Disturbed soil samples were collected over two days and packaged in plastic-coated aluminum bags.

The soil size fractions were determined by wet sieving with sedimentation analysis of grains smaller than 0.063 mm (Schlögl, 2016). The grain size distribution is 1.3% clay, 22.8% silt, and 75.9% combined sand and gravel. The soil contains 2.57% ± 0.01% organic carbon and 0.221% ± 0.002% nitrogen based on three subsets of milled soil, decantated with hydrochloric acid and analyzed with an Elementar *CNS* analyzer (analysis conducted externally: University of Tübingen, Hydrogeochemistry Workgroup). The solid density of the soil was determined to be 2.667 g/cm^3 using a *Micromeritics AccuPyc II 1340* helium pycnometer.

Secondary TWW was collected at least once per week from a municipal wastewater treatment plant in Darmstadt, Germany, and used as inflow water in the column experiments. The water was collected in pre-rinsed 15-L or 25-L gray-tinted glass jugs. In the TWW, nitrate averaged 1.96 mg(N)/L and dissolved organic carbon averaged 7.3 mg(C)/L (Table 2-1). The analytical methods are described in Chapter 2.1.4.

The following DON concentrations were measured in the inflow water for Column II: 2.1 ± 0.2 mg/L (3rd wetting), 1.4 ± 0.2 mg/L (5th wetting), and 1.5 ± 0.2 mg/L (8th wetting). The low (1.4 mg/L) and high (2.1 mg/L) are taken to indicate the range of DON concentrations for the purpose of calculating the mass of DON infiltrated over the course of the short-term experiment (section 3.2.5). These DON concentrations were also used in calculating the δ^{15}N-DON of the inflow water (Section 3.2.7).

A subset of 16 samples of the inflow TWW were measured for dissolved organic carbon. Samples were filtered (0.45 µm) immediately after collection, acidified with hydrochloric acid to a pH of ~2, and measured within four weeks after sample collection with a *Shimadzu TOC V* elemental analyzer.

Table 2-1. Composition and variation of the inflow TWW. The summarized data reflect samples collected for the long-term experiment.

	Nitrate nitrogen mg(N)/L	Ammonium nitrogen mg(N)/L	Dissolved organic carbon mg(C)/L
Min	1.07	0.02	2.7
Mean	1.96	0.17	7.3
Median	1.74	0.11	6.6
Max	4.36	0.76	14
n	35	35	16

2.1.2 Column experiments and sampling

Particles larger than 10 mm were removed with a sieve and the soil was mixed in a large container to promote homogeneity. The columns were packed with soil by first placing a ca. 2 cm layer of quartz sand (Dorfner GmbH, Hirschau, Germany) in the bottom of each column and then pumping treated wastewater (i.e. normal inflow water) from below as soil was filled from above. The volume of TWW added was measured to determine total porosity. The level of the added soil was kept slightly above the rising water table to avoid density-based separation (e.g. of organic and inorganic particles) and the soil was periodically stirred with a stainless-steel rod to promote uniformity. Soil was added to about 7 cm below the top of the column (5 cm below the bottom of the lid), leaving headspace for water to pond before infiltrating into the soil.

The experimental columns consisted of an acrylic glass pipe (length: 1 m, inner diameter: 0.19 m) connected to a lid and base plate, also made out of acrylic glass. Inflow water was stored in a 15-L glass jug, pumped out via polytetrafluoroethylene (PTFE) tubing, through a peristaltic pump using a short (~20 cm) section of Tygon® tubing, and to the column through another section of PTFE tubing and a stainless-steel threaded connector. Flow was from the top of the column downward, in order to conduct infiltration with wetting and drying cycles in a similar manner to field applications. The outflow was collected in a bucket, which was weighed empty and full to obtain the volume of water (assumed density 0.998 g/cm3).

Cycles were typically three to four days of wetting and three to four days of drying. During the 16th wetting period in the short-term experiment, a tracer test lasting 15 days was conducted. The hydraulic loading was approximately 7 cm/d in the long-term experiment and 3.5 cm/d in the short-term experiment, due to differences in hydraulic conductivity, resulting in the exchange of 1-2 pore volumes during each wetting phase. The long-term experiment lasted 615 days and the short-term experiment 140.5 days. A schematic of the columns is presented in Figure 2-1 and a photograph of one of the columns (Column II) is shown in Figure 2-2. Construction of the sampling ports is illustrated in Figure 2-3.

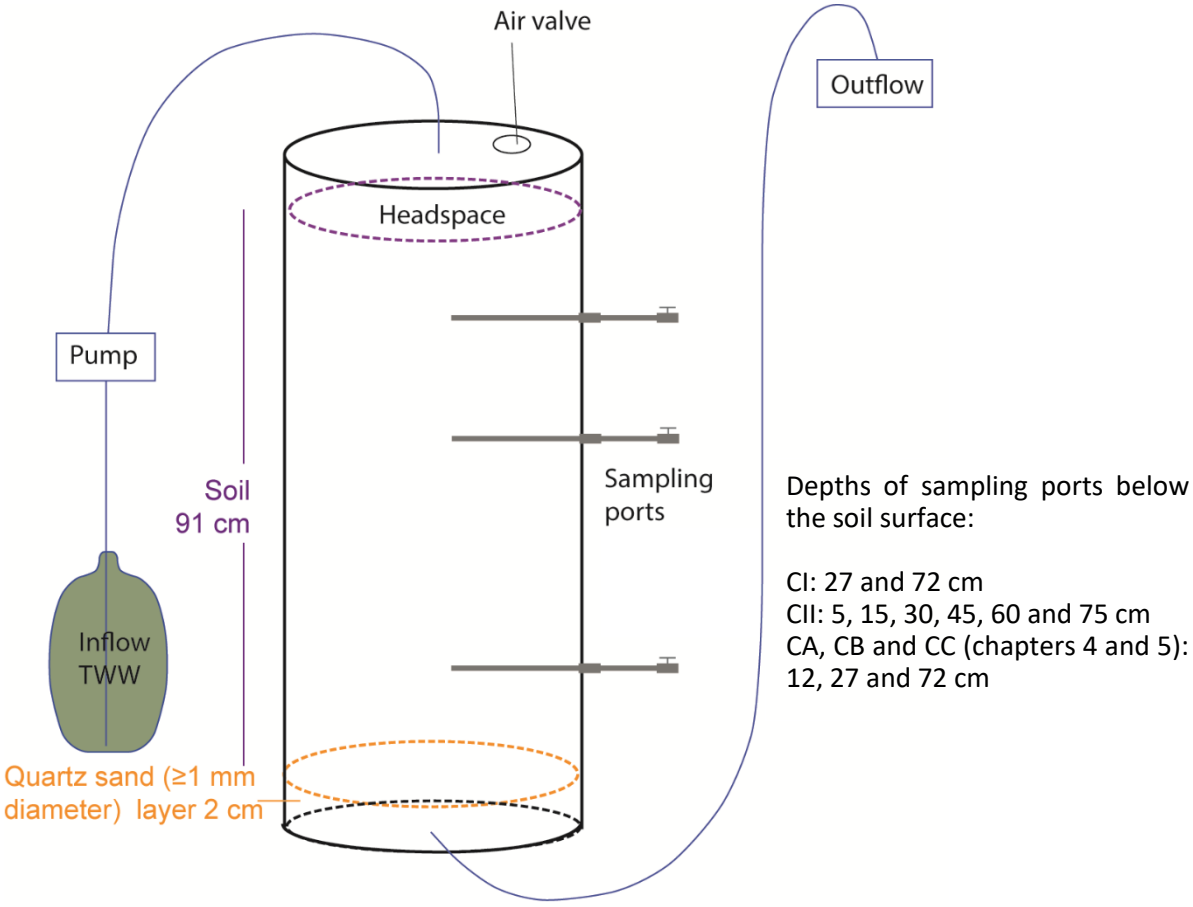

CA = Column A, CB = Column B, CC = Column C (Chapters 3 and 4).

Figure 2-1. Schematic of the experimental columns. CI = Column I, CII = Column II.

Figure 2-2. Photograph of Column II during a drying phase

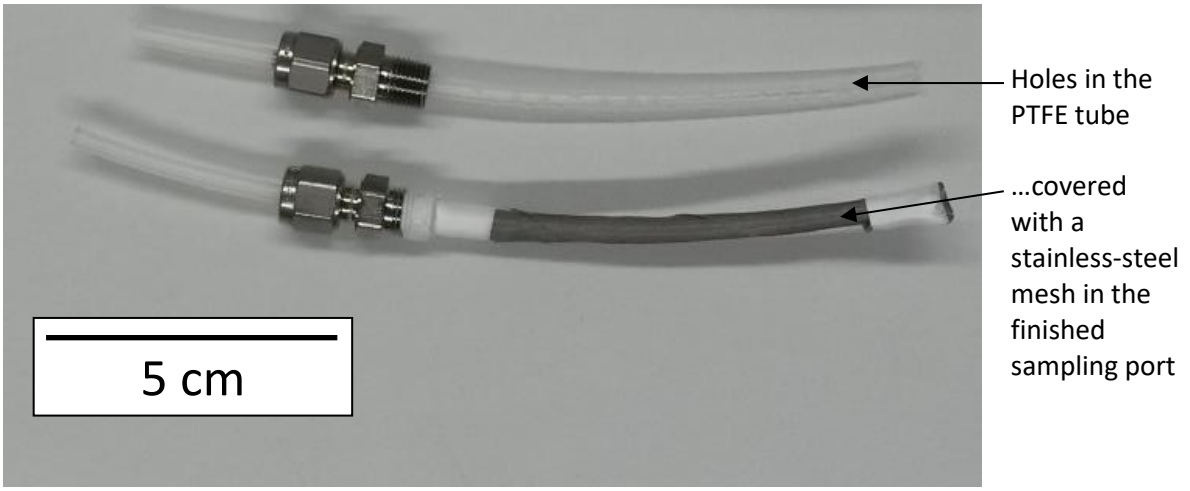

Figure 2-3. Sampling port construction

Sampling at the end of wetting phases was conducted by first taking a sample from the uppermost port and then proceeding downward, in the direction of the water flow. In this way, samples were collected with as little disruption as possible to the flow velocity at the time of sampling at each port. Samples were collected in polypropylene or high-density polyethylene sample bottles. Measurement of pH was done using a WTW *Multi 340i* meter and pH electrode, immediately following sample collection.

In order to obtain samples of water present in the pore space at the end of the drying phases, a method called “first flush” sampling was developed. The premise of the first flush sampling is that residual pore water is carried near the top of the rising water table during the filling of the columns. While water was pumped into the columns, samples were collected as soon as water began to flow out of each sampling port, starting with the lowest sampling port (75 cm) and working upwards as the water table rose. All ports were opened beforehand and samples were taken as soon as the first flush of water came out of the ports. The focus of first flush sampling was on nitrogen species, which are sensitive to changes in oxidation-reduction conditions. To evaluate the impact of mixing of pore water (the water targeted for sampling) with inflow water, the composition of the inflow water was also measured. Further, during one first flush sampling event, sodium bromide salt was added to the inflow water and the bromide ion used as a tracer for the portion of inflow water sampled. The background concentration of bromide in the soil columns is low (usually less than 1.5 mg/L). The bromide ion was measured in all samples using ion chromatography. The bromide concentration found in each sample then allowed estimation of how much inflow water was sampled and therefore how much of the sample contained pore water.

2.1.3 Oxygen and oxidation reduction potential

To monitor conditions related to nitrification and denitrification, oxygen concentrations were measured with a Presens oxygen sensing system from GmbH (Regensburg, Germany). Sensor spots (type *PS3t*, detection limit 0.001 mg/L) were fixed to the inside of the column walls at depths below the soil surface of 0, 2, 7, 12, 19.5, 27, 42, 57, and 72 cm on Column I (concentration-depth profiles collected) and 15 cm on Column II (time series collected). Oxygen concentrations were read using a fiber-optic cable connected to a Presens *Fibox3* control unit.

In the short-term experiment, ORP was measured using an in-situ probe (similar to the probe used by Vorenhout et al. (2004)) custom made by Paleo Terra (Amsterdam, the Netherlands) and a QIS (Oosterhout, the Netherlands) *QM710X* reference electrode (3.0 Molar KCl saturated with AgCl). Measurement of ORP was done in order to have a continuous indication of the oxidation-reduction state of the soil, through all parts of the wetting and drying cycles. The in-situ probe consists of platinum sensors at five depths. The reference electrode was placed in the uppermost part of the soil, where it serves as a reference for any one of the five platinum tip sensors. The platinum sensors and reference electrode were connected to a Campbell Scientific *CR800* data logger, which made voltage measurements for each platinum sensor. The voltage measurements were adjusted to values of a standard hydrogen electrode by adding 212 mV to each measurement and are then referred to as Eh.

2.1.4 Ions and total bound nitrogen

Water samples were measured for nitrate, bromide, and acetate with an *882 Compact IC plus – Anion* (carbonate eluent) and for ammonium with a Metrohm *882 Compact IC plus – Cation* (dicarboxylic acid and nitric acid eluent) (both devices from Metrohm, Herisau, Switzerland). Samples were diluted prior to measurement, resulting in detection limits of approximately 0.025 mg/L for nitrate, 0.1 mg/L for acetate and 0.05 mg/L for ammonium. Acetate was measured along with inorganic anions (Krata et al., 2009) after calibrating with an acetate standard solution (Carl Roth, Karlsruhe, Germany).

The mass of ions passing each sampling location over the duration of the experiments is calculated from the ion concentrations and measured flow volume. The calculations were performed using trapezoidal numerical integration of all available data points. The width of each trapezoid corresponded to the elapsed flow volume between the sampling events and the upper slope of each trapezoid connected the concentrations from consecutive sampling events. The areas of all trapezoids were summed to obtain total mass.

Selected samples of inflow water were measured for total bound nitrogen (tNb) using the U.S. Geological Survey alkaline persulfate digestion method (Patton and Kryskalla, 2003), adapted for measurement of nitrate by ion chromatography as follows: 2 mL of each sample was combined with a solution of potassium persulfate in potassium hydroxide and then heated in a closed vessel for 1 hour at 148°C. Afterwards, the samples were allowed to cool to room temperature. Then, they were diluted 30 times and nitrate was measured by ion chromatography. The digestion reagent contained nitrogen, so triplicate reagent blanks were carried through the entire process to correct the results for reagent nitrogen. Standards of urea (organic nitrogen) were also carried through the process.

2.1.5 Isotopes

Samples were kept frozen prior to isotope analysis. Subsamples were used for measurement of isotopes in ammonium and nitrate. Analysis of samples for isotopes was done by an external laboratory: Helmholtz Centre for Environmental Research - UFZ, Department of Catchment Hydrology.

Samples for $\delta^{15}N$ analysis of ammonium were prepared based on a modified Kjeldahl method that is suitable for sample volumes smaller than 50 mL. Pure sulfuric acid (0.05 N) was added to 50 mL aliquots of the water samples upon defrosting to preserve ammonium. After adjusting alkaline conditions by adding 32% NaOH solution and bromothymol blue for visual pH control, sample ammonium was transferred to a trapping flask containing 0.05N H_2SO_4 by distillation for 30 minutes. Any trapping liquid was evaporated in a sand bath at 80°C. The solid residue was homogenized and weighed for combustion in an elemental analyzer (vario isotope cube, Elementar) connected to an isotope ratio mass spectrometer (IsoPrime100).

Measurement of stable isotopes of nitrate ($\delta^{15}N$ and $\delta^{18}O$) was conducted on 0.2 micron filtered (sterile cellulose acetate membranes) with 10 mL aliquots of the original defrosted samples. Stable isotope ratios were measured on a GasbenchII/delta V plus combination (Thermo) using the denitrifier method for simultaneous determination of $\delta^{15}N$ and $\delta^{18}O$ in the measuring gas N_2O, produced by controlled reduction of sample nitrate (Sigman et al., 2001; Casciotti et al., 2002; McIlvin and Casciotti, 2011).

Apparent enrichment factors (ε) of nitrate were calculated from results of the inflow and a sample collected from depth in the soil by solving

$$\delta = \delta_0 + \varepsilon \cdot \ln(C/C_0) \quad (1)$$

for ε, where δ is the measured isotopic ratio at depth, δ_0 is the measured isotopic ratio in the inflow water, C is the nitrate concentration at depth, and C_0 is the nitrate concentration in the inflow water. Samples of the inflow TWW were measured for tNb concentration and isotopes. With results for tNb and DIN, DON concentrations were calculated by difference:

$$C_{DON} = C_{tNb} - C_{DIN} \quad (2)$$

δ_{15}N-DON is calculated by mass balance:

$$\delta_{15}N\text{-}DON = (\delta_{15}N\text{-}tNb * C_{tNb} - \delta_{15}N\text{-}NO_3 * C_{NO3}) / C_{DON} \quad (3)$$

Samples were prepared for tNb isotope measurements by first evaporating the water at 60°C in a sand bath to a volume of 15 to 20 mL, which was then placed in a concentrator (Eppendorf *Concentrator 5301*) until only solid remained. As for isotope analysis of NH_4, aliquots of the homogenized solid were then combusted in an elemental analyzer (*vario isotope cube*, Elementar) connected to an isotope ratio mass spectrometer (IsoPrime100). Some samples were measured after longer storage time (frozen at 20°C, ca. 5-12 months after collection) and more solid material appeared stuck to the walls of the HDPE sample bottles, resulting in lower solid yields. Results from these samples are discarded and only results from samples frozen for a short time (less than 9 weeks) before analysis are reported. For these samples, no precipitate or material stuck to the sample bottle was visible.

Samples for measurement of $\delta^{15}N$ in the original soil were milled to a grain size of <100 µm. Approximately 30 mg of milled soil was combusted in an elemental analyzer (*vario isotope cube*, Elementar) connected to an isotope ratio mass spectrometer (IsoPrime100).

Nitrogen and oxygen isotope results are reported in delta notation ($\delta^{15}N$, $\delta^{18}O$) as part per thousand (‰) deviation relative to the standards AIR for nitrogen and VSMOW for oxygen (Equation 1), where R is the ratio of the heavy to light isotopes (e.g. $^{15}N/^{14}N$; $^{18}O/^{16}O$).

$$\delta_X\ (‰) = [(R_{sample} - R_{standard}) / R_{standard}] \times 1000 \quad (4)$$

The standard deviation of the nitrogen isotope analysis of nitrate, ammonium and tNb is ± 0.4 ‰. Oxygen isotope analysis of nitrate is conducted with a precision of better than ± 1.6 ‰. For calibration of nitrogen and oxygen isotope values of nitrate samples, the reference nitrates IAEA-N3 ($\delta^{15}N$: +4.7 ‰ AIR; $\delta^{18}O$: +25.6 ‰ VSMOW) USGS32 ($\delta^{15}N$: +180 ‰ AIR; $\delta^{18}O$: +25.7 ‰ VSMOW), USGS 34 ($\delta^{15}N$: -1.8 ‰ AIR; $\delta^{18}O$: -27.9 ‰ VSMOW), and USGS 35 ($\delta^{15}N$: +2.7 ‰ AIR; $\delta^{18}O$: +57.5 ‰ VSMOW) were used. Calibration of ammonium and tNb isotope values was based on the standards USGS 25 ($\delta^{15}N$ = -30.4 ‰), USGS 26 ($\delta^{15}N$ = 53.70 ‰) and an internal standard NH4-0 ($\delta^{15}N$ = 0 ‰).

2.1.6 Batch sorption experiments

Batch experiments were conducted with post-experiment soil from Column A (see Chapter 3), in which continuous infiltration was conducted for 495 days. Soil from a column with continuous infiltration was chosen to first characterize sorption on a sample of the soil affected only by processes occurring during infiltration. The sample was collected in the range of 5 to 15 cm depth and stirred wet to promote homogeneity. The soil was then frozen and later freeze-dried to prevent microbial activity. Grains larger than 2 mm were discarded. Then, two subsamples each consisting of approximately 3 g, 8 g, 20 g, and 42 g soil were weighed, with the exact mass recorded for use in calculating the water-to-sediment ratios.

Aqueous solutions were mixed by adding NaCl, KCl, $MgCl_2$, $CaCl_2$, and NH_4Br (Solution B only) to deionized water (18 MOhm). The compositions of these solutions and the mean composition of the TWW are shown Table 2-2. Solution A contained a very low concentration of ammonium in order to test for desorption of NH_4^+. To test for new sorption of NH_4^+, NH_4Br was added to Solution B. The remaining cations except for calcium were present in Solutions A and B at similar concentrations as in the TWW. In the case of calcium, it is assumed that equilibration between the water and the calcite in the soil initially increases the calcium concentration in any occurrence of water-soil contact, whether a column or batch experiment.

Table 2-2. Composition of a representative sample of TWW and batch experiment aqueous solutions, in mmol/L.

	Na^+	K^+	Mg^{2+}	Ca^{2+}	NH_4^+	Cl^-	Br^-	NO_3^-	SO_4^{2-}	pH
Representative TWW sample	4.92	0.58	0.67	1.95	0.01	4.87	<0.02	0.12	0.88	7.35
Solution A	4.63	0.55	0.82	0.63	0.02	6.09	0.01	0.00	0.00	8.17
Solution B	4.63	0.55	0.83	0.63	0.66	6.09	0.66	0.00	0.00	8.17

The representative TWW sample was infiltrated in Column A beginning on Day 76 of that experiment. Solutions A and B: pH from PHREEQC (Parkhurst and Appelo, 1999) simulations, assuming all missing charge was from HCO_3^-.

2.2 Results and discussion

Results of the long-term experiment (Column I) are presented and discussed to characterize ammonium concentrations and some aspects of redox conditions during the wetting and drying cycles. Results of the short-term experiment (Column II) are then presented, first establishing relevant redox conditions and then moving to ammonium concentrations and stable isotopes in nitrogen species.

Total porosity values of 0.45 and 0.44 were determined from the volume of TWW pumped in while filling Columns I and II, respectively. Based on the measured soil solid density of 2.667 g/cm^3, a bulk density of 1.5 g/cm^3 was calculated for each column.

2.2.1 Wetting periods

Oxygen concentrations at the beginning of a selected wetting period in the long-term experiment are shown in Figure 2-4. Oxygen concentrations decreased to (near) zero in only 2-8 hours after starting wetting periods in the depth range of 2-12 cm, allowing conditions to become more reducing. It is presumed that depletion of oxygen occurred over a similar time period during other wetting periods.

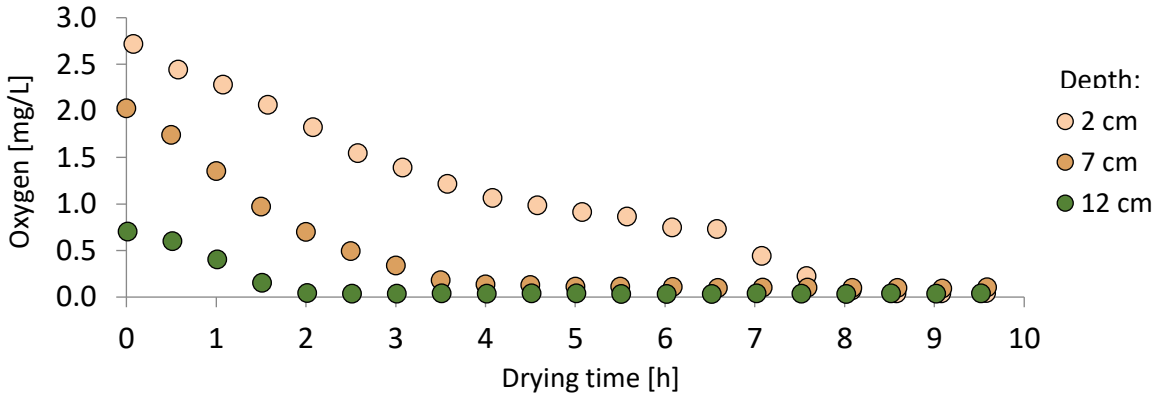

Figure 2-4. Oxygen concentration at three depths in Column I

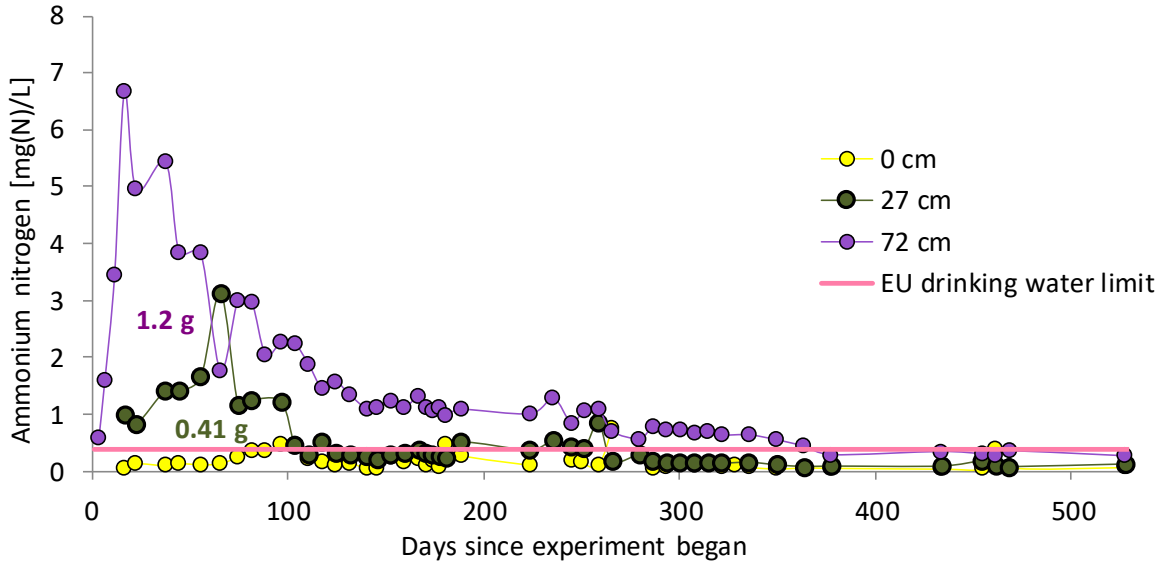

Figure 2-5. Ammonium nitrogen concentrations measured during the long-term experiment relative to the EU drinking water limit

Ammonium concentrations rose in the beginning of the experiment, peaking at 6.68 mg of nitrogen per liter [mg(N)/L] after 17 days at 72 cm depth and at 3.13 mg(N)/L after 66 days at 27 cm depth (Figure 2-5). Concentrations were above the EU Water Framework Directive limit for the first ~100 days in samples from 27 cm depth and the first ~360 days in samples from 72 cm depth. Ammonium concentrations plotted against cumulative flow volume, used for trapezoidal integration to calculate the mass, are shown in Table 2-3. The resulting ammonium nitrogen masses of 0.41 g passing 27 cm depth and 1.2 g passing 72 cm depth are shown on Figure 2-5. The end-of-wetting sampling of Column I shows that if TWW were infiltrated through this soil in a field MAR scheme, it would send a plume of ammonium to the aquifer.

Table 2-3. Ammonium concentration relative to cumulative flow volume in Column I

Cumulative flow volume [L]	Ammonium nitrogen [mg(N)/L] passing 27 cm depth	Ammonium nitrogen [mg(N)/L] passing 72 cm depth
0	0	0
34	n.a.	0.6
47	n.a.	1.6
60	n.a.	3.4
72	1.0	6.7
88	0.8	4.9
110	1.4	5.4
126	1.4	3.8
153	1.6	3.8
173	3.1	1.8
191	1.2	3.0
208	1.2	3.0
224	n.a.	2.0
233	1.2	2.3
247	0.4	2.2
259	0.3	1.9
271	0.5	1.4
282	0.3	1.6
294	0.3	1.3
311	0.3	1.1
321	0.2	1.1
330	0.3	1.2
343	0.3	1.1
352	0.4	1.3
360	0.3	1.1
364	0.3	1.1
371	0.3	1.1
377	0.2	1.0

Cumulative flow volume [L]	Ammonium nitrogen [mg(N)/L] passing 27 cm depth	Ammonium nitrogen [mg(N)/L] passing 72 cm depth
392	0.5	1.1
435	0.4	1.0
450	0.5	1.3
461	0.4	0.8
471	0.4	1.1
479	0.8	1.1
487	0.2	0.7
503	0.3	0.6
511	0.2	0.8
519	0.1	0.7
527	0.1	0.7
536	0.1	0.7
544	0.1	0.7
551	0.1	0.6
569	0.1	0.6
587	0.1	0.5
603	0.1	0.4
620	0.1	0.3
695	0.1	0.3
723	0.2	0.3
732	0.1	0.3
742	0.1	0.3
823	0.1	0.3
Total mass [g(N)]	**0.41**	**1.2**

n.a. = not analyzed

2.2.2 Drying periods

Samples collected using the first flush technique contain a mixture of inflow water and pore water, in its condition at the end of the drying period. To observe the proportion of inflow water in the collected samples, sodium bromide was added to the inflow water for first flush sampling conducted at the end of the 13th drying period (bromide C_0 = 11.5 mg/L, with background concentrations from the end of the previous wetting period < 0.5 mg/L). Analyzed concentrations of the soil pore water samples compared to the inflow water showed bromide C/C_0 of 0.49 (2 cm depth), 0.45 (7 cm), 0.23 (27 cm), 0.18 (57 cm) and 0.29 (72 cm). Based on these results, it is presumed that all first flush samples contain some pore water, likely a portion ≥~0.7 at 27 cm and greater depths. This pore water is thought to have been mobilized along the infiltration flow path to the sampling port.

Concentrations of nitrate in first flush and end of wetting samples from a selected portion of the experiment are shown in Figure 2-6. Concentrations of nitrate rose substantially during the drying periods, as the pore water-inflow water mixture contained higher concentrations of nitrate than the inflow water in most cases, except for 72 cm depth. The highest concentrations of nitrate were found in samples from 27 cm depth. At 72 cm depth, oxygen concentrations were near or below detection limits and nitrate concentrations in the first flush samples were 0.15 mg(N)/L or lower (except for Day 136, 1.1 mg(N)/L). Based on the higher nitrate concentrations at depths other than 72 cm, it appears likely that nitrification of ammonium occurred during the drying periods, as was reported by Miller et al. (2006) and Hernández-Martínez et al. (2016).

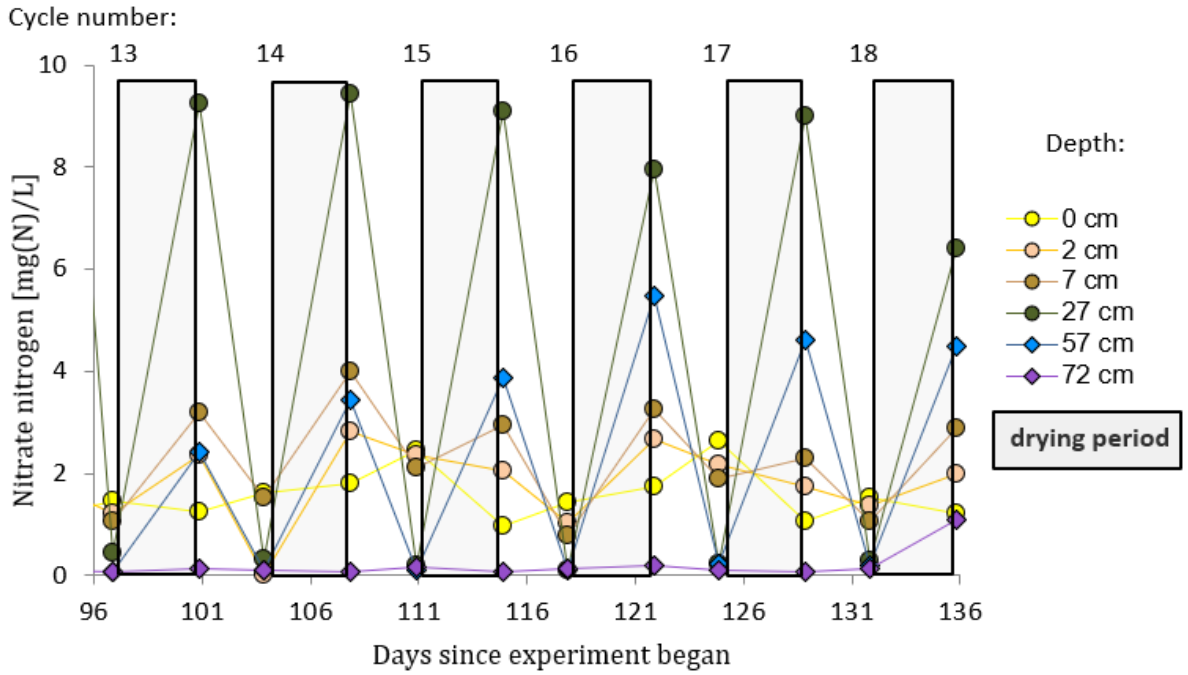

Figure 2-6. Nitrate nitrogen concentrations measured during end of wetting and first flush (end of drying periods) sampling during a selected portion of the long-term experiment

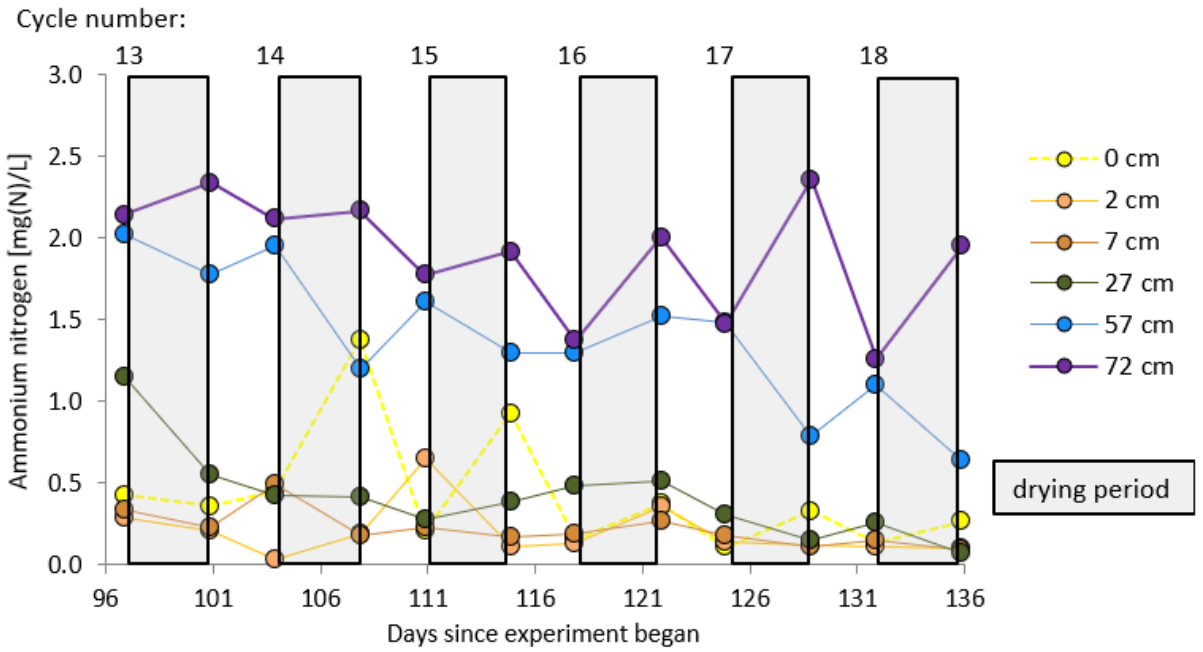

Figure 2-7. Ammonium nitrogen concentrations measured during end of wetting and first flush (end of drying periods) sampling during a selected portion of the long-term experiment

At depths between 12 and 42 cm, oxygen concentrations at the end of the wetting periods increased slightly through time (Figure 2-8). This may indicate depletion of labile organic carbon (i.e. BDOC) from the soil and/or residual TWW, such that less anaerobic respiration occurred in successively later drying periods. Although the pore water in the first flush samples could have originated anywhere from the soil surface down to the respective sampling port, at 27 cm depth, elevated concentrations of ammonium during the wetting periods coincide with replenishment of oxygen during the drying periods (Figure 2-8), providing both mass of ammonium and potential for nitrification. Below about 50 cm, the soil remained water saturated during the drying periods, resulting in near-zero oxygen concentrations. Decreases in concentration of ammonium in the first flush samples (Figure 2-7), compared to the previous wetting period, were observed fairly consistently at 57 cm depth, but they do not correspond in magnitude to the increases in nitrate concentration. At 72 cm depth, first flush ammonium concentrations were higher than during the wetting periods. However, the column remained close to saturation here during the drying periods, so possibly ammonium may have continued to form with stagnant water present in the pore space. At other depths, first flush concentrations were similar to those measured in samples from the end of wetting periods. The lack of a clear trend toward lower ammonium concentrations in first flush samples could be due to variation in the inflow water ammonium concentration and/or possible desorption of ammonium as concentrations lowered, preventing large fluctuations in concentration.

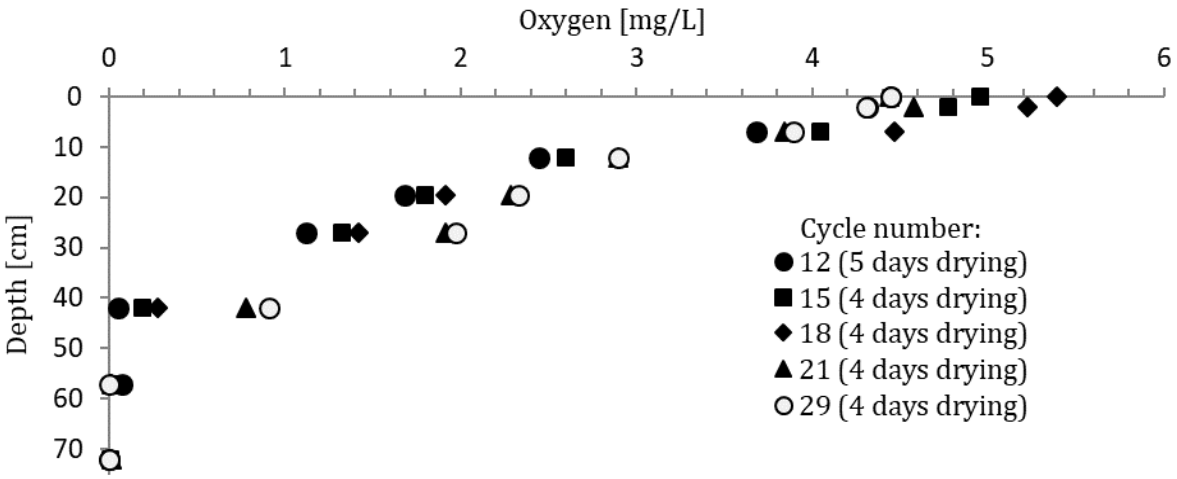

Figure 2-8. Oxygen concentrations decreased with depth in the soil at the end of drying periods in the long-term experiment.

Overall, the long-term experiment (Column I) showed that ammonium concentrations rise during infiltration of treated wastewater through the experimental soil and that some ammonium may be nitrified during drying periods. The following sections present the short-term experiment (Column II), in which nitrogen cycling was investigated in more detail by collecting ORP, acetate and stable isotope data.

2.2.3 Oxygen and oxidation reduction potential

ORP measurements illustrate a clear difference in redox condition between the wetting and drying periods (Figure 2-9). During wetting phases, Eh reached approximately -200 mV at all depths. This Eh is similar to that found by Dhondt et al. (2003) during autumn and winter, a time period for which they show that DNRA was responsible for at least some nitrate reduction. In the present study, reducing conditions were present everywhere in the soil during wetting periods. During drying phases, Eh recovered to ~400 mV in the upper part of the soil, while remaining essentially unchanged from 45 cm downward. The soil remained water saturated during the drying periods from ~50 cm depth downward. Beginning on day 104, a tracer test was conducted, with a wetting length of 15 days, resulting in an extended time period with Eh around -200 mV at all depths.

The maximum Eh reached during drying periods at 15 cm depth was low through the 11th drying (~Day 75) and then was substantially higher during the following drying periods. A similar trend was observed in oxygen concentrations, which are shown in Figure 2-10. The increase in oxygen concentration and

Eh in later wetting periods may have resulted from depletion of the system of labile organic carbon (e.g. acetate), so that less anaerobic respiration occurred. Oxygen concentrations generally increased beginning at 0.5 – 0.75 days after drainage began. Drying periods lasted about 2.6 days.

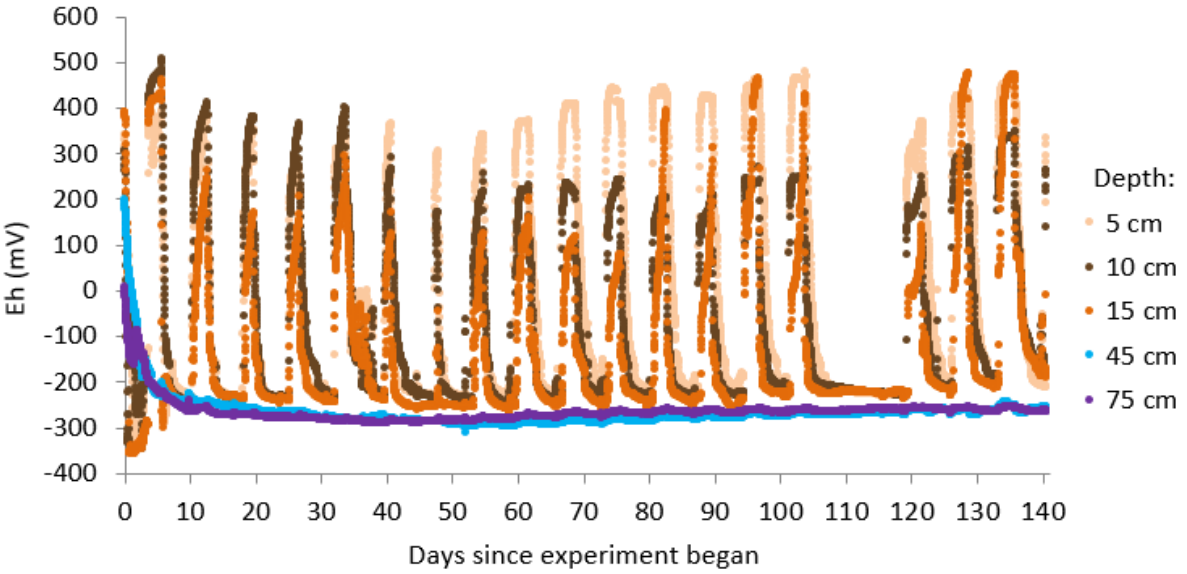

Figure 2-9. Oxidation reduction potential in Column II

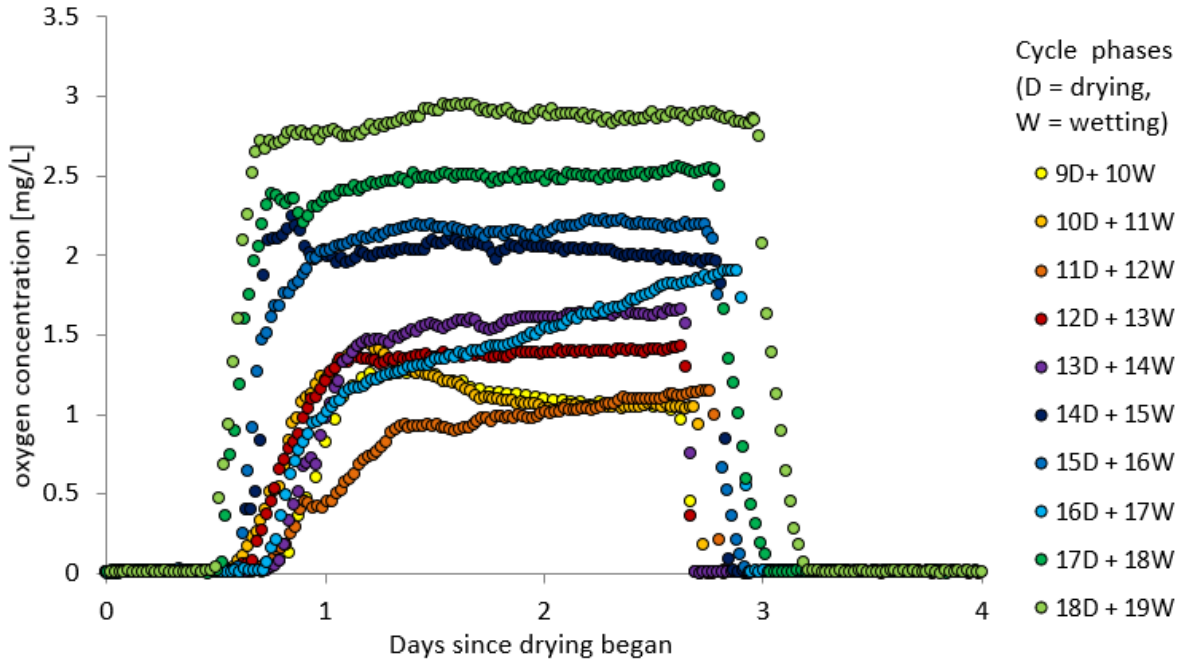

Figure 2-10. Oxygen concentrations measured 15 cm below the soil surface

With the oxidizing conditions in the upper part of the soil, the potential for nitrification of ammonium was present. The interpretation that ammonium is nitrified during drying periods is also consistent with the higher nitrate concentrations found during first flush sampling (Chapter 2.2.2). In studies infiltrating TWW in which ammonium was the dominant form of inorganic nitrogen, some ammonium is nitrified during drying periods and then denitrified during wetting periods, with retention of ammonium in the soil appearing to play a role (Miller et al., 2006; Hernández-Martínez et al., 2016).

2.2.4 Acetate

Acetate is a form of labile organic carbon. It can be formed in soils by anaerobic decomposition of a variety of plant substances (Acharya, 1935), which the experimental soil contained in the form of fragments of roots and plant stems. While acetate is commonly produced through fermentation of more complex forms of organic matter, it can then act as an electron donor in denitrification (Paul and Beauchamp, 1989) or DNRA (van den Berg et al., 2017). Acetate concentrations were highest in the beginning of the experiment and at depth in the soil (Figure 2-11).

In considering possible sources of the ammonium, it has been shown that with higher labile organic carbon to nitrate ratios, nitrate reduction is driven from denitrification toward DNRA (Buresh and Patrick, 1978; Yin et al., 2002; Yoon et al., 2015). Jørgensen (1989) found that denitrification occurred close to the soil surface but that nitrate reduction switched to DNRA with increasing depth, in as little as 1 cm from the soil surface. Based on the occurrence of high acetate concentrations, the conditions needed for DNRA may have been present in the earlier stages of the experiment and at greater depths in the soil. Van den Berg et al. (2016) showed that at acetate to nitrate molar ratios of ~1 and higher, DNRA occurred (to some extent concurrently with denitrification) in activated sludge taken from a wastewater treatment plant. In the short-term experiment, acetate and nitrate were both above detection limits in many samples from 15 cm and 30 cm depth, particularly early in the experiment. In these samples, the acetate to nitrate molar ratio was always 8 or higher, indicating the presence of conditions under which DNRA occurs.

A local peak in acetate concentrations is seen in the fourth sampling event, which was performed at the end of a wetting phase in which the flow rate was lowered due to technical problems with column operation. The slower water flow results in longer contact time for the water with the soil, which might have allowed higher production of acetate.

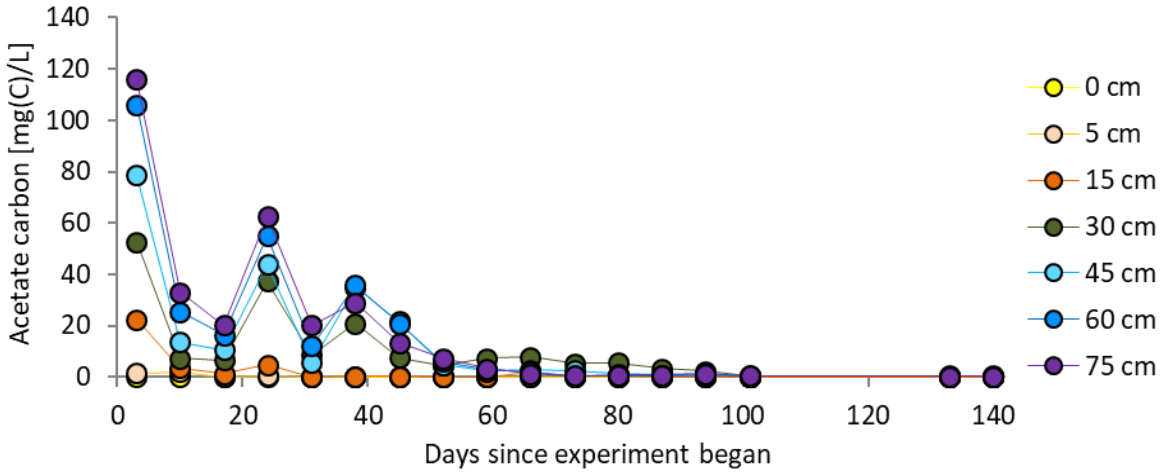

Figure 2-11. Acetate carbon concentrations in inflow and pore water over the course of the short-term experiment

2.2.5 Ammonium

Ammonium concentrations in the short-term experiment rose to as high as 13.94 mg(N)/L (Figure 2-12). The pattern over time was similar to Column I, with concentrations peaking after 38 days at 30 cm depth and 52 days at 75 cm depth, although a less pronounced second peak is seen at some depths. Ammonium was present in the beginning at all measured depths, but then generally decreased progressively over time with depth. Results from the fourth sampling event (24 days) were slightly higher than in the fifth sampling event, showing a local peak. The local peak in ammonium concentrations seen in the fourth sampling (24 days) may be due to the flow conditions described in the previous section. Ammonium concentrations plotted against cumulative flow volume are shown in Appendix A.

The short-term experiment (Column II) lasted for 140.5 days, during which a total of 113 L of TWW was infiltrated. Based on the flow volume at sampling times and ammonium nitrogen concentrations shown in Table 2-4, 0.54 g(N) of ammonium was observed in the water at 30 cm depth and 0.78 g(N) at 75 cm depth. A total of 0.26 g(N) of nitrate was infiltrated. Compared to the 0.78 g(N) of ammonium at 75 cm depth, not enough nitrate was infiltrated to account for all of the mass of ammonium observed. If inflow DON remained in the range of 1.4 to 2.1 mg/L over the duration of the experiment, the mass of DON infiltrated was in the range of 0.16 to 0.24 g(N), which is also not enough to account for all of the ammonium formed. Further, when the infiltrated masses of nitrate and assumed DON are summed, a total of 0.38 to 0.50 g(N) was infiltrated, compared to 0.78 g(N) of ammonium observed at 75 cm depth.

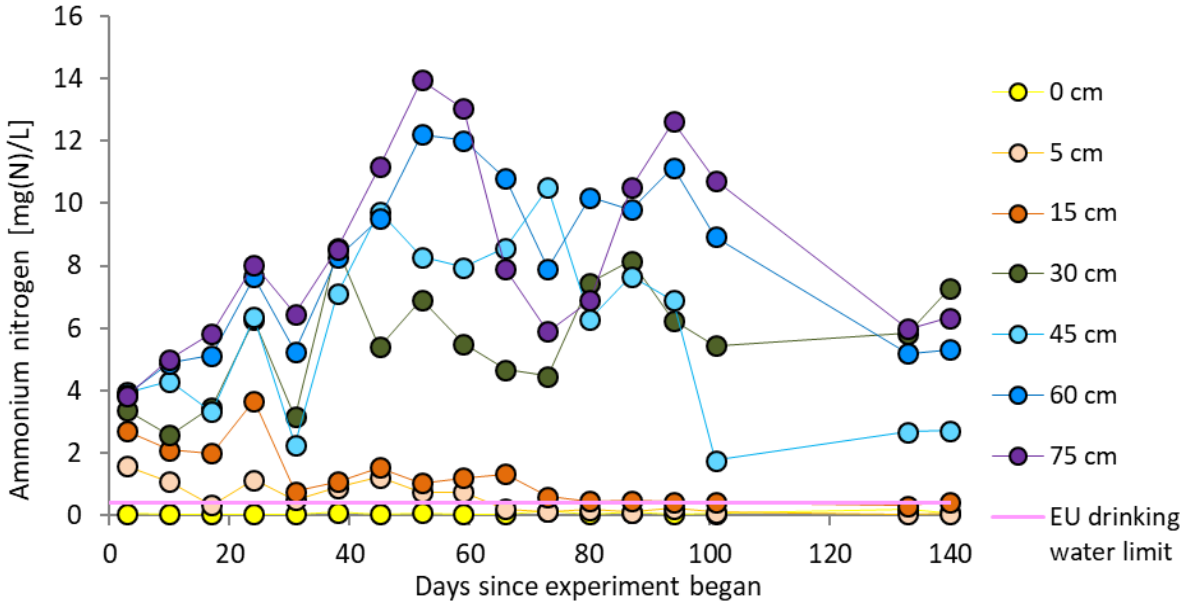

Figure 2-12. Ammonium nitrogen concentrations in pore water samples over the course of the short-term experiment

Table 2-4. Ammonium concentration relative to cumulative flow volume in Column II

Flow volume (L)	Ammonium nitrogen [mg(N)/L] 30 cm depth	Ammonium nitrogen [mg(N)/L] 75 cm depth
0	0	0
15	3.4	3.8
27	2.6	5.0
36	3.5	5.8
39	6.3	8.0
48	3.2	6.5
55	8.6	8.5
61	5.4	11.2
65	6.9	13.9
70	5.5	13.0
74	4.7	7.9
79	4.5	5.9
83	7.5	6.9
87	8.2	10.5
88	6.2	12.6
92	5.4	10.7
109	5.8	6.0
113	7.3	6.3
Total mass [g(N)]	**0.54**	**0.78**

Another possible source of the ammonium is the soil. The soil contained 0.2% nitrogen by mass. 32,446 g of soil were added to the column to a depth of 88 cm. Of this mass, 85% (75 cm / 88 cm) is assumed to lay between 0 cm and 75 cm depth. Therefore, 27,652 g of soil was present between 0 cm and 75 cm depth, of which 0.2% was nitrogen, equivalent to 55 g. As the total mass of infiltrated nitrogen appears to be less than the mass of ammonium, it is likely that soil nitrogen was a source for at least some of the ammonium.

In Column I, with the higher flow rate, only 0.33 g(N) of ammonium was observed at 72 cm depth through a flow volume of 110 L (37.7 days), the total flow volume through Column II. However, comparing equal time intervals, 0.83 g(N) of ammonium was observed through 140.7 days in Column I (311 L of cumulative flow, almost three times the flow volume through Column II for the same amount of time), which is close to the 0.78 g(N) of ammonium at 75 cm depth in Column II (140.5 days). More ammonium was observed in Column II at 30 cm depth (0.54 g) than in Column I at 27 cm depth (0.78 g) over the duration of the Column I experiment, but ammonium concentration remained high (5.4 – 7.3 mg(N)/L) in the last three sampling events in Column II. This comparison suggests that if the experiment in Column II had been continued, the mass of ammonium observed passing 27 cm depth could have equaled that observed in Column I. Thus, it appears that longer reaction time allows for more ammonium formation and that time, rather than flow volume, appears to have been the more critical factor in how much mass of ammonium formed. Thus, in addition to the mass balance, the similarity of the temporal pattern suggests that the soil was a prominent source of the ammonium because if the main source of the ammonium were in the TWW, flow rate should have had an influence on how much ammonium forms.

2.2.6 Stable isotopes in nitrate

Most samples were measured for stable isotopes of oxygen (^{18}O) and nitrogen (^{15}N) in nitrate. Results of $\delta^{15}N\text{-}NO_3$ and $\delta^{18}O\text{-}NO_3$ for all samples from 0 to 15 cm depth are shown in Figure 2-13. Samples from 5 cm depth are more enriched overall in ^{15}N and ^{18}O than the inflow (0 cm depth), and samples from 15 cm depth are overall more enriched in the heavy isotopes than the samples from 5 cm depth.

Results for individual sampling events are shown in Appendix A and consistently show enrichment of ^{15}N and ^{18}O at 5 cm depth relative to the 0 cm sample for the respective wetting period (with the exception of ^{15}N in the 13th wetting period). Where isotopes were detected in samples from 15 cm depth, in most cases these also show enrichment relative to the 5 cm sample from the same wetting

period. Overall, these observations are consistent with studies using dual isotopes that clearly show the occurrence of denitrification (e.g., Böttcher et al., 1990; Mengis et al., 1999).

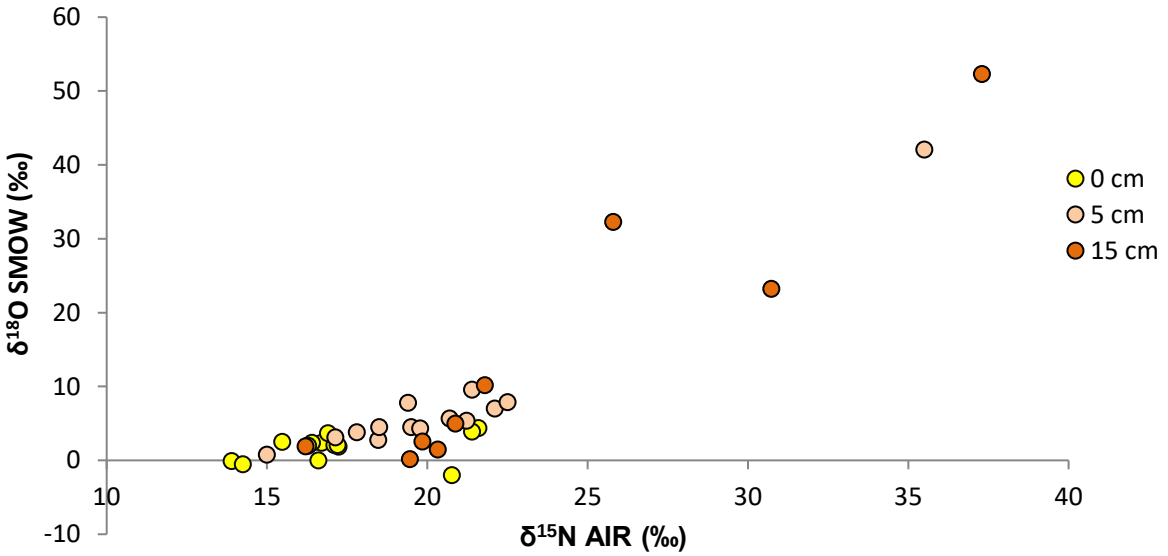

Figure 2-13. Dual isotope plot of ^{15}N and ^{18}O in all samples analyzed over the course of the experiment

The $\delta^{15}N$ versus natural log-normalized nitrate concentration (Appendix A, Figures A-4, A-5, A-10, A-12 and A-19) plots linearly between 0 cm and 15 cm depth in five sampling events (out of nine sampling events with isotope detection at all three depths). Such a linear relationship can result from denitrification (Mariotti et al., 1981). In some other cases the slope becomes shallower with either the 15 cm or 30 cm sample; this might be a result of nitrate reduction switching (partially) to DNRA, but knowledge of isotopic fractionation during DNRA is limited.

In general, enrichment of ^{15}N and ^{18}O is apparent in the data, but when all of the data points are viewed together as in Figure 2-13, considerable variation from the linear relationship that is expected for denitrification is seen. This is partly a result of variable isotopic composition of the inflow TWW. In the soil pore water samples, multiple processes (e.g. denitrification and DNRA) could have occurred simultaneously in different microenvironments, resulting in interfering isotopic signals.

Viewing individual sampling events (Appendix A, Figures A-1a – A-19a; stable isotopes were not measured in samples from the 11th, 16th, 17th and 18th wetting periods), the dual isotope results mostly show enrichment of both N and O between 0 and 15 cm depth. However, in samples from the 13th wetting period, nitrate became depleted in ^{15}N. This could be a result of process variation in different pores with water samples representing combinations of different microenvironments. Where the

slope changes with the 15 cm sample (6th, 9th and 15th wetting periods) or the 30 cm sample (5th wetting period), it is possible that by these depths, nitrate reduction had (partially) switched from denitrification to DNRA. Rayleigh enrichment factors (ε) for ^{15}N were calculated based on the inflow and 5 cm depth samples (Appendix A, Figures A1c – A19c). The result from the 15 cm sample fit on this curve in some cases (e.g. 4th wetting) but fell below it in many other cases. This could be a result of concurrent denitrification and DNRA.

Enrichment factors based on the concenteration-15N relationship resulting from denitrification typically range from about −11 to −33 ‰, with lower absolute values likely being associated with faster reaction rates (Mariotti et al., 1982). Overall, the mean apparent enrichment factor based on the 0 and 5 cm samples and Equation 1 was −7.2 ‰ but with considerable variation between wetting periods (Figure A-1). These values overall do not seem to be consistent with denitrification as a single enrichment process. Dhondt et al. (2003) found a nitrate 15N enrichment factor of −6.2‰ that likely was influenced by DNRA as a competing process with denitrification. In the soil-TWW system, it may also be that denitrification and DNRA were competing nitrate reduction processes, with variation in apparent enrichment factors due to relative predominance of one process over the other.

Chen and Macquarrie (2005) evaluated nitrate dual isotope data in six studies in which denitrification likely occurred, finding ^{18}O to ^{15}N fractionation ratios in the range of 0.48 to 0.67, while Carrey et al. (2014) found a ratio of 0.93. In the present study, the slope of dual isotope plots for individual wetting periods (Figure 2-14) is outside of this range for a substantial number of wetting periods. Higher enrichment of O relative to N is seen in the earlier wetting periods, when the higher acetate concentrations were present, a factor which is thought to drive nitrate reduction toward DNRA. In a column study with lake sediments, DNRA was inferred to have occurred in the early stages of infiltration (Carrey et al., 2014). The lower fractionation ratios from the 5th wetting onward (except for the 10th wetting) could indicate a change in the dominant nitrate reducing process from DNRA to denitrification.

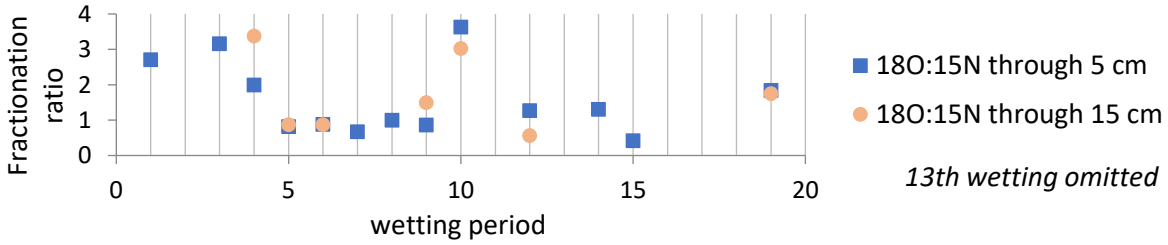

Figure 2-14. ^{18}O:^{15}N fractionation ratios over the course of the experiment

In some samples from 30 cm and deeper, nitrate concentration was sufficient to detect isotopic ratios. In these cases, $\delta^{15}N\text{-}NO_3$ became lighter with depth (Appendix A) and in some cases lighter than the inflow (2nd, 4th and 19th wetting phases). Samples from 30 cm and greater depth collected during the 2nd and 19th wetting periods also contained high $\delta^{18}O$ values (above 40 ‰). Aerobic respiration resulting in even small changes in oxygen concentration can cause a substantial increase of $\delta^{18}O$ in remaining oxygen (Aggarwal et al., 1997). The increase in the heavier oxygen isotope ^{18}O is a kinetic effect, similar to the increase in ^{15}N during denitrification (Knöller et al., 2011). Thus, the observed high $\delta^{18}O$ values in samples from 30 cm and greater depth during these two wetting periods suggest that microbial activity was also present in the deeper portion of the soil.

The lower $\delta^{15}N\text{-}NO_3$ values suggests the presence of an additional, isotopically lighter nitrogen source contributing to the nitrate pool. A lighter nitrogen source that was present is ammonium (Section 2.2.7). The isotopically lighter nitrate-nitrogen provides an indication, in addition to the first flush sampling results (Section 2.2.2), that nitrification of ammonium occurred during the drying periods. The fact that this lighter nitrate-nitrogen is only (with the exception of the 13th wetting) found at greater depths (30 cm and deeper) is consistent with the interpretation that it formed during the previous drying period and then was flushed downward during the next wetting period, at the end of which sampling was conducted.

2.2.7 Stable isotopes in ammonium and its possible origin

Stable isotopes of ammonium and its possible sources are shown in Figure 2-15. $\delta^{15}N\text{-}NH_4^+$ is similar to $\delta^{15}N$-Soil, although in most samples the ammonium is isotopically somewhat heavier than the soil nitrogen. Because of the similarity, the soil nitrogen is a likely source of at least some of the ammonium. Most of the $\delta^{15}N\text{-}NH_4^+$ values are higher than the $\delta^{15}N$-soil value, which is likely an effect of nitrification during the drying periods and/or DNRA during the wetting periods. Nitrification would result in isotopically lighter nitrate-nitrogen, leaving isotopically heavier ammonium-nitrogen behind in the portion of ammonium that remained at the end of the drying periods. DNRA would convert nitrogen from the isotopically heavier nitrate (Figure 2-15) to ammonium. With the soil as a main source of the ammonium, it is likely that the $\delta^{15}N\text{-}NH_4^+$ values are increased from the value of the $\delta^{15}N$-soil through a combination of both DNRA (wetting periods) and nitrification (drying periods). While nitrate is a possible source for some of the ammonium, DON in the inflow water appears to be isotopically similar to or lighter than the soil. Thus, DON does not appear to be an important source of the ammonium.

At 30 cm depth, $\delta^{15}N\text{-}NH_4^+$ rose in the beginning to a maximum of 10.3‰ on Day 17, then declined thereafter. As ammonium may be retarded in the soil, the peak on Day 17 may be an additional indication that ammonium formed from an isotopically heavier source (nitrate) in the early stages of infiltration, with this source becoming less important over time. The high concentrations of acetate in the early stages of the experiment (Figure 2-11) provided a labile carbon source that has been shown to drive the nitrate reduction system toward DNRA (van den Berg et al., 2016).

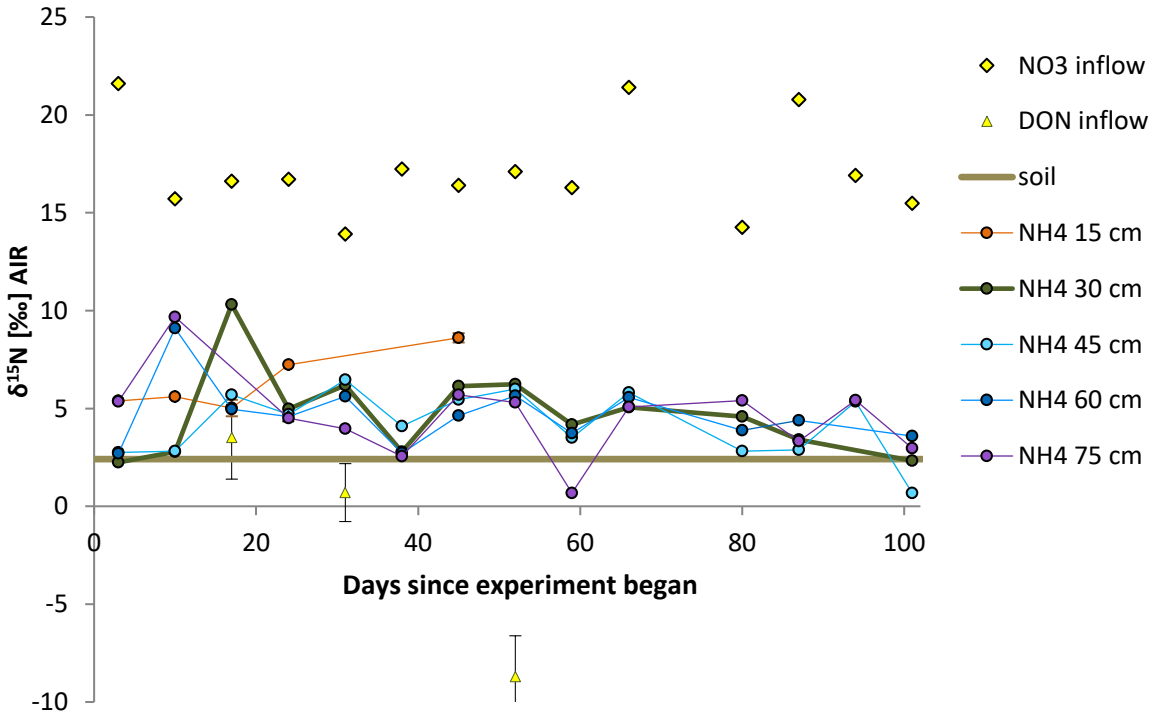

Figure 2-15. $\delta^{15}N$ in ammonium in comparison to $\delta^{15}N$ in the soil nitrogen, inflow water nitrate and inflow water DON

2.2.8 Sorption of ammonium

Batch experiments with post-experiment soil and two different aqueous solutions (one with ammonium spiked, the other unspiked) resulted in the sorbed and desorbed concentrations shown in Figure 2-16. On this graph, sorbed ammonium is represented by positive values on the vertical axis and desorbed ammonium by negative values. In the unspiked starting solution, ammonium concentration was very low (0.32 mg(N)/L), as was the case with the TWW used as inflow in the column experiments. In these batch experiments, ammonium concentrations were higher in the final solution after shaking, indicating that ammonium had desorbed. Furthermore, these results indicate that ammonium sorbed to the soil during the column experiment, even with calcium was present at higher concentrations and

having a higher valence than ammonium, which tends to result in calcium having a higher affinity to a solid exchanger than ammonium (Appelo and Postma, 2005). However, some layered silicate minerals show a preference for ammonium over calcium, and soil organic matter may also play a role in sorption (Okamura and Wada, 1984). Sorption of ammonium in the presence of variable calcium concentrations was also found in a study of clay-rich (8.5% and 32%) agricultural soils, with a preference for ammonium over calcium (Agbenin and Modisaemang, 2015). In the present study, results from the eight samples plot linearly, with a y-axis intercept of -17 mg/kg, indicating that 17 mg of ammonium-N per kg of soil was sorbed. The -17 mg/kg of sorbed ammonium was subtracted from the concentrations shown in Figure 2-16 in order to plot a linear isotherm (Figure 2-17). The slope of the isotherm gives a linear sorption coefficient (K_d) of 3.14 kg/L.

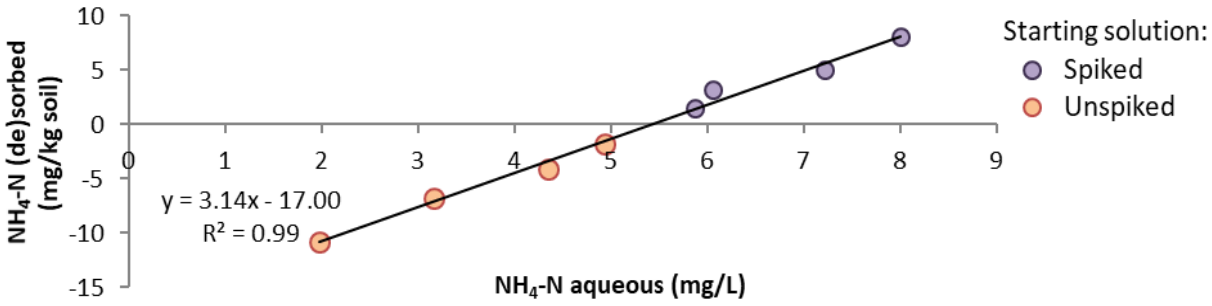

Figure 2-16. Results of the batch experiments with and without spiked ammonium

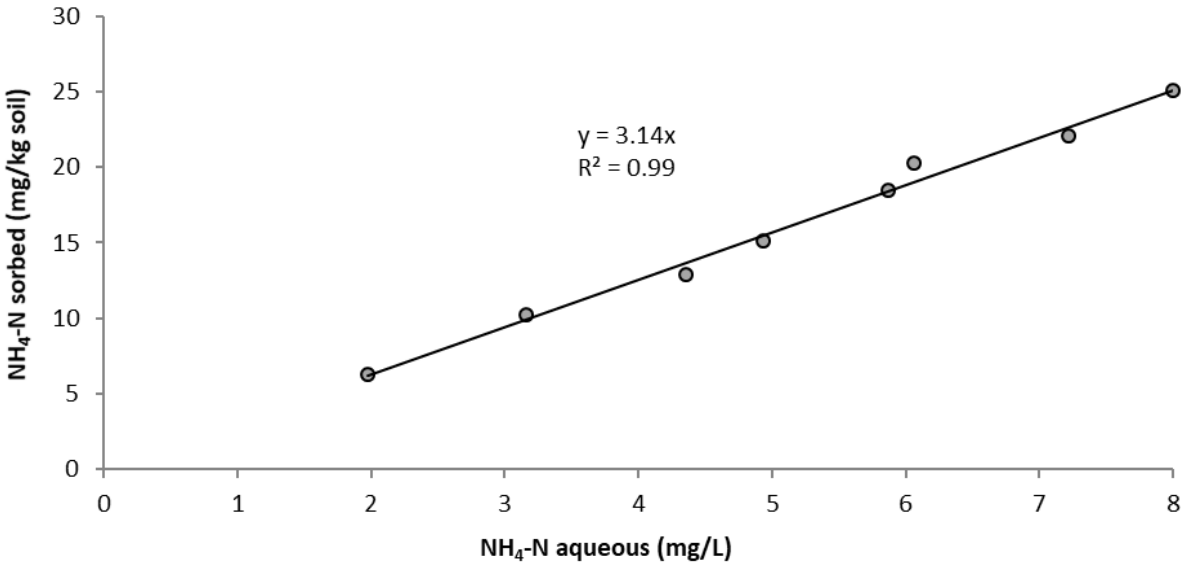

Figure 2-17. Sorption isotherm for ammonium nitrogen from the batch experiment with post-experiment soil from Column A

The aqueous solution used contained cations in concentrations representative of the TWW, except for ammonium (spiked series) and calcium (Table 2-2). With the desorption that occurred in the unspiked samples and the spiked ammonium, the isotherm covers the concentration range of approximately 2 - 8 mg/L of ammonium nitrogen. In the column experiments, ammonium concentration reached a maximum of 6.7 in Column I and 13.9 in Column II. The concentration range of the isotherm is therefore representative of pore water ammonium-nitrogen concentrations (> 2 mg/L). The calcium concentration in the starting solution was lower than in the TWW sample. However, calcium concentrations increased after shaking in all batch samples to concentrations ranging from 1.28 mmol/L (3.17 g of soil) to 2.89 mmol/L (41.35 g of soil), which are higher than the concentration in the TWW.

Assuming comparability of these batch sorption experiments with the Column I and Column II experiments operated with wetting and drying cycles, the linear isotherm shows that ammonium sorbs to the soil under the infiltration conditions. Retardation of ammonium during transport, through sorption and desorption, is therefore a likely process affecting the temporal pattern of observed ammonium concentrations. The peak ammonium concentrations observed at greater depths (e.g. 72 cm in Column I and 75 cm in Column II) therefore suggests that the peak of ammonium production occurred sometime before the peak concentrations.

Applying the K_d value to the Column II experiment, the retardation factor (R_f) of ammonium during transport can be calculated:

$$R_f = 1 + \rho_s K_d (1-n)/n \quad (5)$$

where ρ_s is the solid density of the soil and n is the porosity. Application of the K_d value assumes that sorption was reversible, i.e. desorption also occurred in equilibrium with the water concentration.

Using the porosity (0.44) determined while filling Column II and the solid density (2.667 g/cm^3), a retardation factor of 12 results. Assuming that the K_d is representative for the duration of the Column II experiment, the retardation factor means that ammonium traveled at 1/12th of the water seepage velocity. It is therefore likely that much of the ammonium formed early in the experiment and that the observed peaks came later as a result of retardation during transport. However, the occurrence of secondary peaks at 30 and 75 cm depth in the time range of Days 87 – 94 (Figure 2-12) suggests that some additional ammonium also formed later in time.

3 Fate of non-antibiotic pharmaceuticals

The following sections present the methods for and results of the fate of non-antibiotic pharmaceuticals under three different infiltration conditions. Tables B-1 and B-2, documenting all extraction replicates and the complete mass balance, respectively, are provided in Appendix B.

3.1 Materials and methods

3.1.1 Soil and inflow water

The soil (described in Chapter 2.1.1) contains pristine (not decayed) organic matter originating from plants, which may help degrade TrOCs (Lim et al., 2008). The inflow water for the experiments was secondary TWW, as described in Chapter 2.1.1. Total dissolved organic carbon (DOC) concentration (including the BDOC and non-biodegradable fractions) averaged 7.3 mg/L (Chapter 2.1.1) and ranged from 2.7 to 14 mg/L based on a subset of 16 samples, which were filtered (0.45 µm) immediately after collection, acidified with hydrochloric acid to a pH of ~2 and measured within four weeks after sample collection on a *Shimadzu TOC V* elemental analyzer.

Infiltration of water with higher organic matter concentrations may increase biomass in the upper ~30 cm of soil (Rauch-Williams and Drewes, 2006) or specifically promote biofilm growth (Zhao et al., 2009; Vidal-Gavilan et al., 2014), which could lead to increased sorption of the pharmaceuticals (Dobor et al., 2012). Infiltration water with lower BDOC tends to lead to increased degradation of TrOCs such as pharmaceuticals, as bacteria are starved of more favorable carbon sources (Rauch-Williams et al., 2010; Hoppe-Jones et al., 2012; Alidina et al., 2014b).

Carbamazepine (1.3 ± 0.2 µg/L), diclofenac (5.3 ± 1.0 µg/L), gemfibrozil (0.2 ± 0.2 µg/L) and naproxen (0.2 ± 0.2 µg/L) were consistently detected in the TWW. Worldwide, maximum concentrations between ~5 and 20 µg/L have been reported for these four compounds in secondary effluent (Verlicchi et al., 2012). To better see changes in concentration and for better comparison, these compounds plus fenoprofen were spiked with 20 µg/L, resulting in relatively high but occurring concentrations. The antibiotics doxycycline, sulfadimidine and sulfamethoxazole are each found in untreated wastewater (Verlicchi et al., 2012) as well as in the aquatic environment (Kümmerer, 2009). Sulfamethoxazole and doxycycline are also found in TWW and present medium or higher environmental risk (Verlicchi et al., 2012). To create one inflow solution with elevated concentrations of these environmentally occurring

compounds to investigate the influence of higher concentrations on the fate of other compounds, they were also spiked in the inflow water for one of the columns. The compounds carbamazepine, diclofenac sodium salt, fenoprofen calcium salt hydrate, gemfibrozil, naproxen, as well as the antibiotics doxycycline, sulfadimidine and sulfamethoxazole were purchased from Sigma Aldrich (Germany); all were of analytical grade. The log octanol-water coefficients (K_{ow}), solubilities in water and acid dissociation constants (pK_a) of the compounds are shown in Table 3-1. The pharmaceuticals diclofenac, fenoprofen, gemfibrozil and naproxen occur predominantly as anions at a pH of 7.

Table 3-1. Properties of the non-antibiotic pharmaceutical compounds investigated in this study

Compound	Chemical formula	log K_{ow}[a]	Water solubility at 25°C[b] (mg/L)	pK_a
Carbamazepine	$C_{15}H_{12}N_2O$	(2.25); 2.45 (Dal Pozzo et al., 1989)	17.7	13.9 (Jones et al., 2002)
Diclofenac	$C_{14}H_{11}Cl_2NO_2$	(4.02); 4.51 (Avdeef et al., 1998)	4.5	4.2 (Jones et al., 2002) 3.99 (Avdeef et al., 1998)
Fenoprofen	$C_{15}H_{15}O_3$	3.90	30.1	4.5[c]
Gemfibrozil	$C_{15}H_{22}O_3$	4.77	5.0	4.4[c]
Naproxen	$C_{14}H_{14}O_3$	(3.10); 3.18 (Jones et al., 2002)	145	4.2 (Jones et al., 2002)

[a]first value listed is calculated value from EPI SUITE, KOWWIN v1.68 (US EPA, 2012); [b]calculated value from WSKOW v1.41 (US EPA, 2012), using the log K_{ow} value that does not appear in parentheses; [c]data from www.drugbank.ca, accessed 12 March 2018

3.1.2 Column experiments, sampling and monitoring

The three soil columns are referred to as Column A, Column B and Column C. Column A was run with continuous infiltration and Columns B and C with wetting and drying cycles (typically 3-4 days wetting followed by 3-4 days drying). Soil was filled in the columns as described in Chapter 2.1.2. The column construction is shown in Figure 2-1; sampling ports were located at depths of 12, 27 and 72 cm below the soil surface. Column A was packed with soil on 8 November 2014 and the soil was unpacked on 17 March 2016, for a total of 495 days of continuous infiltration. Columns B and C were packed on 28 November 2014 and the soil was unpacked on 13 March 2016, for a total of 471 experimental days consisting of wetting and drying cycles. The column experiments were conducted at a constant ambient temperature of 21 °C. The column sides were wrapped with aluminum foil to prevent ambient light from entering the system.

The columns consisted of an acrylic glass pipe (length: 1 m, inner diameter: 0.19 m) connected to a lid and base plate, also made out of acrylic glass. Inflow water was stored in glass jugs and pumped into the column as described in Chapter 2.1.2. The hydraulic loading was approximately 7 cm/d. During drying phases, the soil remained (near) saturation below approximately 50 cm depth, as no supplemental suction was applied at the column outlet. At the beginning of each wetting phase and during the initial filling of the continuous column, an air valve in the column lid was left open to allow gas to escape as air left the pore space. The column outflow tubing extended from the bottom of the column upwards to above the top of the soil column (Figure 2-1), thus promoting saturated conditions as the filling process progressed.

Sampling ports consisted of a stainless-steel screen (30 µm pore size) wrapped around perforated 3 mm inner diameter PTFE tubing connected via a glass connector to 6 mm inner diameter PTFE tubing. The sampling ports were passed through the columns through drilled and threaded holes in the column walls, using PTFE tape between the column wall and a stainless-steel threaded connector. At the outer end of the 6 mm PTFE tubing, a two-way valve made of polyvinylidene fluoride was attached, which was left closed except when samples were collected. After opening each valve, sample collection began after ~3 mL of uncollected water emerged from the port.

Table 3-2 shows the experimental stages for each column. The Column A experiment (495 days) lasted slightly longer than the Columns B and C experiments (471 days). The Columns B and C experiments were intended to begin only a few days after Column A, but technical problems with column construction delayed the start. Spiking of the pharmaceuticals began approximately two months after all three experiments were running. The beginning of spiking was done on the same calendar day for all columns due to practical reasons involving the sampling and analysis schedule. Methanol (MeOH) was added to the inflow water for 95 days in Columns A and B and 133 days in in Column C. The slightly longer duration in Column C was to check for any changes in experimental parameters compared to Column B as the system recovered. On one occasion during the pre-spiking period, a sample was collected from the column outflow. The flowpath to the outflow is through an additional ~15 cm of experimental soil and a ~2 cm layer of quartz sand. The outflow connector is stainless steel and the sample flowed through PTFE tubing to a glass collection jug (pre-rinsed with acid and deionized water).

Immediately after the experiments were ended, soil for triplicate extraction samples was collected from an ~2 cm interval at the depth of each sampling port. Column A and B received inflow TWW spiked with only the non-antibiotic compounds, while the TWW for Column C was additionally spiked

Table 3-2. Overview of experimental stages

	Column A	Column B	Column C
Experiment duration	495 days (08/11/2014 – 17/03/2016)	471 days (28/11/2014 – 13/11/2016)	471 days (28/11/2014 – 13/11/2016)
Begin spiking pharmaceuticals	Day 83 (30/01/2015)	Day 63 (30/01/2015)	Day 63 (30/01/2015)
MeOH added to inflow	Day 156 – 251 19% of experiment duration (13/04/2015 – 17/07/2015)	Day 136 – 231 20% of experiment duration (13/04/2015 – 17/07/2015)	Day 136 – 269 28% of experiment duration (13/04/2015 – 24/08/2015)

with the antibiotics doxycycline, sulfadimidine and sulfamethoxazole. The relatively long time period of the experiments was chosen to better capture processes over a timescale appropriate for MAR applications. Further, compared to single compounds in isolation, the presence of a mixture of compounds is expected to result in longer degradation half-lives for many compounds, including naproxen and gemfibrozil (Monteiro and Boxall, 2009; Dodgen and Zheng, 2016). Longer degradation half-lives have also been reported for cambisol soils (Kodešová et al., 2016), which are similar in terms of poor soil development to the rendzina soil used in this study.

During an initial two-to-three-month acclimation period (Table 3-2), unspiked TWW was infiltrated. Greater degradation of several TrOCs following a 2-3 month acclimation period, compared to 1.5-3 weeks, has been reported (Maeng et al., 2011a; Hoppe-Jones et al., 2012). Since the TWW contains background concentrations of most of the spiked compounds, this initial period served as an opportunity for the microbial community to adapt to the conditions, before concentrations of the studied compounds were increased.

After the initial acclimation period, the concentrations of the target pharmaceuticals were spiked in the inflow water through the end of the experiments. Concentrated supplement solutions of the non-antibiotic pharmaceuticals in milli-Q water were prepared; dissolution was aided by stirring and/or placing the solutions in a sonic bath. The supplement solutions were added (up to 3 mL of solution per 1 L of TWW) to each jug of TWW immediately before first use. For 95 days for Columns A and B and 133 Days for Column C (Table 3-2), the pharmaceutical spiking solutions were created by dissolving the needed mass of substance in a mixture of MeOH and milli-Q water (ca. 50%-50%), of which 1 mL was added to 1 L of TWW. This resulted in an additional ca. 150 mg/L of BDOC (some of which could have been degraded in the inflow, with lower concentrations when the water reached the sediment), which

may promote higher microbial populations (Vidal-Gavilan et al., 2014). However, the higher BDOC concentrations could reduce degradation of the pharmaceuticals (Hoppe-Jones et al., 2012), especially in the upper ~30 cm of soil where BDOC may be mostly degraded (Rauch-Williams and Drewes, 2006). The three antibiotics were added to a separate milli-Q water solution, which was added to the inflow water for Column C only. Actual concentrations of the pharmaceuticals in the soil column inflow water may vary from the target concentration of 20 µg/L due to varying concentrations already in the TWW, the possibility of degradation in the inflow water before it was sampled and the possibility of incomplete dissolution and mixing of the spiking solutions.

Sampling ports were located at depths of 12, 27 and 72 cm below the soil surface. The ports were constructed from inert materials, namely PTFE and stainless steel. Samples were collected at the end of selected wetting phases from Columns B and C and concurrently from Column A. Samples were collected in 125 mL or 250 mL glass bottles and refrigerated (5 °C) within minutes. Samples were shipped overnight to the analytical laboratory and analyzed within seven days. A separate sample (10 mL) was collected and pH was measured with a WTW electrode and meter.

ORP was measured in Column B using an in-situ probe, similar to that used by Vorenhout et al. (2004) and manufactured by Paleo Terra (Amsterdam, the Netherlands), and a QIS (Oosterhout, the Netherlands) reference electrode (3.0 Molar KCl saturated with AgCl). The in-situ probe consists of platinum sensors at depths of 2, 7, 12, 42 and 72 cm below the soil surface. The reference electrode was placed in the uppermost part of the soil. The platinum sensors and reference electrode were connected to a Campbell Scientific CR800 data logger. Voltage measurements were made every 30 minutes and adjusted to values of a standard hydrogen electrode by adding 212 mV to each measurement (Franson, 1992) to calculate Eh.

3.1.3 Pressurized liquid extraction

At the conclusion of the experiments, soil from the columns was unpacked. Samples were taken from horizontal zones approximately 2 cm thick at the depth of the sampling ports, wrapped in aluminum foil and plastic bags, and frozen. Later, the samples were thawed, mixed thoroughly and a sub-sample of approximately 100 g was selected, re-frozen, freeze-dried, sieved to 2 mm and smaller (removing inorganic clasts only), and then milled. Triplicate samples were selected from the milled sample. A blank (original soil, no spiking) was also extracted and measured.

Replicate samples from Column A at 12 cm depth as well as Column C at 12 and 72 cm depths (hereafter referred to as A-12, C-12 and C-72, respectively) were spiked with pharmaceuticals (approximately 0.20 µg/g) in order to test the extraction recovery. These samples were chosen to obtain variation in sample depth and infiltration mode. A spiking solution was prepared with the target pharmaceuticals added at concentrations of 0.50 µg/mL in acetone (Carl Roth, ≥99.5%). 15 g of soil sample was weighed in a small glass beaker (pre-rinsed with acetone), 6 mL of spiking solution was pipetted into the beaker, 3 mL of unspiked acetone also pipetted and then the mixture of sample and acetone was stirred thoroughly for several minutes. The samples were then aged for 7-8 days before extraction.

A number of studies using pressurized liquid extraction of pharmaceutical compounds have shown that mixing water (or acidified water) with a polar organic solvent results in good recoveries (Nieto et al., 2010; Runnqvist et al., 2010). Nieto et al. (2007) extracted carbamazepine, diclofenac and naproxen (among 11 compounds total) from sewage sludge samples using different combinations of solvents, comparing water versus acidic water combined with MeOH, with the best recoveries found using a mixture (1:1) of 50 mM H_3PO_4 and MeOH (recoveries of 71% and better for the compounds analyzed in the current study). Kinney et al. (2006) extracted carbamazepine, gemfibrozil and sulfamethoxazole (among other compounds) from soil samples using a 3:7 ratio of water to acetonitrile. Radjenović et al. (2009) extracted 31 pharmaceuticals from sewage sludge samples with a mixture of water and MeOH, in ratios of 1:1, 2:1 and 1:2 as well as pure MeOH. Gemfibrozil was recovered better with an excess of MeOH, while the remaining compounds that are also analyzed in the present study were recovered better with an excess of water. Most compounds were recovered better at a temperature of 100 ^{o}C, except for gemfibrozil which was recovered better at 75 °C (Radjenović et al., 2009). Further, recovery of gemfibrozil has been shown to decrease with temperatures above 60 °C (Barron et al., 2008).

Based on the above studies, the two solvents chosen were 50 mM ortho-phosphoric acid and MeOH. 50% H_3PO_4 (extra pure) and LC-MS-grade MeOH (ROTISOLV, ≥99.95%) were purchased from Carl Roth (Germany). The phosphoric acid was diluted with Milli-Q water to 50 mM. The extraction was performed with a Dionex *Accelerated Solvent Extractor 300* in three stages. First, a solution of 7:3 H_3PO_4:MeOH was used at 60 °C, to target the most polar compounds. Second, a solution of 3:7 H_3PO_4:MeOH was used at 60 °C, to target gemfibrozil. Third, following the second step which should extract gemfibrozil well, the temperature was increased to 100 °C and the same solvent as in the first

step was used, to extract as much as possible of any remaining compounds. Following each cycle, the cell was rinsed with 100% of the cell volume and purged with nitrogen gas for two minutes.

For the pressurized liquid extraction, 4.0 g of milled soil was mixed with quartz sand (pre-rinsed with acetone followed by ultrapure water) to expose as many surfaces of the soil as possible and filled into a stainless steel cell (volume ca. 33 mL) with additional quartz sand at the top and bottom and glass fiber filters at the ends. These conditions, combined with the parameters described above, resulted in extracts of ~140 mL for all three cycles combined.

The extracts were condensed and refrigerated prior to analysis. For the analysis of diclofenac, fenoprofen, gemfibrozil and naproxen, solid phase extraction (SPE) was utilized. With extracts containing a mixture of MeOH and water, the MeOH content of the samples had to be reduced to obtain effective SPE recovery. The mass of soil extracted and the method detection limits allowed for dilution of the samples with water. However, Nieto et al. (2007) diluted samples to a MeOH content of 4-8% before using SPE but found unsatisfactory recoveries (less than 10%) using this method (these authors then used an analysis method that did not require SPE for remaining samples). Therefore, to further reduce the MeOH content of the samples in the current study, the extracts were evaporated within minutes following completion of the extraction: the total extract volume was placed in an open glass beaker (pre-rinsed with acetone) and placed in a 55 ^{o}C water bath, with a fan increasing airflow over the top of the samples. In this manner, the samples were evaporated to volumes of ca. 86 mL for spiked post-experiment soil samples and ca. 75 mL for all other samples. The evaporation was performed under a fume hood with minimal exposure to ambient light. In addition to reducing the total sample volume, MeOH was expected to evaporate preferentially. To confirm this, test samples of MeOH in deionized water were evaporated to different volumes and analyzed on an elemental carbon analyzer (Elementar *LiquiTOC II*), with the results indicating that for the sample volumes stated and the dilutions performed, the MeOH content should be <0.5%.

3.1.4 Analysis of pharmaceutical and dissolved ionic compounds

Analysis of samples for pharmaceutical compounds was done by an external laboratory: IWW Water Centre, Department of Water Quality. The acidic pharmaceuticals diclofenac, fenoprofen, gemfibrozil and naproxen were analyzed using an *Agilent 6890* gas chromatograph with an *Agilent 5973* mass spectrometry detector following SPE at a pH of 2, elution and derivatization (Deutsches Institut für Normung, 2003). Quantification was performed by internal calibration using 4-chlorobenzoic acid as

an internal standard. SPE was performed using Biotage *ENV+ Isolute* 200mg, 3 mL (line 205) cartridges. Prior to SPE, samples from the column experiments were diluted by factors ranging from 20x to 500x. Carbamazepine, doxycycline, sulfadimidine and sulfamethoxazole were analyzed using a Waters *UPLC Acquity H Class, Xevo TQ-S* liquid chromatograph with tandem mass spectrometry detection via direct injection of an aliquot of the sample. Quantification was done by standard addition. Within each sample series blank control as well as quality control samples were measured. The detection limits for undiluted samples were between 0.01 and 0.05 µg/L and the precision between 12 and 15% for the non-antibiotic compounds (Table 3-3). Precision for each compound was determined from analyses of drinking water.

For analysis of the extraction samples, the entire sample volume was used in order to quantify all extracted mass. The condensed extract was poured into a dilution flask, then the sample bottle was rinsed with milli-Q water and this water was also poured into the dilution flask, to transfer all of the condensed extract. Extracts of the spiked post-experiment samples were diluted to a total volume of 1606 mL. Extracts of all other samples were diluted to a total volume of 1011 mL. SPE was performed with 1 L of the diluted sample.

Table 3-3. Detection limits (undiluted samples) and precision

Compound	Detection limit (µg/L)	Relative standard deviation (%)
Carbamazepine	0.01	12
Diclofenac	0.01	15
Fenoprofen	0.02	12
Gemfibrozil	0.02	15
Naproxen	0.01	15
Doxycycline	0.05	49
Sulfadimidine	0.01	12
Sulfamethoxazole	0.01	17

During the column experiments, samples were collected and measured for ions, total iron and total manganese. For measurement of common anions and cations, samples were filtered immediately after collection through 0.45 µm filters and then measured with the Metrohm (Herisau, Switzerland) devices *882 Compact IC plus – Anion* and *882 Compact IC plus – Cation*. Samples were diluted 5x, resulting in detection limits for nitrate of approximately 1 mg/L. Samples for total iron and total manganese were acidified to a pH of ~2 with hydrochloric acid immediately after collection and then measured with a *contrAA 300* atomic absorption spectrometer (AAS) (Analytik Jena, Jena, Germany).

3.1.5 Mass balance

3.1.5.1 Pre-spiking mass

During the initial phase of the experiments, the inflow water was not spiked and was sampled three times. The mass of each pharmaceutical infiltrated during this period was calculated as the mean of the three measurements times the flow volume from the first water infiltrated to when spiking of the pharmaceuticals began. During the pre-spiking period, one sample per column was collected from the column outflow. The results from these outflow samples (one per column) were used to estimate the minimum amount of pre-spiking mass passing the sampling ports.

Some uncertainty in the fate of mass from the pre-spiking period exists because no samples from the ports were analyzed. For compounds for which the pre-spiking mass was greater than 1% of the total mass infiltrated, the attenuated mass and inferred degraded mass were calculated in two scenarios: 1) assuming that all pre-spiking mass passed each port in the water phase and 2) assuming that a minimum amount of pre-spiking mass passed each port in the water phase, with the minimum amount based on the concentration measured in a sample collected from the column outflow (approximately 90 cm below the soil surface). To calculate this minimum mass passing, it is assumed that the concentration at the outflow increased linearly from the beginning of infiltration (concentration of zero) until when spiking began. The sampled concentration was used to calculate the slope of the above line and from that the estimated mass.

3.1.5.2 Numerical integration for mass passing each sampling point

To obtain the mass passing each sampling point in the water phase, results from the column experiments sampling were tabulated relative to cumulative outflow volume and the area under each data series calculated using trapezoidal numerical integration. To propagate measurement variability through the integration and the following data evaluation, the calculation was performed stochastically. For each sampling result, a value was chosen randomly from a normal distribution defined by the concentration and the relative standard deviation in Table 3-3. Between each two sampling results, another concentration value was included in the stochastic calculation. This value was allowed to vary randomly within a defined range, to include uncertainty in concentrations at times when no sampling was performed. Following mass calculation for each sampling point, the mass attenuated from the water phase was calculated for each sampling depth by subtracting the mass passing the respective depth from the mass infiltrated. Accumulated uncertainties were propagated as follows:

$$\delta M_i = (\delta M_{i,a}^2 + \delta M_{i,b}^2)^{1/2} \quad (6)$$

where δM_i is the accumulated uncertainty in mass of compound *i*, $\delta M_{i,a}$ is the uncertainty from the stochastic calculation at sampling point *a* and $\delta M_{i,b}$ is uncertainty at sampling point *b*.

To obtain the water-phase mass of each pharmaceutical compound at the sampling locations, the concentration versus flow volume data series were integrated by trapezoidal numerical integration. In order to propagate measurement variability through this step, stochastic calculation was performed: each sampling result was represented by a random value from a normal distribution based on the concentration result and the relative standard deviation in Table 3-3. Stochastic calculation was performed 10,000 times (10k) and then 20,000 times (20k). The mean and standard deviation from the 10k set of calculations were compared to the 20k calculations, to ensure that the calculated mass and standard deviation were the same to at least one decimal place with milligram units. The following paragraphs describe cases in which assumptions were made to enable calculation and comparison of results.

Samples were collected seven times during the spiking phase of the experiment, but not immediately at the beginning or the very end. Numerical treatment of concentration values at the flow volumes of the beginning of spiking and end of the experiments at each sampling point was as follows:

- The inflow concentration when spiking began is assumed to be the inflow concentration from the first spiking-period sampling, allowing random normally distributed variation based on the relative standard deviation in Table 3-3.
- Concentrations in the soil pore water (i.e. all sampling ports) when spiking began are constrained by the range between the pre-spiking outflow and pre-spiking inflow concentrations, with the range extending one standard deviation below the outflow concentration and one standard deviation above the pre-spiking inflow concentration. Concentrations were varied randomly within this range.
- The inflow concentration at the end of the experiments is constrained by the last two inflow sample concentrations. The concentration was varied randomly within the range of one standard deviation below the lower value to one standard deviation above the higher value.
- Concentration in the soil pore water at the end of the experiments is assumed to be the same as the last sampling result. A random value was chosen from a normal distribution based on the relative standard deviation in Table 3-3.

The inflow and sampling ports A-72 cm, B-12 cm and B-72 cm were each sampled seven times. For the remaining sampling ports, only six concentration results are available. To apply equal numerical treatment, a concentration value was assigned randomly, for each missing data point and each stochastic iteration, within a range defined based on available data as follows:

- Concentrations are not available for the first sampling round for Column C. The concentration values at this time were constrained between the pre-spiking outflow concentration minus one standard deviation and the first available sample results from Column C (second sampling round) plus one standard deviation. Concentrations are not available for the first sampling round for the sampling ports A-27 cm and B-27 cm. The concentration values at the corresponding flow volume were constrained by the results from the sampling ports at 12 cm (in all cases the higher concentration) and 72 cm depth, with the range extending from one standard deviation below the 72 cm result to one standard deviation above the 12 cm result.
- Concentrations are not available for the fourth sampling round for the sampling port A-12 cm. The concentration values at this flow volume were constrained by the inflow concentration and the results from the A-27 cm sampling port, with the range extending from one standard deviation below the lower value (A-27 cm) to one standard deviation above the higher value (inflow).

The data points and values assigned as described above (where concentration results are lacking) are hereafter referred to as core values. To assess the impact of uncertainty in concentrations between the core values, seven interpolated values were calculated for each sampling location and stochastic iteration. First, a random flow volume was chosen between each of seven pairs of successive flow volumes corresponding to the eight data points. Then, a concentration value was chosen randomly from the interval of one standard deviation below the minimum value to one standard deviation above the maximum value. Each pair of concentration value and flow volume was used in the stochastic mass calculation (trapezoidal integration), in addition to the core values, to allow for the possibility that concentrations changed at unknown flow volumes in between the sampling events. No interpolated value was calculated between the last sampling (eighth core value) and the concentration value assigned for the end of the experiments.

3.1.5.3 Calculation of cumulative sorbed mass

After the experiments were ended, soil samples were collected from the same three depths as the sampling ports and extractions were performed to determine sorbed concentrations. Mass sorbed to the soil was calculated from results of the extraction samples. Concentrations measured in the samples

were multiplied by the total volume after dilution to obtain the mass recovered. Then, relative recoveries were calculated:

$$R_i = (m_s - m_{us}) \cdot 100\% / M \quad (7)$$

where R_i is the relative recovery of compound i, m_s is the measured mass from the spiked sample, m_{us} is the measured mass from the unspiked sample and M denotes the spiked mass determined by laboratory balance measurement. All recoveries were determined from the mean of triplicate measurements of spiked samples and of the unspiked post-experiment soil.

The total sorbed concentration for each sample and compound was calculated as follows (units resulting from each step in parentheses): the concentration results of each liquid sample were multiplied by the total volume after dilution (µg/sample), divided by the 4-g mass of solid sample used in the extraction (µg/g) and scaled for extraction efficiency by dividing by R_i (no change to units), the mean recovery per compound of the three spiked post-experiment soil samples. The total sorbed concentration (mean of available replicates) was then assumed to be the sorbed concentration everywhere within a soil cylinder: the uppermost cylinder (12 cm soil sample) begins at the soil surface and extends to 19.5 cm (halfway between the upper two sampling ports), the middle cylinder (27 cm soil sample) extends from there down to 49.5 cm (halfway between the 2nd and 3rd sampling ports) and the lower cylinder (72 cm soil sample) extends from this boundary down to 72 cm (depth of the 3rd sampling port). The mass sorbed in each cylinder is calculated as the product of the following parameters: total sorbed concentration for the respective sample, soil solid density, porosity and respective cylinder volume. The cumulative mass sorbed at each sampling port depth is then calculated by summing the mass sorbed in each block and then multiplying by the portion of the block that is above the sampling port depth. Accumulated error was calculated as the standard deviation of all replicates, propagated through each step of the calculations.

3.1.5.4 Fate of infiltrated pharmaceutical mass

Where differences (outside the margin of propagated errors) exist between attenuated mass and sorbed mass, the remaining mass is inferred to have been degraded (likely in large part aided by microbial activity). Of the total mass of each compound infiltrated, the percent passing (in the water phase), sorbed and degraded is thereby calculated.

3.2 Results and discussion

3.2.1 Column experiments

Total porosity values of 0.41, 0.44 and 0.44 were determined from the volume of TWW pumped in while filling Columns A, B and C, respectively. Based on the measured soil solid density of 2.667 g/cm^3, bulk density values of 1.6 g/cm^3 (Column A) and 1.5 g/cm^3 (Columns B and C) were calculated. Redox conditions in Column B varied in response to wetting and drying cycles, similarly to the conditions observed in Column II (Chapter 2.2.3). Figure 3-1 shows four drying and four wetting periods during the middle of the experiment, after conditions stabilized. Eh rose to values above 400 mV in the upper part of the soil (0-15 cm depth) during drying periods, while gradually dropping to values around -200 mV during wetting phases. At 75 cm depth, Eh remained relatively constant, just below -200 mV. A long wetting period was conducted starting on Day 262, with Eh at all depths stabilizing below -210 mV (the brief rise in values on Day 268 corresponds with collection of samples, which could have introduced oxygen to the system). The long wetting period is analogous to continuous infiltration and it is thus presumed that conditions in Column A were similar to those in Figure 3-1 from ~Day 270 through 280, if not more reducing. Furthermore, it is presumed that Eh in Column C was similar to Column B, since both were operated with wetting and drying cycles. While MeOH was added to the column inflow water (Days 136 – 231), the minimum Eh values did not drop below the displayed minimum values (~-200 mV), but during drying periods, the maximum values were lower than the peaks seen in Figure 3-1.

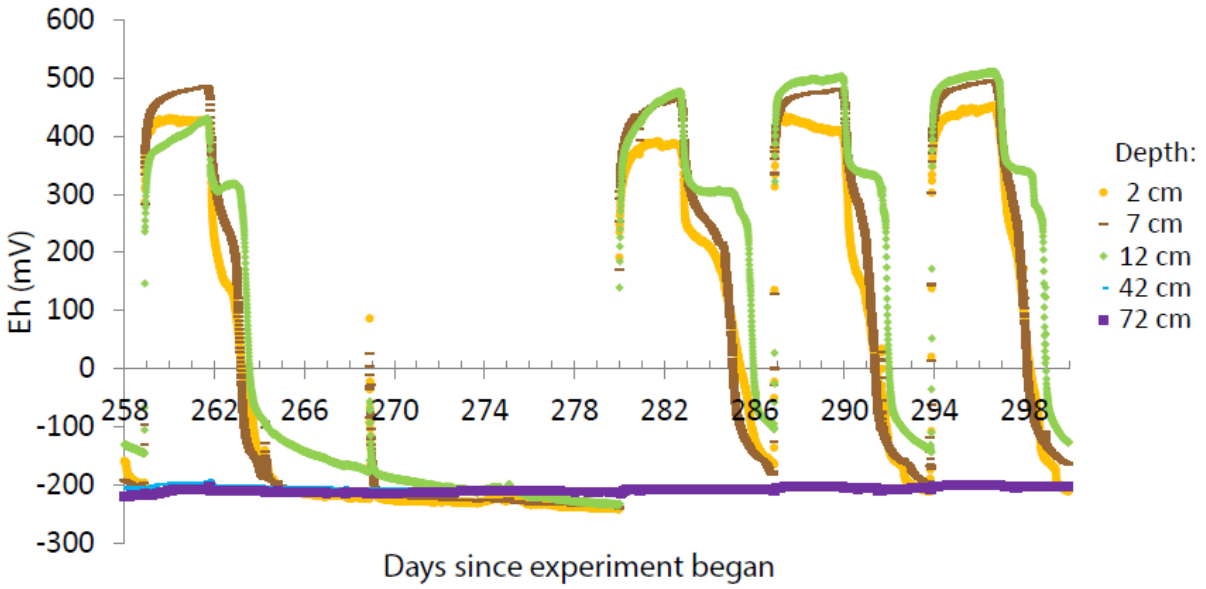

Figure 3-1. Oxidation reduction potential in Column B during the middle of the experiment

While ORP gives an indication of redox conditions, the concentrations of two electron acceptors, oxygen and nitrate, are commonly used to classify conditions as oxic or anoxic (oxygen) and aerobic or anaerobic (nitrate). Figure 2-4 and Figure 2-10 show that in Columns I and II, oxygen concentrations were close to zero during most of the wetting periods. Therefore, anoxic conditions are assumed for the wetting periods.

Table 3-4 shows average nitrate concentrations from the second half of the experiments, after conditions had stabilized. Nitrate concentrations in Column A averaged 0.3 mg/L or less, suggesting that anaerobic conditions prevailed at all three depths sampled. Nitrate concentrations remained above 0.5 mg/L at 12 cm depth in Column B and through 27 cm depth in Column C, indicating that aerobic conditions were more prevalent. The prevalence of aerobic or anaerobic conditions is relevant in particular to the fate of diclofenac, which has been reported to degrade under nitrate reducing conditions (Zwiener and Frimmel, 2003; Rauch-Williams et al., 2010).

Table 3-4. Average nitrate concentrations (mg/L) during the second half of the experiments

Depth	**Column A** ***(n=17)***	**Column B** ***(n=18)***	**Column C** ***(n = 18)***
0 cm	8.1	8.1	8.1
12 cm	0.3	1.5	2.4
27 cm	0.1	0.5	0.7
72 cm	0.3	0.4	0.4

Table 3-5 shows concentrations of the non-antibiotic pharmaceuticals in samples collected during the pre-spiking period. Samples of inflow water were collected on three different days during the pre-spiking period. The entry in the "±" column is the standard deviation of the results of the three samples. Samples of the column outflow were collected on one occasion during the pre-spiking period of the experiments. An anticipated measurement error range could be calculated with the relative standard deviations in Table 3-3, but has not been as it would be small compared to measurement errors in later samples. Total pre-spiking flow volumes (beginning of the experiments until spiking began) were 412 L, 179 L and 176 L for Columns A, B and C, respectively. Flow volume from the time sampling of the outflow was performed (Day 32 for Column A and Day 11 for Columns B and C) until spiking began was 178 L, 134 L and 132 L for Columns A, B and C, respectively. These flow volumes were used for calculation of the mass passing all sampling ports in the water phase.

Table 3-5. Pre-spiking concentrations and mass

	Carbamazepine		Diclofenac		Fenoprofen		Gemfibrozil		Naproxen	
		±		±		±		±		±
Sampled concentration (µg/L)										
inflow (n=3)	1.2	0.2	4.7	1.1	<0.02		0.10	0.11	0.13	0.10
outflow A (n=1)	0.12		1.47		<0.02		<0.02		<0.01	
outflow B (n=1)	0.04		<0.05		<0.10		<0.10		<0.05	
outflow C (n=1)	0.05		<0.05		<0.10		<0.10		<0.05	
Pre-spiking mass infiltrated (mg)										
Column A	0.51	0.06	1.9	0.5	--		0.043	0.047	0.052	0.041
Column B	0.21	0.03	0.78	0.19	--		0.017	0.019	0.021	0.017
Column C	0.21	0.03	0.78	0.18	--		0.017	0.019	0.021	0.017
Minimum pre-spiking mass passing the sampling ports (mg)										
outflow A	0.044		0.53		--		--		--	
outflow B	0.014		--		--		--		--	
outflow C	0.017		--		--		--		--	

-- = not calculated because compound below detection limit in corresponding sample(s)

Figure 3-2 shows pharmaceutical concentrations at the sampling locations along the columns over time (cumulative infiltrated volume) after spiking began. Sample pH ranged from 6.9 to 7.4, suggesting that diclofenac, fenoprofen, gemfibrozil and naproxen were predominantly anionic (Table 3-1). Concentrations in general decreased with depth. In the following discussion of soil pore water concentrations, increasing concentrations at a specific depth over time are expected if sorption (retardation) occurred, while lower than inflow concentrations in the absence of increasing concentrations in time could be a result of degradation.

Concentrations of carbamazepine increased gradually over time at 72 cm depth in all columns, a pattern that could indicate retarded breakthrough of the compound due to sorption. Complete breakthrough was achieved or almost achieved by the end of the experiment at 12 and 27 cm depth. Carbamazepine's affinity to sorb is higher in soils with higher organic carbon content (Chefetz et al., 2008; Walker et al., 2012) and other column studies have shown retarded breakthrough (Chefetz et al., 2008; Banzhaf et al., 2012). Considerable mass passed 72 cm depth over the duration of the experiments, with more mass remaining in the water in Column A (5.4 mg, see Table 3-6) compared to Columns B and C (2.5 and 2.7 mg, respectively).

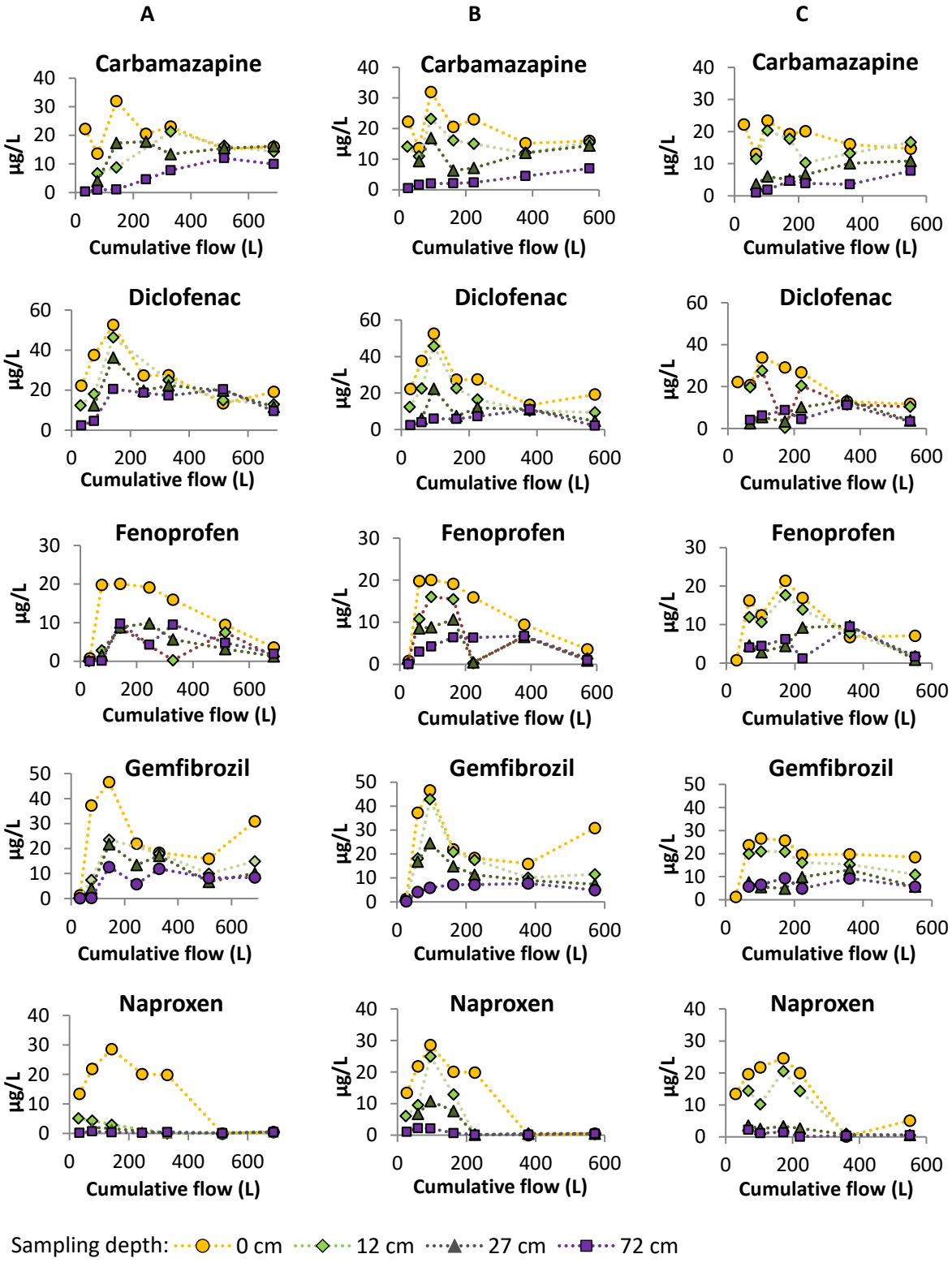

Figure 3-2. Measured concentrations of the non-antibiotic pharmaceuticals

In contrast to carbamazepine, naproxen concentrations do not show increasing trends over time. Concentrations decreased by 13%-50% from the inflow to 12 cm depth (Columns B and C, sampling

events 1 through 4) and further to 38% or less of inflow concentrations in the 27 and 72 cm samples. Concentrations decreased more quickly with depth in Column A (38% or less of inflow concentrations in sampling events 1-5), where the Eh is presumed to have been around -200 mV or lower, compared to Column B (Figure 3-2), where Eh values around 500 mV were reached during drying periods (Figure 3-1). The lack of concentration increases through time (except for sampling events 1-3 in Column B) together with decreases in concentration with depth indicate low retardation but high degradation of naproxen.

The calculated mass passing the depth of each sampling port in the water during the spiking phase of the experiments, based on the sampling results presented in Figure 3-2 and using the trapezoidal numerical integration method, are shown in Table 3-6. The standard deviation of the set of results from the stochastic calculation is shown under "±".

Table 3-6. Mass passing each sampling location in the water phase during the spiking phase of the experiments.

Sampling location	Carbamazepine		Diclofenac		Fenoprofen		Gemfibrozil		Naproxen	
		±		±		±		±		±
	mg	mg	mg	mg	mg	mg	mg	mg	mg	mg
A0	15.0	0.7	19.5	1.2	9.2	0.5	18.3	1.2	9.2	0.9
A12	11.8	0.5	16.1	1.1	3.9	0.6	10.9	0.7	1.9	0.7
A27	10.6	0.4	14.4	0.9	3.4	0.2	8.6	0.7	0.56	0.06
A72	5.4	0.3	11.4	0.7	3.8	0.3	6.1	0.4	0.29	0.02
B0	12.2	0.6	15.3	0.9	7.1	0.5	15.0	1.1	6.5	0.7
B12	9.3	0.4	10.2	0.7	3.8	0.4	9.9	0.7	2.9	0.3
B27	7.1	0.4	6.1	0.5	2.9	0.4	6.9	0.4	1.6	0.2
B72	2.5	0.2	4.0	0.5	2.8	0.3	3.9	0.2	0.40	0.03
C0	10.9	0.4	12.0	0.7	6.5	0.4	12.0	0.5	6.8	0.7
C12	8.6	0.4	8.2	0.7	5.2	0.4	9.3	0.5	4.3	0.5
C27	4.9	0.2	4.5	0.5	3.3	0.4	5.1	0.4	1.0	0.1
C72	2.7	0.2	4.0	0.5	2.9	0.4	4.2	0.3	0.45	0.04

Sampling location is indicated in the format column-depth (e.g. A12 = Column A, 12 cm depth), where a depth of 0 denotes the inflow.

While the concentration trends indicate sorption as the main attenuation mechanism for carbamazepine and degradation as the main mechanism for naproxen, the trends are less clear for diclofenac, fenoprofen and gemfibrozil (Figure 3-2). Concentrations of diclofenac increased over time at 72 cm depth through the sixth sampling event, when soil pore water concentrations reached inflow concentration in all three columns, suggesting sorption, although concentrations decreased in the last

sampling. In Column A, where Eh is presumed to have been around -200 mV, more mass of diclofenac remained in the water at 72 cm depth over the duration of the experiment compared to carbamazepine, while less diclofenac remained in the water at this depth in Columns B and C, where Eh fluctuated in response to wetting and drying cycles (Figure 3-1).

Concentrations of fenoprofen and gemfibrozil in general show decreases with depth in all three columns (Figure 3-2). Some increases in concentration over time are visible, but limited to 3-4 consecutive sampling events (e.g. fenoprofen and gemfibrozil at 72 cm in Column B, at the beginning of the experiment). This may indicate that some sorption occurred, but does not suggest sorption as the main attenuation mechanism. The mass of fenoprofen remaining in the water over the duration of the experiments appears similar at all depths in Columns A and B compared to the inflow concentration, while in Column C, there was clearly mass attenuated between 12 and 27 cm depths. Unlike fenoprofen, attenuation of gemfibrozil is apparent at all depths and all columns, except for 72 cm depth in Column C. This suggests the attenuation of gemfibrozil occurred over at least the range of redox conditions seen in Figure 3-1. The mass remaining in the water at 72 cm depth over the duration of the experiments is similar for both compounds and all columns.

Concentrations of the pharmaceuticals in the inflow water varied from the spiking target of 20 µg/L. Possible reasons include variations in the concentration in the unspiked TWW, degradation of the compounds while in the inflow jugs before the water was infiltrated and incomplete dissolution and mixing of the spiking solutions. Unspiked inflow water was sampled seven times (three times during the pre-spiking period and four times during the spiking period), with results shown in Table 3-7. While the concentrations in these seven samples of unaltered TWW varied somewhat, such variations do not appear to be large enough to explain the variation seen in the inflow samples in Figure 3-2. Fenoprofen is not shown in Table 3-7 because it was not detected in the inflow water samples.

The remaining possibilities for the variation seen in the spiked inflow water are degradation of the spiked compounds and incomplete dissolution and/or mixing in the spiking solution. The compounds were added to a spiking solution in masses planned to result in spiking concentrations of 20 µg/L. However, if the compounds were not completely dissolved and/or mixed within the spiking solution, when the spiking solution was added to the TWW, in some cases too little of a compound would have been delivered to the inflow TWW while in other cases too much would have been added.

Table 3-7. Concentrations of the pharmaceuticals in unspiked TWW

Sample number	Experiment day number (Column A)	Carbamazepine (µg/L)	Diclofenac (µg/L)	Gemfibrozil (µg/L)	Naproxen (µg/L)
1	0	1.2	3.9	0.01*	0.05
2	43	1.4	4.2	0.07	0.09
3	94	1.1	5.9	0.23	0.24
4	109	1.2	5.0	0.23	0.52
5	131	1.4	6.8	0.29	0.43
6	166	1.6	6.1	0.5*	0.25*
7	201	1.5	5.5	0.15*	0.09
	minimum	1.1	3.9	0.01*	0.05
	mean	1.3	5.3	0.2	0.2
	maximum	1.6	6.8	0.29	0.52

* not detected, numerical value is half the detection limit

To further evaluate the reason for and impact of concentration variation in the spiked inflow water on the mass balance, the mass calculated from the sampling concentrations (as listed in Table 3-6, 0 cm depth samples) is compared to the sum of the native TWW mass plus the intended spiked mass as follows:

- A plausible range for the native TWW mass is calculated as the total infiltrated spiked inflow volume times the minimum concentration of each compound as well as the infiltrated volume times the maximum concentration of each compound in Table 3-7.
- The intended spiked mass is calculated as the total infiltrated spiked volume times the planned spiking concentration of 20 µg/L.

The results of this comparison are shown in Figure 3-3. In general, the calculated masses match or are similar to the expected masses for carbamazepine, diclofenac and gemfibrozil. This suggests that the masses calculated from the sampling results are more or less accurate over the duration of the experiments. In the case of fenoprofen and naproxen, less mass was calculated from the sampling results than is to be expected from the spiking method.

As fenoprofen was not detected in the unspiked inflow water samples, it is plausible that it was readily degraded in the TWW. Although naproxen was detected in six of the seven unspiked samples, in general its concentrations were low (Figure 3-6) and it is also plausible that some of the spiked mass was degraded before sampling. As sampling was conducted at the end of the wetting periods, the sampling results reflect the *minimum* amount of mass infiltrated, if some of it may have been degraded while in the inflow jugs.

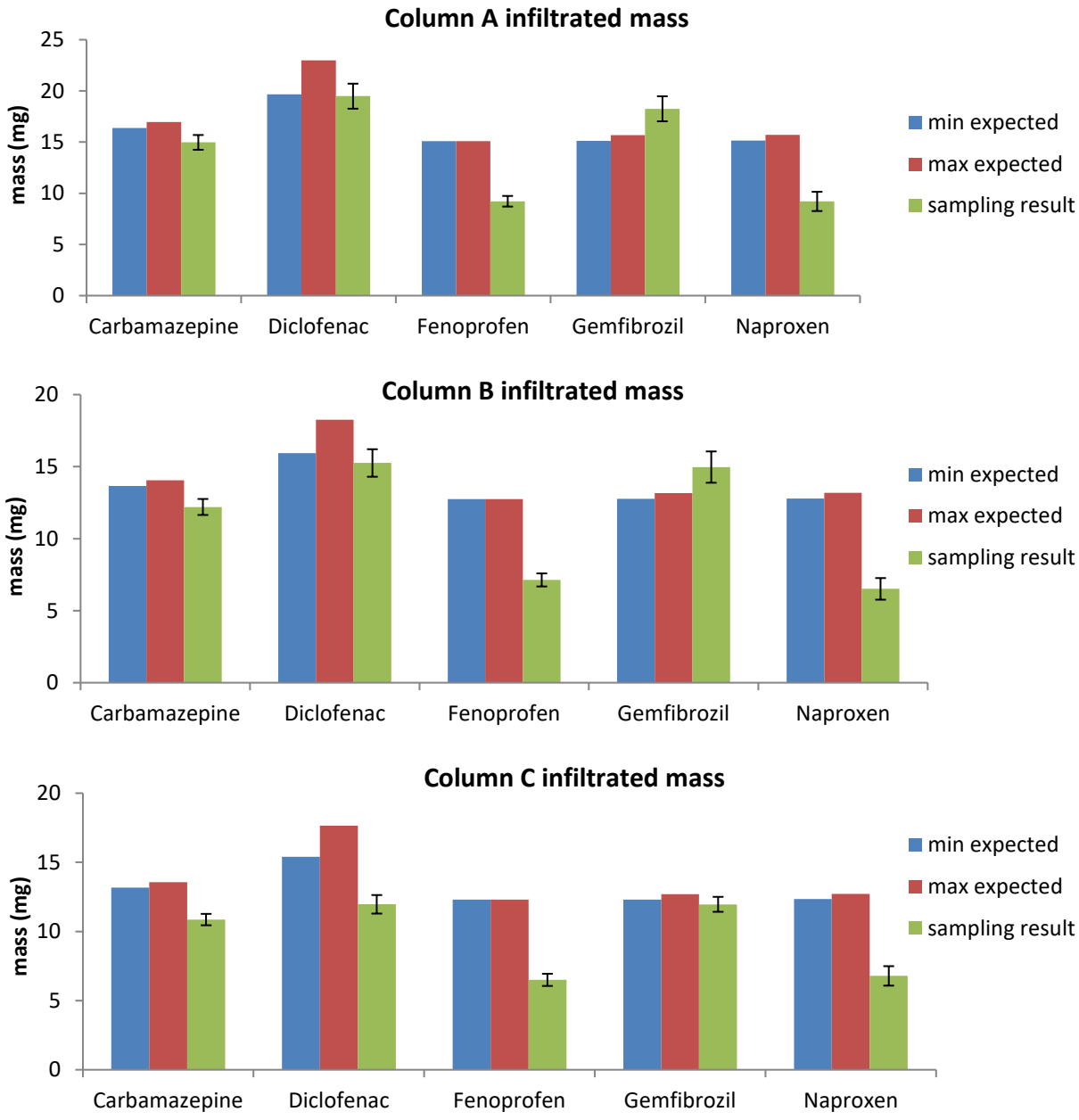

Figure 3-3. Comparison of the expected spiked mass to the spiked mass calculated from the sampling results

The effect of underestimation of the infiltrated mass on the overall mass balance is therefore predictable: if the infiltrated mass is underestimated, the only place any "missing" infiltrated mass could be accounted for is in the mass degraded at depth in the soil. Thus, if it is the case that some mass degraded in the inflow water before infiltration, then the degraded mass totals will underestimate the actual mass degraded.

Comparing the pre-spiking mass in Table 3-5 to the sum of the spiking-period infiltrated mass (Table 3-6, 0 cm values) and Table 3-6 values for each soil column and compound, the pre-spiking mass as a percentage of total mass infiltrated is listed in Table 3-8. For carbamazepine and diclofenac, the pre-spiking mass is greater than 1% of the total mass infiltrated. Therefore, the additional uncertainty of the fate of the pre-spiking mass will be considered for these compounds. For fenoprofen, gemfibrozil and naproxen, the pre-spiking mass is less than 1% of the total mass infiltrated. Uncertainty of the fate of the pre-spiking mass of these three compounds is therefore neglected.

Table 3-8. Pre-spiking mass as a percentage of total mass infiltrated

	Carbamazepine	Diclofenac	Fenoprofen	Gemfibrozil	Naproxen
Column A	3.3%	9.0%	0.04%[1]	0.2%	0.6%
Column B	1.7%	4.9%	0.02%[1]	0.1%	0.3%
Column C	1.9%	6.1%	0.03%[1]	0.1%	0.3%

[1]Fenoprofen was not detected in each of the three inflow samples (measured undiluted, detection limit 0.02 µg/L); value shown is assuming a pre-spiking concentration of half the detection limit.

The concentrations of the antibiotic compounds in Column C versus the cumulative volume of water flow through the soil are shown in Figure 3-4. Concentrations of the antibiotics in Column C decreased with depth, with the concentration at 27 cm depth being 50% or less of the inflow concentration (except for sulfadimidine in the sixth sampling event). In this chapter, the antibiotics are considered only as an infiltration condition. Their fate is discussed in Chapter 4.

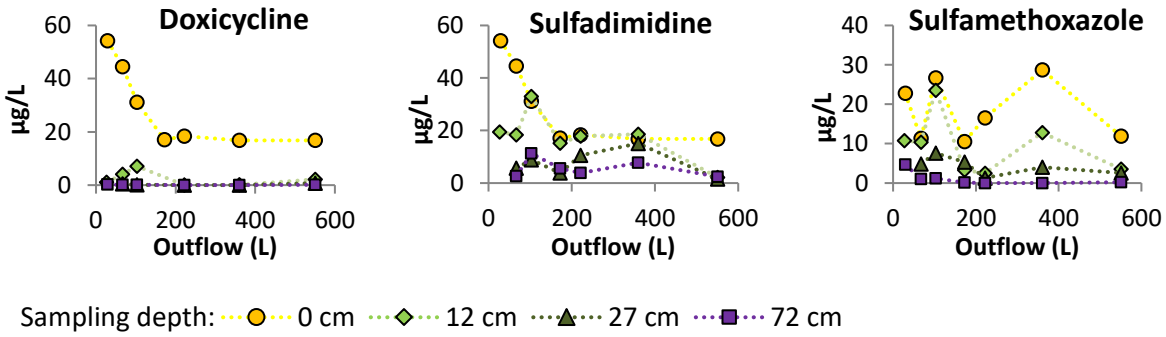

Figure 3-4. Measured concentrations of the antibiotic pharmaceuticals in Column C

3.2.2 Sorbed pharmaceutical mass

Extraction of spiked and unspiked samples of the post-experiment soil showed mean relative recoveries of the spiked mass, calculated from triplicate experimental samples and triplicate spiked

samples using Equation 7 (the measured concentration in the extract of the spiked sample minus the measured concentration in the extract of the unspiked sample, divided by the known spiked mass), ranging from 64% for gemfibrozil to 82% for carbamazepine (Table 3-9). These relative recoveries are typical for extraction of pharmaceuticals and other TrOCs from organic-rich matrices, where recovery depends on e.g. the sample matrix, compound extracted and solvent or combination of solvents used (Runnqvist et al., 2010; Nieto et al., 2010). Results from the extraction of all soil samples are shown in (Figure 3-5), where the expected total sorbed concentration is the mean measured concentration divided by the mean extraction efficiency (Table 3-9), with percentage converted to a decimal. In Appendix B, Table B-1 lists results of all replicates without correction for recovery, while Table B-2 shows the cumulative sorbed masses from the top of the soil to each sampling point.

Of the five compounds, carbamazepine sorbed the most, followed by diclofenac and gemfibrozil. Less sorption of fenoprofen occurred and almost none of naproxen. Carbamazepine has a log K_{ow} of 2.45 and has been reported to sorb in several studies (Matamoros et al., 2008; Banzhaf et al., 2012; Hebig et al., 2017). Although carbamazepine and diclofenac (log K_{ow} 4.51) dissolved in TWW have been shown to have similar affinities to sorb in an organic-rich sediment (Chefetz et al., 2008), in comparing the Column A results, about twice as much sorption of carbamazepine occurred compared to diclofenac at 12 cm and 27 cm depth.

Table 3-9. Relative recovery of spiked mass of the pharmaceutical compounds from three soil samples and the average relative recovery

Sample		**CMP**	**DCF**	**FEN**	**GMB**	**NX**
A 12cm	Mean (%)	80%	47%	62%	56%	65%
	Standard deviation (%)	*39%*	*10%*	*5.1%*	*3.7%*	*5.9%*
C 12cm	Mean (%)	87%	77%	69%	73%	67%
	Standard deviation (%)	*47%*	*3.9%*	*2.1%*	*4.1%*	*2.4%*
C 72cm	Mean (%)	79%	76%	64%	65%	66%
	SD (%)	*27%*	*2.4%*	*1.2%*	*4.2%*	*2.0%*
Mean	Mean (%)	82%	67%	65%	64%	66%
	Standard deviation (%)	22%	3.7%	1.9%	2.3%	2.2%

CMP = carbamazepine, DCF = diclofenac, FEN = fenoprofen, GMB = gemfibrozil, NX = naproxen

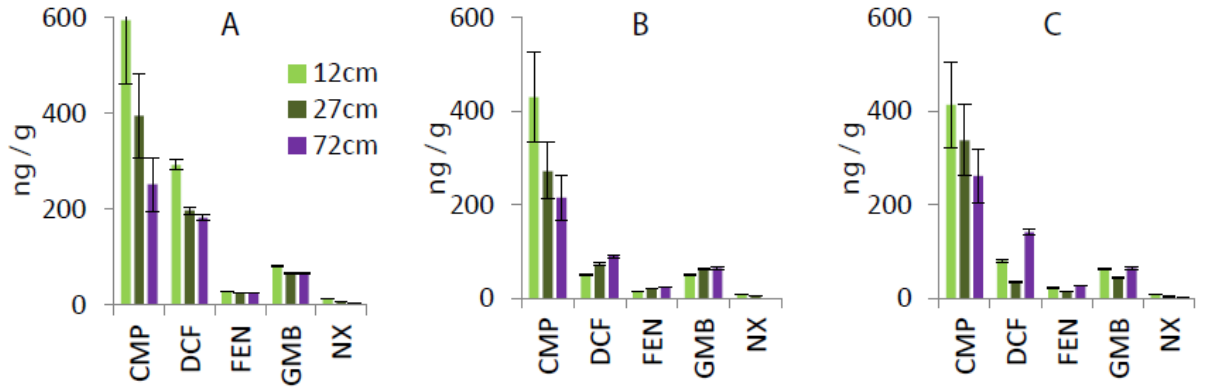

Figure 3-5. Calculated total sorbed mass of the non-antibiotic pharmaceutical compounds extracted from soil samples

The mean and standard deviation of three replicates is shown, except only two replicates were analyzed for Column B samples 12 cm and 72 cm, Column C sample 27 cm and Column C sample 72 cm for CMP. CMP = carbamazepine, DCF = diclofenac, FEN = fenoprofen, GMB = gemfibrozil, NX = naproxen.

The quantity of sorption of the compounds generally followed the order carbamazepine > diclofenac > gemfibrozil > fenoprofen > naproxen. The latter four compounds all have log K_{ow} values above 3, but they are also anionic. Sorption of these anionic pharmaceuticals can be aided by complexation with multivalent cations (Bui and Choi, 2010). Sorbed concentrations of carbamazepine decreased with depth (Figure 3-5), but up to 5.4 mg passed 72 cm depth in the water phase and concentrations were still increasing at the end of the experiments (Figure 3-2). This suggests that sorption did not reach equilibrium and was still occurring when infiltration was ended.

Aside from carbamazepine, the only other instance of a compound showing clear decreases in sorbed concentration with depth is diclofenac in Column A. In the remaining cases, sorbed concentrations do not appear to decrease with depth. However, considerable mass of all compounds (Table 3-6) except naproxen was observed in the water phase at 72 cm depth (Figure 3-2). With fenoprofen and gemfibrozil, concentrations in the water phase were generally lower, limiting sorption. On the other hand, sorbed diclofenac concentrations increased with depth in Columns B and C. With aerobic conditions generally present through 27 cm depth, degradation may have occurred until nitrate was depleted, with lower concentrations then limiting diclofenac sorption in the upper part of the soil.

3.2.3 Fate of pharmaceutical mass

The fate of mass is divided into three categories: passing in the water phase, sorbed to the soil and degraded into some other compound(s). The first two totals were calculated from measured data,

while the third is inferred from the mass balance. Figure 3-6 presents these results, cumulative from the top of the soil down to each sampling depth, in terms of absolute mass and percentage of the infiltrated mass (mass passing 0 cm). The complete mass balance is also shown in Table B-2.

Of the infiltrated carbamazepine mass, 73% or more is calculated to have sorbed by 72 cm depth in all columns. A small amount of degraded mass (up to 14%) is indicated by the mass balance, but is close to or within the cumulative uncertainty range. Several studies have found that carbamazepine is recalcitrant (Clara et al., 2004; Scheytt et al., 2006; Patterson et al., 2011; Durán-Álvarez et al., 2015) but degradation was reported for a soil with high (1%) organic carbon content (Banzhaf et al., 2012). Carbamazepine was the most persistent compound among 19 pharmaceuticals analyzed in a field-based study of soil irrigated with TWW (Kinney et al., 2006). Results of the present study are consistent with findings that carbamazepine is not degraded, as all cases of missing mass lie within the margin of propagated uncertainties.

Although diclofenac has a high log K_{ow} (above 4), it is an anion at neutral pH (pK_a around 4, Table 3-1). The compound exhibited low sorption in organic-poor soils (Lin and Gan, 2011) but has been observed to sorb in soils with 1% or greater organic carbon content (Banzhaf et al., 2012; Chefetz et al., 2008). With the soil with a relatively high organic matter content in the present study, the extraction results clearly indicate sorption of diclofenac (Figures 3-3 and 3-4). Sorption of diclofenac may also be aided by complexation with multivalent cations (Bui and Choi, 2010). The double-valent cations calcium and magnesium were present in the inflow water at concentrations ranging from 7.2 to 53 mg/L and 34 to 175 mg/L, respectively. Concentrations in pore water samples often increased with depth in the soil. Iron and manganese concentrations measured with AAS showed that in general, concentrations of both increased with depth (they were not detected in the inflow water). Iron concentrations reached 4.0 mg/L in Column A, 12 mg/L in Column B and 9.8 mg/L in Column C. Manganese concentrations reached 4.3 mg/L in Column A, 6.7 mg/L in Column B and 6.6 mg/L in Column C. The presence of these and possibly other multivalent cations therefore presents a possible mechanism for aiding diclofenac sorption. More mass of diclofenac sorbed in Column A (32%) compared to Columns B and C (14% and 19%, respectively), in which water phase concentrations decreased more rapidly with depth.

Degradation of diclofenac is inferred for the columns with wetting and drying cycles, in which more than half of the mass is inferred degraded by 27 cm depth. Diclofenac has been shown to degrade under oxic conditions (Gröning et al., 2007) with a range of degradation products (Jewell et al., 2016) and for anoxic conditions with nitrate present (Rauch-Williams et al., 2010; Banzhaf et al., 2012).

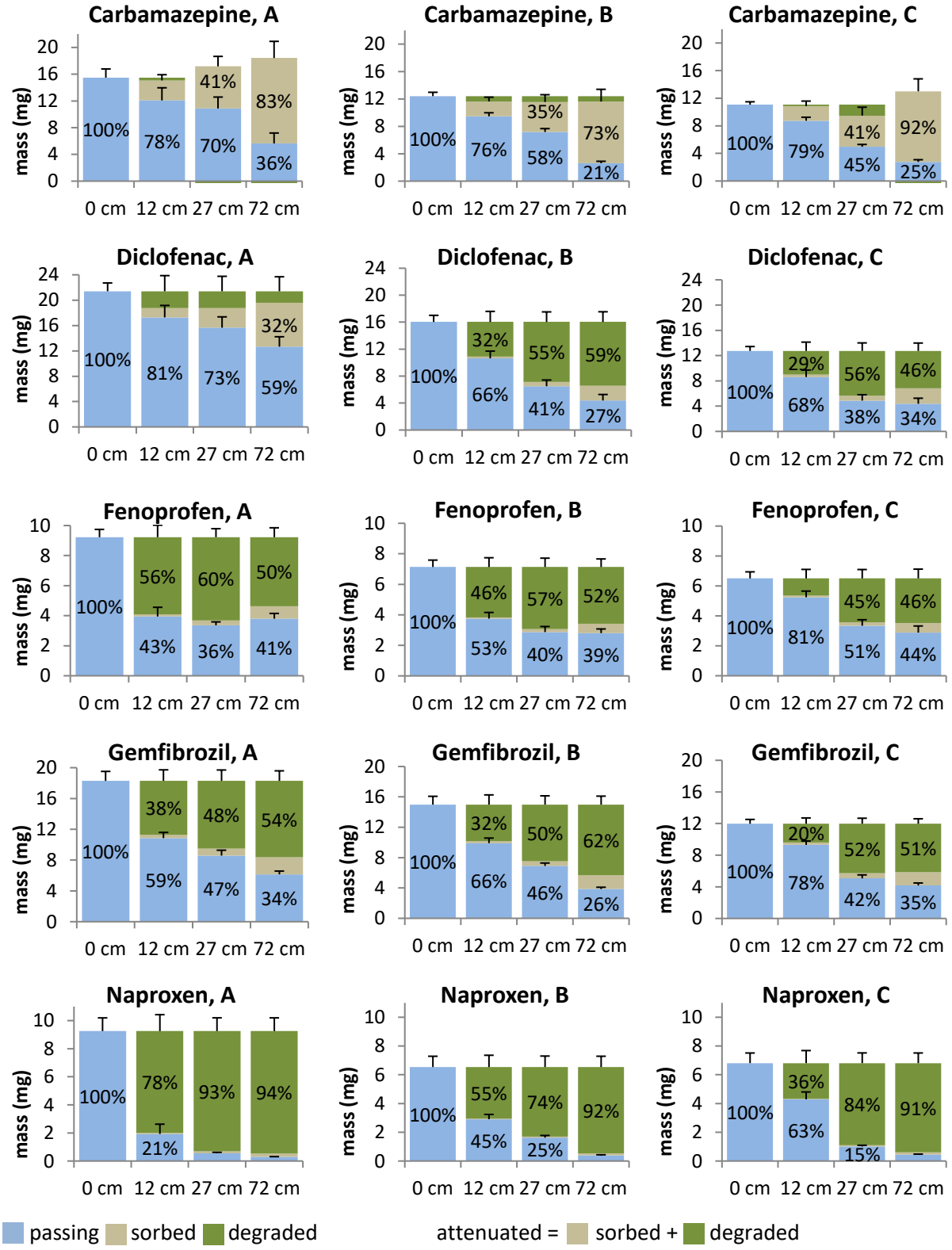

Figure 3-6. Fate of mass infiltrated during the column experiments

Percentages of the total mass infiltrated are cumulative from the soil surface down to the depth indicated. Error bars display only the positive portion of propagated uncertainties. Some error bars (small uncertainties) are omitted. A = Column A, B = Column B, C = Column C.

A few studies have found better degradation of diclofenac under denitrifying conditions than oxic conditions (Zwiener and Frimmel, 2003; Rauch-Williams et al., 2010; Banzhaf et al., 2012). Nitrate concentrations decreased with depth in all three columns (Table 3-4), with the greatest rate of decrease in Column A and the slowest rate of decrease in Column C.

In the presence of high concentrations of humic substances but little labile organic matter, diclofenac may be more readily degraded as microorganisms utilize it as an alternative energy source (Maeng et al., 2012; Alidina et al., 2014). In Column A, where conditions were anoxic and nitrate concentrations were typically low (Table 3-4), a small amount of degradation (9 to 12% of infiltrated mass) is calculated but lies within or close to the cumulative uncertainty range. Overall, these results suggest that wetting and drying cycles are necessary to have enough electron acceptors (oxygen and/or nitrate) present for diclofenac degradation to occur. Hellauer et al. (2017b) reported increased degradation of diclofenac with a sequential aeration step following BDOC-rich infiltration, which is a condition similar to wetting and drying cycles. He et al. (2016) reported only ~15% more degradation of diclofenac with cyclic compared to continuous infiltration, but through a soil with very low (0.02%) organic carbon content. With the more organic-rich soil in the present study, however, degradation appears to be more dependent on infiltration mode: at least 46% of diclofenac was degraded with wetting and drying cycles, compared to little (i.e. within the margin of propagated errors) or no degradation with continuous infiltration.

About half of the infiltrated mass of fenoprofen is inferred to have degraded, probably with all degradation occurring by 12 cm depth in Columns A and B and by 27 cm depth in Column C. In contrast, 91% or more of infiltrated naproxen is inferred degraded in each column. In a study of degradation in wastewater treatment, degradation rates of fenoprofen were similar to (equal or slightly larger than) those of naproxen (Chen et al., 2015). The lack of degradation of fenoprofen at depth in the present study might indicate that it does not degrade anaerobically. A study infiltrating river water under oxic conditions also showed degradation of fenoprofen (Maeng et al., 2011a). Although conditions in Column A were likely more reducing due to continuous infiltration, the low concentrations of nitrate present in Column A may have been enough to support aerobic degradation through 12 cm depth. Around 9-10% of the fenoprofen mass was found to sorb.

Similar to fenoprofen, about half of infiltrated gemfibrozil is inferred to have been degraded, while up to 14% attenuated by sorption. Unlike fenoprofen, inferred degradation of gemfibrozil increases progressively with depth in each column (with the exception of the similar results for 27 and 72 cm

depth in Column C), suggesting that it is degraded both aerobically and anaerobically (Table 3-4). Maeng et al. (2011a) found little degradation of gemfibrozil in column experiments infiltrating river water through silica sand (oxic conditions), while Alidina et al. (2014b) found that degradation increases strongly with a lower BDOC to refractory organic matter ratio. As this ratio likely decreased along the flowpath in the present study without much difference between continuous versus cyclic infiltration, the results here are consistent with the findings of Alidina et al. (2014a,b) that degradation depends on the nature of organic matter present, rather than on specifics of the microbial community.

Nearly all the mass of naproxen that entered the soil columns was degraded by 72 cm depth. Only 2-3% of the infiltrated mass sorbed. Naproxen is known to be degraded in many aqueous environments, including MAR applications (Rauch-Williams et al., 2010; Maeng et al., 2011a). By 12 cm depth, 78% of the infiltrated mass had already been degraded in Column A but 45% or more of the mass was still in the water phase in the other two columns at this depth. Based on these observations, it is possible that degradation of naproxen is more efficient under anaerobic conditions for this water-soil system, which would contrast with another study that found degradation of naproxen only under aerobic conditions (Lin and Gan, 2011).

Antibiotics were added to the inflow water of Column C to evaluate whether their presence in greater concentrations affected degradation of the other pharmaceutical compounds. At 12 cm depth, fenoprofen, gemfibrozil and naproxen show more degradation in Column B (no antibiotics spiked) than Column C (antibiotics spiked). Furthermore, nitrate concentrations at depths of 12 and 27 cm were highest in Column C (Table 3-4). Both of these observations could be due to the elevated concentrations of antibiotics suppressing microbial activity until they were attenuated. The difference is especially large for fenoprofen and naproxen. However, by 72 cm depth, the difference in degraded mass is much less. The spiked antibiotics themselves showed some attenuation by 12 cm and more with greater depth (Figure 3-4). The decrease in concentration of these three antibiotics in the water phase by 72 cm depth coincides with the portion of mass degraded in Column C becoming similar to Column B. Therefore, the antibiotics' presence may slow degradation of other compounds. Liu et al. (2009) incubated soil with sulfamethoxazole and sulfadimidine at concentrations between 1 and 100 mg/kg and found substantially decreased microbial respiration (an indicator of activity) with higher antibiotic concentrations. Another study similarly found changes in microbial communities, including relatively more fungal biomass, when sulfonamide antibiotics (including sulfamethoxazole and sulfadimidine) were added with a carbon source to soil (Gutiérrez et al., 2010). In a study of soil samples containing a single compound compared to samples with a mixture of compounds, Monteiro

and Boxall (2009) found less degradation of naproxen in the samples with a mixture, which included sulfadimidine. The finding here of less degradation of other compounds is thus plausible in view of these previous studies.

4 Fate of antibiotic pharmaceuticals

This chapter presents evaluation of the fate of the antibiotic pharmaceuticals spiked in the inflow water for Column C. The materials and methods follow those described in Chapter 3.1 and are only briefly expanded on here with respect to the antibiotic compounds.

4.1 Materials and methods

4.1.1 Properties of the antibiotic pharmaceutical compounds

The antibiotics doxycycline, sulfamethoxazole and sulfadimidine are soluble in water and have relatively low log K_{ow} values (Table 4-1). Compared to the non-antibiotic pharmaceutical compounds (Chapter 4), these antibiotics are less hydrophobic, as indicated by lower K_{ow} values, and more soluble in water. While the K_{ow} reflects the hydrophobicity of a compound, Wegst-Uhrich et al. (2014) also consider D_{ow}, which compares the sum of ionized and non-ionized species of a solute in octanol to the same sum in water. Software-estimated D_{ow} values for sulfadimidine were lower than estimated K_{ow} values, and both fall in the lower end of literature-reported K_d values (Wegst-Uhrich et al., 2014). The lower D_{ow} compared to K_{ow} values could indicate that ionized species of sulfadimidine play a role in sorption.

Table 4-1. Chemical properties of sulfamethoxazole and sulfadimidine

Compound	Chemical formula	log K_{ow}	Water solubility (mg/L)
Doxycycline	$C_{22}H_{24}N_2O_8$	-0.02 [a]	630 [b]
Sulfamethoxazole	$C_{10}H_{11}N_3O_3S$	0.89 [a]	610 [a]
Sulfadimidine	$C_{12}H_{14}N_4O_2S$	0.76 [a]	1,500 [a]

[a] from US EPA (2012); [b] from https://pubchem.ncbi.nlm.nih.gov/compound/doxycycline, accessed 21 June 2019.

Sulfamethoxazole has been found to degrade in several studies. In a soil column study using bank filtration water (containing TWW mixed with other surface water) and a quartz sand, which limited sorption to <10% of total mass, Baumgarten et al. (2011) found that sulfamethoxazole degraded, with elimination rates dependent on redox conditions, adaptation time and initial concentration. In general, higher degradation was found for aerobic conditions and with lower initial concentration. Degradation increased after an initial adaptation period, which was shorter for higher inflow concentrations of sulfamethoxazole and also shorter with higher BDOC concentrations. At a sulfamethoxazole inflow

concentration of 4 µg/L, Baumgarten et al. (2011) found attenuation of 95% of the inflow mass, due predominantly to degradation. In a study with soil richer in organic matter (1% organic carbon), Banzhaf et al. (2012) found that attenuation of sulfamethoxazole was closely correlated with denitrification (i.e. degradation of nitrate to nitrite, then nitrite to a gaseous product), suggesting that when denitrification occurs, it controls sulfamethoxazole degradation. Sorption did not appear to be a significant attenuation process under the experimental conditions (Banzhaf et al., 2012).

Sulfadimidine has been found to sorb to soils. For loamy soils and similar concentration ranges as with sulfadimidine in the present study (0 – 60 µg/L), K_d values of 0.95 – 22.28 were found by Wegst-Uhrich et al. (2014), with K_d typically decreasing over the pH range 5 to 9. Fan et al. (2011) investigated four soils, two of which have total organic matter contents in the range of 7.5% (close to the value of 6.8% of the soil in the present study). For these soils, K_d values of 1.25 and 1.99 L/kg are reported, with corresponding K_{oc} values of 16.7 and 26.5 (Fan et al., 2011). Sorption of sulfadimidine in several soils has been explained with a linear-regression model that accounts for both anionic and neutral aqueous species (Lertpaitoonpan et al., 2009). Degradation of sulfadimidine in soils has also been reported (Fan et al., 2011).

4.1.2 Extraction

The choice of solvent, or a mixture of solvents, is a decisive factor in the recovery of different compounds, with similar polarity between solvent and target compound leading to better recoveries (Nieto et al., 2010). The extraction method, described in Chapter 3.1.3, was planned primarily to optimize recovery of five non-antibiotic pharmaceuticals. Those compounds have higher log K_{ow} values (2.25 – 4.77) than the antibiotics discussed here. The methanol-phosphoric acid mixtures used in the extraction could lead to lower recoveries of the antibiotics compared to the lower-polarity non-antibiotic compounds (Chapter 3.2.2).

4.2 Results and discussion

4.2.1 Column experiment

Concentrations of the antibiotics doxycycline, sulfadimidine and sulfamethoxazole decreased with depth in the soil (Figure 3-4). At 12 cm depth, doxycycline concentration decreased during all sampling events (concentrations between <0.05 and 7.1 µg/L) relative to the inflow water (0 cm depth). Sulfamethoxazole concentrations decreased in six of the seven sampling events (concentrations 2.5 –

23.5 µg/L), while sulfadimidine concentration decreased in three of the six sampling events (2.16 – 19.4 µg/L) at 12 cm depth relative to the inflow water. At 27 cm depth, the highest measured doxycycline concentration was 0.77 µg/L, and in three cases the compound was not detected. Sulfamethoxazole concentrations were in the range of 1.3 – 7.6 µg/L, while sulfadimidine was detected in the range of 1.53 – 15.1 µg/L. At 72 cm depth, doxycycline was detected at 0.21 and 0.11 µg/L in the first two samples, respectively, and remained below the detection limit thereafter. Sulfamethoxazole was detected at 4.7 µg/L during the first sampling event, then remained at or below 1.2 µg/L thereafter and was not detected (<0.01 µg/L) in the 5th and 6th samples. Sulfadimidine was detected in all samples, at concentrations ranging from 2.6 to 11.3 µg/L.

Measurements of ORP in Column II (Figure 2-9) and Column B (Figure 3-1) showed that Eh reached levels above +400 mV during drying periods, while it sunk to about -200 mV during wetting periods. In Column I, oxygen was consumed within eight hours at 2 – 12 cm depth at the beginning of a wetting period (Figure 2-4) and remained at zero through the wetting periods (observed in Column II, Figure 2-10). It is therefore presumed that anoxic conditions were generally present and Eh sunk gradually over time during the wetting periods.

Degradation of TrOCs is often dependent on redox conditions and organic matter composition and content (Maeng et al., 2011b). A study of bank filtration showed that sulfamethoxazole attenuated better under anoxic conditions (Heberer et al., 2008). However, many redox-dependent pathways and degradation products exist for sulfamethoxazole (Rodriguez-Escales and Sanchez-Vila, 2016). As a wide range of redox conditions existed during the wetting and drying cycles, degradation is likely accountable for at least some of the observed decreases in sulfamethoxazole concentration.

Sulfadimidine is a polar compound (low log K_{ow}; Table 4-1.). Fan et al. (2011) found that sulfadimidine and an even more polar degradation product were removed from the water phase by sorption that was strongly correlated with soil organic matter content. Sorption of sulfadimidine is generally inversely correlated with pH, and in particular may increase below 7.4 due to hydrophobic partitioning of a non-ionized species (Lertpaitoonpan et al., 2009). Both sorption and degradation are therefore possible mechanisms for decreases in sulfadimidine concentrations.

4.2.2 Sorbed mass and overall fate of antibiotic mass

The extraction resulted in mean recoveries of 43% for sulfamethoxazole and 19% for sulfadimidine (Table 4-2), while doxycycline was not detected in the extracts from any samples (including the spiked samples) of the post-experiment soil. These recoveries are considerably lower than the recoveries between 64% and 82% for the non-antibiotic pharmaceuticals. In a study investigating sewage sludge samples, Lillenberg et al. (2009) used a 1:1 (based on volume) acidic aqueous solution of (36 mM H_3PO_4, 10 mM citric acid monohydrate):acetonitrile, which is similar to the extraction solutions in this study (50 mM H_3PO_4:MeOH in 2:1 and 1:2 volume ratios), in that both are mixtures of an acidic aqueous solution and a polar organic solvent. Mean recoveries from the sewage sludge samples were 95% for doxycycline (10% with a second type of SPE cartridge), 90 - 96% for sulfamethoxazole and 43 - 53% for sulfadimidine (Lillenberg et al., 2009). The comparably lower recoveries of these compounds in the present study could have been affected by neutralization of the acid by carbonate minerals in the soil. It is noteworthy that a better recovery was found for sulfamethoxazole compared to sulfadimidine in the extraction in both the present study and in Lillenberg et al. (2009).

Table 4-2. Recoveries of the antibiotics sulfadimidine (SDM) and sulfamethoxazole (SMX) from post-experiment soil, reported as mean and standard deviation of duplicate samples (triplicate samples at 12 cm depth) in percent.

Sample	SDM	SMX
12 cm	22 ± 16	45 ± 15
72 cm	17 ± 10	41 ± 7
Mean	19 ± 8	43 ± 14

As doxycycline was not recovered from the post-experiment soil, even from the spiked samples, the fate of the compound cannot be determined from the available data. Doxycyline may exist in colloidal form in both water and when sorbed to sediment (Zaranyika et al., 2015). A multi-step sample preparation method and HPLC analysis at a pH of 3 was used by Zaranyika et al. (2015) to measure doxycycline. Therefore, to determine the fate of doxycycline in a wet soil environment, a sample treatment and analytical method specifically designed to measure doxycycline may be needed. In the present study, doxycycline was measured using the method described in Chapter 3.1.4, for simultaneous determination of several compounds.

The extraction results do provide information useful for inferring the fate of sulfadimidine and sulfamethoxazole. From the post-experiment soil samples, only 8 ng/g of sulfamethoxazole was

recovered in the sample from 12 cm depth, while sulfamethoxazole was not detected in the samples from 27 and 72 cm depths. Recovered mass of sulfadimidine was 61, 45 and 61 ng/g in the samples, respectively. It is noteworthy that distinctly more mass of sulfadimidine was recovered compared to sulfamethoxazole, despite the higher recovery found for sulfamethoxazole (Table 4-2). This suggests that the results provide, at the least, an indication that sorption was an important process for sulfadimidine, despite the mean recovery of only 19%. The interpretation of sorption being an important processes for sulfadimidine is consistent with the findings of previous studies (Fan et al., 2011; Wegst-Uhrich et al., 2014). The apparent total sorbed mass, calculated as the recovered mass divided by the mean extraction recovery rate, is shown in Figure 4-1. Just over 300 ng/g of sulfadimidine is projected for the 12 cm and 72 cm samples, while 240 ng/g is calculated for the 27 cm sample. Considering deviations of the replicate samples, the results suggest that a range of about 240 – 300 ng/g sorbed mass is plausible. This would be consistent with a linear sorption mechanism, which has been demonstrated for sulfadimidine by Lertpaitoonpan et al. (2009).

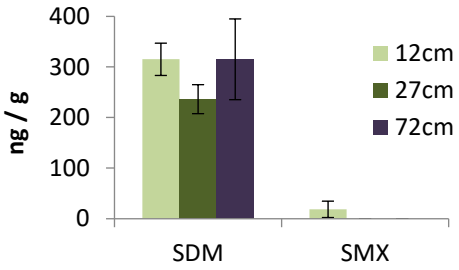

Figure 4-1. Apparent total sorbed mass in the post-experiment soil samples

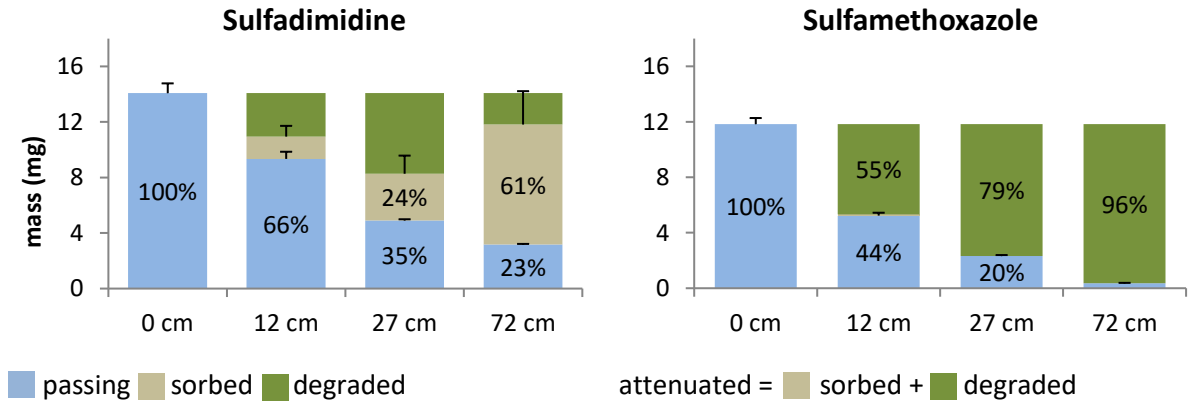

Figure 4-2. Fate of mass of sulfadimidine and sulfamethoxazole infiltrated during the column experiment

Percentages of the total mass infiltrated are cumulative from the soil surface down to the depth indicated. Error bars display only the positive portion of propagated uncertainties.

The mass balances for sulfadimidine and sulfamethoxazole are shown in Figure 4-2, which further illustrates that sorption was an important attenuation mechanism for sulfadimidine. Although sorption of sulfadimidine has been found in previous studies (Fan et al., 2011; Wegst-Uhrich et al., 2014), it has also been found to degrade in wastewater treatment (Pérez et al., 2005) and in soils with similar organic matter content to the present study (Fan et al., 2011). The mass balance for sulfadimidine also suggests that some mass of the compound degraded. If this is the case, sorption of sulfadimidine may have delayed or prevented even more degradation under these infiltration conditions.

Meanwhile, the mass balance for sulfamethoxazole shows increasing attenuation of the compound at each sampling point, with nearly all of the infiltrated mass attenuated by 72 cm depth. As sulfamethoxazole was not detected in the extracts from the deeper soil samples (27 and 72 cm depths), the (most important) attenuation mechanism is inferred to be degradation. Approximately 96% of sulfamethoxazole mass was inferred to have been degraded, which is similar to the finding of Baumgarten et al. (2011) for an inflow concentration of 4 µg/L that 95% of sulfamethoxazole was degraded. Nitrate was present in the inflow water and generally attenuated between 0 cm and 27 cm depth (Table 3-4). It is therefore plausible that at least some, if not most, of the degradation of sulfamethoxazole was linked to the process of denitrification, as was found by Banzhaf et al. (2012).

Degradation is presumed to have been aided by microbes. For microbial degradation to occur in a new or changed environment, the time needed for the microbial community to adapt to the conditions and then obtain peak efficiencies degrading compounds (adaptation time) is an important parameter. An adaptation time of about nine months was found for degradation of sulfamethoxazole in a study of bank filtration (Bertelkamp et al., 2016), compared to 3-12 months found by Baumgarten et al. (2011). In the latter study, it was found that attenuation was high in the presence of higher BDOC concentrations, but that at lower BDOC concentrations, degradation rates were also high after a longer adaptation time. In the present study, adaptation time might have been relatively short, given the acetate (a form of BDOC) concentrations (Figure 2-11) measured. However, the role of the soil organic matter and BDOC on microbial adaptation and degradation rates, both initially and when BDOC concentrations decrease after the initial leaching, is a topic that warrants further research.

5 Environmental implications and conclusions

5.1 Nitrogen cycling and redox conditions

In two separate column experiments, ammonium was produced during infiltration of TWW through a soil containing >2% organic carbon and >0.2% organic nitrogen. Based on mass balance and isotopic data, soil nitrogen appears to be an important source of the ammonium, if not the main source. While soils with considerable organic matter have certain advantages for MAR, implementers of MAR schemes should be aware of the potential to form ammonium with concentrations exceeding the EU water framework directive limit in the infiltrating water. As ammonium concentrations first increased to an initial peak and then decreased, MAR applications should be planned with the view that ammonium might be generated during an initial phase of infiltration.

Results of this study of nitrogen compounds suggest that nitrification occurs during drying phases and a combination of denitrification and DNRA during wetting phases. While denitrification of at least some of the nitrate in the inflow TWW appears to have occurred, several indications of DNRA were also observed: high acetate-to-nitrate ratios early in the experiments and in the 15-30 cm depth range in the soil, Eh values below zero and often below -200 during wetting periods, high $\delta^{15}N$ of nitrate in the inflow water combined with $\delta^{15}N$ of ammonium greater than that of the soil and that increased early in the experiment, and isotopic enrichment factors that are lower than enrichment factors typically found for denitrification occurring alone. The high ^{18}O:^{15}N ratios may also be a result of DNRA, although this warrants further research. For implementation of MAR schemes, the occurrence of DNRA is important in that it lowers the nitrogen elimination rate of the system. As opposed to gaseous products of denitrification, nitrate-nitrogen reduced to ammonium will remain in the system, either as ammonium or later nitrified back to nitrate. This cycling of ionic nitrogen forms presents the potential to deliver a plume of ammonium and/or nitrate to the aquifer.

The sorption batch experiments demonstrated that ammonium sorbs to the same soil during infiltration with TWW, which implies that ammonium was retarded during transport through the soil. Results of the column experiments suggest that, under wetting and drying cycles, some ionic nitrogen mass may be eliminated by nitrification during drying periods and denitrification during the subsequent wetting period. Further research could focus on the partitioning of nitrate reduction between denitrification (eliminating nitrogen mass from the system) and DNRA (conservation of nitrogen mass in the system). The length of wetting and drying cycles, particularly in the beginning of infiltration when concentrations of acetate and other labile organic carbon compounds can be

expected to be high, may be a tool to influence partitioning between denitrification and DNRA and thereby how much DIN mass remains in the soil-groundwater system.

5.2 Fate of non-antibiotic pharmaceuticals

The non-antibiotic pharmaceuticals were all found to attenuate under each of the three investigated infiltration conditions. Sorption was found to account for mass attenuation in the order carbamazepine > diclofenac > gemfibrozil > fenoprofen > naproxen. To the extent pharmaceutical mass sorbs to the soil in field MAR applications, it poses a risk, as it could later desorb and be transported toward the aquifer. If desorbed, some compounds (e.g. gemfibrozil) could be expected to be degraded under anaerobic conditions (if present) at greater depth, while others might not be degraded at all (e.g. carbamazepine) or only degraded if aerobic conditions are present (e.g. diclofenac). For planning of MAR sites, sorption of compounds should be considered together with the potential for desorbed compounds to later degrade, in the context of the (expected) unsaturated zone and aquifer redox conditions.

A substantial amount of mass degradation is inferred for all compounds except for carbamazepine. If degradation of contaminant mass to small, non-toxic molecules is complete (e.g. to CO_2 and H_2O) or the remaining degradation products are non-toxic, this mass attenuation mechanism should improve water quality during MAR, potentially in a sustainable manner. The difference in inferred degradation of diclofenac between the columns shows that for this compound, wetting and drying cycles are useful in promoting degradation, likely due to oxidizing conditions during drying periods slowing nitrate attenuation in comparison to continuous infiltration. Wetting and drying cycles may therefore be beneficial to the fate of diclofenac and possibly other organic micropollutants, while having only slight to no negative effect on compounds that degrade anaerobically (gemfibrozil and naproxen). With degradation observed over a wide range of redox conditions, selecting a soil with substantial organic matter content appears to be a viable approach to attenuating a range of pharmaceutical compounds. In Column C, less degraded mass was found with elevated antibiotic concentrations. The concentrations of these compounds should be monitored and the treatment effectiveness of the uppermost part of the soil should be evaluated with antibiotic concentrations in mind, in terms of these contaminants themselves and their effects on the attenuation of other compounds.

5.3 Fate of antibiotic pharmaceuticals

The two sulfonamide antibiotics evaluated show differing environmental fates. In the case of sulfadimidine, sorption is an important process. Sorption can be aided by high soil organic carbon content (Lertpaitoonpan et al., 2009). Sorption and degradation of the antibiotic sulfadimidine are both processes that occur during infiltration through soils with similar organic matter content (Fan et al., 2011). While sorption could have prevented more degradation of sulfadimidine over the time frame of the column experiment, if coupled with desorption when concentrations are lower, the net effect would be retardation during transport. A higher retention time in the soil could have the effect of increasing degradation in the long term.

Meanwhile, degradation was an important process affecting the fate of sulfamethoxazole. Results of this study suggest that the redox conditions promoted degradation of substantial mass of the compound under the infiltration conditions of a relatively organic-rich soil and TWW. If nitrate is present in the MAR system and conditions for denitrification exist (i.e. presence of sufficient BDOC), degradation of sulfamethoxazole may be promoted (Banzhaf et al., 2012). As nitrate is also a chemical of concern in groundwater in general (Almasri, 2007) as well as in MAR systems (Miller et al., 2006; Barry et al., 2017; Schmidt et al., 2012), potential exists to optimize degradation of these two pollutants simultaneously in the presence of sufficient BDOC.

To better attenuate higher mass loads of sulfamethoxazole, a soil capable of leaching BDOC might be beneficial toward degrading greater mass, at least during the initial stages of infiltration. In the study of nitrogen cycling (Chapter 2), it was observed that acetate (a form of BDOC) concentrations were highest in the beginning of infiltration (Figure 2-11), then decreased over time. Leaching of BDOC from soil organic matter could, then, be a process that is well-timed to help reduce mass of sulfamethoxazole reaching the aquifer during the early stages of MAR, when adaptation times might otherwise be longer (as noted in Section 4.2.2, this topic warrants further research). Therefore, potential exists to minimize the mass load of sulfamethoxazole reaching an aquifer during infiltration of TWW, dependent on factors such as BDOC availability and redox conditions, and their effects on microbial adaptation time.

5.4 Conclusions

Concentrations of all of the pharmaceutical compounds analyzed in this study, including the antibiotics, decreased during infiltration. Sorption was the main attenuation mechanism for

carbamazepine and an important mechanism for sulfadimidine, while degradation played a role in the attenuation of diclofenac, fenoprofen, gemfibrozil, naproxen and sulfamethoxazole. In the cases of diclofenac and sulfamethoxazole, degradation appears to be linked to the process of denitrification.

An important question in MAR is how to manage infiltration in order to optimize degradation of pollutants. Wetting and drying cycles appear to have resulted in more degradation of diclofenac than continuous infiltration. Furthermore, while denitrification appears to have occurred during continuous infiltration, only wetting and drying cycles offer the opportunity to eliminate DIN mass, through nitrification of ammonium during drying, then denitrification to gaseous nitrogen during the following wetting. Ammonium appears to have formed in large part from nitrogen contained in the soil. Potential to attenuate ammonium depends on sorption and desorption, which increase retention time in the unsaturated zone. With this soil, however, lower infiltration rates and/or shorter wetting periods would be needed to prevent a plume of ammonium from leaching to the aquifer, where it would move slowly due to retardation or be converted to nitrate if oxidizing conditions are present.

To manage this issue in a field MAR application, low volumes of TWW should be infiltrated initially in short infiltration phases (e.g. 1-2 days), and then the recharge volumes and infiltration time could be gradually increased after ammonium concentrations during infiltration decline. This could take years with the experimental soil used in this study, but planning of MAR applications with a longer operational time frame (e.g. decades) in mind may help to further optimize the systems and determine what initial soil organic matter content best balances all water quality considerations.

Overall, this soil with 2.57 % organic carbon resulted in a wide range of redox conditions with wetting and drying cycles, with over half of the infiltrated pharmaceutical mass removed from the water in all cases. The study of nitrogen compounds illustrates that pollutants that can be generated from the soil should be considered and managed. MAR operated with wetting and drying cycles can help degrade some pollutants and offer long-term water quality benefits.

References

Agbenin, J.O., Modisaemang, L., 2015. Calcium-ammonium selectivity of two benchmark soils from Botswana as assessed by competing semi-empirical ion exchange equations. Commun. Soil Sci. Plant Anal. 46, 2757–2773. https://doi.org/10.1080/00103624.2015.1102929

Aggarwal, P.K., Fuller, M.E., Gurgas, M.M., Manning, J.F., Dillon, M.A., 1997. Use of stable oxygen and carbon isotope analyses for monitoring the pathways and rates of intrinsic and enhanced in situ biodegradation. Environ. Sci. Technol. 31, 590–596. https://doi.org/10.1021/es960562b

Ahmed, M.B., Zhou, J.L., Ngo, H.H., Guo, W., 2015. Adsorptive removal of antibiotics from water and wastewater: Progress and challenges. Sci. Total Environ. 532, 112–126. https://doi.org/10.1016/j.scitotenv.2015.05.130

Alidina, M., Li, D., Drewes, J.E., 2014a. Investigating the role for adaptation of the microbial community to transform trace organic chemicals during managed aquifer recharge. Water Res. 56, 172–180. https://doi.org/10.1016/j.watres.2014.02.046

Alidina, M., Li, D., Ouf, M., Drewes, J.E., 2014b. Role of primary substrate composition and concentration on attenuation of trace organic chemicals in managed aquifer recharge systems. J. Environ. Manage. 144, 58–66. https://doi.org/10.1016/j.jenvman.2014.04.032

Almasri, M.N., 2007. Nitrate contamination of groundwater: A conceptual management framework. Environ. Impact Assessment Review 27, 220-242. https://doi.org/10.1016/j.eiar.2006.11.002

Amy, G., Drewes, J., 2007. Soil aquifer treatment (SAT) as a natural and sustainable wastewater reclamation/reuse technology: Fate of wastewater effluent organic matter (EfoM) and trace organic compounds. Environ. Monit. Assess. 129, 19–26. https://doi.org/10.1007/s10661-006-9421-4

Appelo, C.A.J., Postma, D., 2005. Geochemistry, groundwater and pollution, 2nd ed. Taylor & Francis, Boca Raton, Florida, USA.

Avdeef, A., Box, K.J., Comer, J.E.A., Hibbert, C., Tam, K.Y., 1998. Determination of Liposomal Membrane-Water Partition Coefficients of Ionizable Drugs. Pharm. Res. 15, 209–215.

Banzhaf, S., Nödler, K., Licha, T., Krein, A., Scheytt, T., 2012. Redox-sensitivity and mobility of selected pharmaceutical compounds in a low flow column experiment. Sci. Total Environ. 438, 113–121. https://doi.org/10.1016/j.scitotenv.2012.08.041

Barron, L., Tobin, J., Paull, B., 2008. Multi-residue determination of pharmaceuticals in sludge and

sludge enriched soils using pressurized liquid extraction, solid phase extraction and liquid chromatography with tandem mass spectrometry. J. Environ. Monit. 10, 353–361. https://doi.org/10.1039/b717453e

Barry, K.E., Vanderzalm, J.L., Miotlinski, K., Dillon, P.J., 2017. Assessing the impact of recycled water quality and clogging on infiltration rates at a pioneering Soil Aquifer Treatment (SAT) site in Alice Springs, Northern Territory (NT), Australia. Water (Switzerland) 9. https://doi.org/10.3390/w9030179

Batt, A.L., Snow, D.D., Aga, D.S., 2006. Occurrence of sulfonamide antimicrobials in private water wells in Washington County, Idaho, USA. Chemosphere 64, 1963–1971. https://doi.org/10.1016/j.chemosphere.2006.01.029

Baumgarten, B., Jährig, J., Reemtsma, T., Jekel, M., 2011. Long term laboratory column experiments to simulate bank filtration: Factors controlling removal of sulfamethoxazole. Water Res. 45, 211–220. https://doi.org/10.1016/j.watres.2010.08.034

Bekele, E., Toze, S., Patterson, B., Higginson, S., 2011. Managed aquifer recharge of treated wastewater: Water quality changes resulting from infiltration through the vadose zone. Water Res. 45, 5764–5772. https://doi.org/10.1016/j.watres.2011.08.058

Bertelkamp, C., Verliefde, A.R.D., Schoutteten, K., Vanhaecke, L., Vanden Bussche, J., Singhal, N., van der Hoek, J.P., 2016. The effect of redox conditions and adaptation time on organic micropollutant removal during river bank filtration: A laboratory-scale column study. Sci. Total Environ. 544, 309–318. https://doi.org/10.1016/j.scitotenv.2015.11.035

Böttcher, J., Strebel, O., Voerkelius, S., Schmidt, H.L., 1990. Using isotope fractionation of nitrate-nitrogen and nitrate-oxygen for evaluation of microbial denitrification in a sandy aquifer. J. Hydrol. 114, 413–424. https://doi.org/10.1016/0022-1694(90)90068-9

Bouwer, H., 2002. Artificial recharge of groundwater: Hydrogeology and engineering. Hydrogeol. J. 10, 121–142. https://doi.org/10.1007/s10040-001-0182-4

Boxall, A.B.A., Kolpin, D.W., Halling-Sørensen, B., Tolls, J., 2003. Are veterinary medicines causing environmental risks? BMJ 37, 286A-294A. https://doi.org/10.1136/bmj.d7929

Bui, T.X., Choi, H., 2010. Influence of ionic strength, anions, cations, and natural organic matter on the adsorption of pharmaceuticals to silica. Chemosphere 80, 681–686. https://doi.org/10.1016/j.chemosphere.2010.05.046

Buresh, R.J., Patrick, W.H.J., 1978. Nitrate Reduction to Ammonium in Anaerobic Soil. Soil Sci. Soc. Am.

J. 42, 913–918.

Burke, V., Treumann, S., Duennbier, U., Greskowiak, J., Massmann, G., 2013. Sorption behavior of 20 wastewater originated micropollutants in groundwater - Column experiments with pharmaceutical residues and industrial agents. J. Contam. Hydrol. 154, 29–41. https://doi.org/10.1016/j.jconhyd.2013.08.001

Caschetto, M., Colombani, N., Mastrocicco, M., Petitta, M., Aravena, R., 2017. Nitrogen and sulphur cycling in the saline coastal aquifer of Ferrara, Italy. A multi-isotope approach. Appl. Geochemistry 76, 88–98. https://doi.org/10.1016/j.apgeochem.2016.11.014

Casciotti, K.L., Sigman, D.M., Hastings, M.G., Böhlke, J.K., Hilkert, A., 2002. Measurement of the oxygen isotopic composition of nitrate in seawater and freshwater using the denitrifier method. Anal. Chem. 74, 4905–4912. https://doi.org/10.1021/ac020113w

Chefetz, B., Mualem, T., Ben-Ari, J., 2008. Sorption and mobility of pharmaceutical compounds in soil irrigated with reclaimed wastewater. Chemosphere 73, 1335–1343. https://doi.org/10.1016/j.chemosphere.2008.06.070

Chen, X., Vollertsen, J., Nielsen, J.L., Gieraltowska Dall, A., Bester, K., 2015. Degradation of PPCPs in activated sludge from different WWTPs in Denmark. Ecotoxicology 24, 2073–2080. https://doi.org/10.1007/s10646-015-1548-z

Clara, M., Strenn, B., Kreuzinger, N., 2004. Carbamazepine as a possible anthropogenic marker in the aquatic environment: Investigations on the behaviour of Carbamazepine in wastewater treatment and during groundwater infiltration. Water Res. 38, 947–954. https://doi.org/10.1016/j.watres.2003.10.058

Czerwionka, K., Makinia, J., Pagilla, K.R., Stensel, H.D., 2012. Characteristics and fate of organic nitrogen in municipal biological nutrient removal wastewater treatment plants. Water Res. 46, 2057–2066. https://doi.org/10.1016/j.watres.2012.01.020

D'Alessio, M., Yoneyama, B., Ray, C., 2015. Fate of selected pharmaceutically active compounds during simulated riverbank filtration. Sci. Total Environ. 505, 615–622. https://doi.org/10.1016/j.scitotenv.2014.10.032

Dal Pozzo, A., Dontelli, G., Rodriquez, L., Tajana, A., 1989. "In vitro" model for the evaluation of drug distribution and plasma protein-binding relationships. Int. J. Pharm. 50, 97–101. https://doi.org/10.1016/0378-5173(89)90133-6

Deutsches Institut für Normung, 2003. Water quality - Determination of selected phenoxyalkanoic

herbicides, including bentazones and hydroxybenzonitriles by gas chromatography and mass spectrometry after solid phase extraction and derivatization. Berlin, Germany.

Dhondt, K., Boeckx, P., Van Cleemput, O., Hofman, G., 2003. Quantifying nitrate retention processes in a riparian buffer zone using the natural abundance of 15N in NO3-. Rapid Commun. Mass Spectrom. 17, 2597–2604. https://doi.org/10.1002/rcm.1226

Dillon, P., 2005. Future management of aquifer recharge. Hydrogeol. J. 13, 313–316. https://doi.org/10.1007/s10040-004-0413-6

Dillon, P., Pavelic, P., Page, D., Beringen, H., Ward, J., 2009. Managed aquifer recharge: An Introduction, Waterlines Report Series No. 13.

Dobor, J., Varga, M., Záray, G., 2012. Biofilm controlled sorption of selected acidic drugs on river sediments characterized by different organic carbon content. Chemosphere 87, 105–110. https://doi.org/10.1016/j.chemosphere.2011.11.067

Dodgen, L.K., Zheng, W., 2016. Effects of reclaimed water matrix on fate of pharmaceuticals and personal care products in soil. Chemosphere 156, 286–293. https://doi.org/10.1016/j.chemosphere.2016.04.109

Drewes, J.E., Heberer, T., Rauch, T., Reddersen, K., 2003. Fate of Pharmaceuticals During Ground Water Recharge. Ground Water Monit. Remediat. 23. https://doi.org/10.1111/j.1745-6592.2003.tb00684.x

Durán-Álvarez, J.C., Prado, B., González, D., Sánchez, Y., Jiménez-Cisneros, B., 2015. Environmental fate of naproxen, carbamazepine and triclosan in wastewater, surface water and wastewater irrigated soil - Results of laboratory scale experiments. Sci. Total Environ. 538, 350–362. https://doi.org/10.1016/j.scitotenv.2015.08.028

Dutta, T., Carles-Brangarí, A., Fernàndez-Garcia, D., Rubol, S., Tirado-Conde, J., Sanchez-Vila, X., 2015. Vadose zone oxygen (O2) dynamics during drying and wetting cycles: An artificial recharge laboratory experiment. J. Hydrol. 527, 151–159. https://doi.org/10.1016/j.jhydrol.2015.04.048

Eckert, P., Irmscher, R., 2006. Over 130 years of experience with Riverbank Filtration in Düsseldorf, Germany. J. Water Supply Res. Technol. - AQUA 55, 283–291. https://doi.org/10.2166/aqua.2006.040

Essandoh, H.M.K., Tizaoui, C., Mohamed, M.H.A., Amy, G., Brdjanovic, D., 2011. Soil aquifer treatment of artificial wastewater under saturated conditions. Water Res. 45, 4211–4226. https://doi.org/10.1016/j.watres.2011.05.017

Fan, Z., Casey, F.X.M., Hakk, H., Larsen, G.L., Khan, E., 2011. Sorption, fate, and mobility of sulfonamides in soils. Water. Air. Soil Pollut. 218, 49–61. https://doi.org/10.1007/s11270-010-0623-6

Fang, Y., Karnjanapiboonwong, A., Chase, D.A., Wang, J., Morse, A.N., Anderson, T.A., 2012. Occurrence, fate, and persistence of gemfibrozil in water and soil. Environ. Toxicol. Chem. 31, 550–555. https://doi.org/10.1002/etc.1725

Franson, M.A.H. (Ed.), 1992. Standard Methods for the Examination of Water and Wastewater, 18th ed. American Public Health Association, Washington, D.C.

Goren, O., Burg, A., Gavrieli, I., Negev, I., Guttman, J., Kraitzer, T., Kloppmann, W., Lazar, B., 2014. Biogeochemical processes in infiltration basins and their impact on the recharging effluent, the soil aquifer treatment (SAT) system of the Shafdan plant, Israel. Appl. Geochemistry 48, 58–69. https://doi.org/10.1016/j.apgeochem.2014.06.017

Greskowiak, J., Prommer, H., Massmann, G., Nützmann, G., 2006. Modeling seasonal redox dynamics and the corresponding fate of the pharmaceutical residue phenazone during artificial recharge of groundwater. Environ. Sci. Technol. 40, 6615–6621. https://doi.org/10.1021/es052506t

Gröning, J., Held, C., Garten, C., Claußnitzer, U., Kaschabek, S.R., Schlömann, M., 2007. Transformation of diclofenac by the indigenous microflora of river sediments and identification of a major intermediate. Chemosphere 69, 509–516. https://doi.org/10.1016/j.chemosphere.2007.03.037

Gutiérrez, I.R., Watanabe, N., Harter, T., Glaser, B., Radke, M., 2010. Effect of sulfonamide antibiotics on microbial diversity and activity in a Californian Mollic Haploxeralf. J. Soils Sediments 10, 537–544. https://doi.org/10.1007/s11368-009-0168-8

Hadas, A., Sofer, M., Molina, J.A.E., Barak, P., Clapp, C.E., 1992. Assimilation of nitrogen by soil microbial population: NH4 versus organic N. Soil Biol. Biochem. 24, 137–143. https://doi.org/10.1016/0038-0717(92)90269-4

Hamann, E., Stuyfzand, P.J., Greskowiak, J., Timmer, H., Massmann, G., 2016. The fate of organic micropollutants during long-term/long-distance river bank filtration. Sci. Total Environ. 545–546, 629–640. https://doi.org/10.1016/j.scitotenv.2015.12.057

He, K., Echigo, S., Itoh, S., 2016. Effect of operating conditions in soil aquifer treatment on the removals of pharmaceuticals and personal care products. Sci. Total Environ. 565, 672–681. https://doi.org/10.1016/j.scitotenv.2016.04.148

Heberer, T., Massmann, G., Fanck, B., Taute, T., Dünnbier, U., 2008. Behaviour and redox sensitivity of antimicrobial residues during bank filtration. Chemosphere 73, 451–460.

https://doi.org/10.1016/j.chemosphere.2008.06.056

Hebig, K.H., Groza, L.G., Sabourin, M.J., Scheytt, T.J., Ptacek, C.J., 2017. Transport behavior of the pharmaceutical compounds carbamazepine, sulfamethoxazole, gemfibrozil, ibuprofen, and naproxen, and the lifestyle drug caffeine, in saturated laboratory columns. Sci. Total Environ. 590–591. https://doi.org/10.1016/j.scitotenv.2017.03.031

Hellauer, K., Karakurt, S., Sperlich, A., Burke, V., Massmann, G., Hübner, U., Drewes, J.E., 2017a. Establishing sequential managed aquifer recharge technology (SMART) for enhanced removal of trace organic chemicals: Experiences from field studies in Berlin, Germany. J. Hydrol. https://doi.org/10.1016/j.jhydrol.2017.09.044

Hellauer, K., Mergel, D., Ruhl, A.S., Filter, J., Hübner, U., Jekel, M., Drewes, J.E., 2017b. Advancing sequential managed aquifer recharge technology (SMART) using different intermediate oxidation processes. Water (Switzerland) 9, 1–14. https://doi.org/10.3390/w9030221

Hernández-Martínez, J.L., Prado, B., Cayetano-Salazar, M., Bischoff, W.A., Siebe, C., 2016. Ammonium-nitrate dynamics in the critical zone during single irrigation events with untreated sewage effluents. J. Soils Sediments 1–14. https://doi.org/10.1007/s11368-016-1506-2

Hoppe-Jones, C., Dickenson, E.R. V, Drewes, J.E., 2012. The role of microbial adaptation and biodegradable dissolved organic carbon on the attenuation of trace organic chemicals during groundwater recharge. Sci. Total Environ. 437, 137–144. https://doi.org/10.1016/j.scitotenv.2012.08.009

Jewell, K.S., Falas, P., Wick, A., Joss, A., Ternes, T.A., 2016. Transformation of diclofenac in hybrid biofilm--activated sludge processes. Water Res. 105, 559–567. https://doi.org/10.1016/j.watres.2016.08.002

Jones, O.A.H., Voulvoulis, N., Lester, J.N., 2002. Aquatic environmental assessment of the top 25 English prescription pharmaceuticals. Water Res. 36, 5013–5022. https://doi.org/10.1016/S0043-1354(02)00227-0

Kinney, C.A., Furlong, E.T., Werner, S.L., Cahill, J.D., 2006. Presence and distribution of wastewater-derived pharmaceuticals in soil irrigated with reclaimed water. Environ. Toxicol. Chem. 25, 317–326. https://doi.org/10.1897/05-187R.1

Knöller, K., Vogt, C., Haupt, M., Feisthauer, S., Richnow, H.-H., 2011. Experimental investigation of nitrogen and oxygen isotope fractionation in nitrate and nitrite during denitrification.pdf. Biogeochemistry 103, 371–384. https://doi.org/10.1007/s10533-010-9483-9

Kodešová, R., Kočárek, M., Klement, A., Golovko, O., Koba, O., Fér, M., Nikodem, A., Vondráčková, L., Jakšík, O., Grabic, R., 2016. An analysis of the dissipation of pharmaceuticals under thirteen different soil conditions. Sci. Total Environ. 544, 369–381. https://doi.org/10.1016/j.scitotenv.2015.11.085

Kopchynski, T., Fox, P., Alsmadi, B., Berner, M., 1996. The effects of soil type and effluent pre-treatment on soil aquifer treatment. Water Sci. Technol. 34, 235–242. https://doi.org/10.1016/S0273-1223(96)00843-8

Kraft, B., Tegetmeyer, H.E., Sharma, R., Klotz, M.G., Ferdelman, T.G., Hettich, R.L., Geelhoed, J.S., Strous, M., 2014. The environmental controls that govern the end product of bacterial nitrate respiration. Science (80-.). 345, 676–679. https://doi.org/10.1126/science.1254070

Kümmerer, K., 2009. Antibiotics in the aquatic environment - A review - Part I. Chemosphere 75, 417–434. https://doi.org/10.1016/j.chemosphere.2008.11.086

Laws, B. V., Dickenson, E.R.V., Johnson, T.A., Snyder, S.A., Drewes, J.E., 2011. Attenuation of contaminants of emerging concern during surface-spreading aquifer recharge. Sci. Total Environ. 409, 1087–1094. https://doi.org/10.1016/j.scitotenv.2010.11.021

Lertpaitoonpan, W., Ong, S.K., Moorman, T.B., 2009. Effect of organic carbon and pH on soil sorption of sulfamethazine. Chemosphere 76, 558–564. https://doi.org/10.1016/j.chemosphere.2009.02.066

Li, C., Li, B., Bi, E., 2019. Characteristics of hydrochemistry and nitrogen behavior under long-term managed aquifer recharge with reclaimed water : A case study in north China. Sci. Total Environ. 668, 1030–1037. https://doi.org/10.1016/j.scitotenv.2019.02.375

Lillenberg, M., Yurchenko, S., Kipper, K., Herodes, K., Pihl, V., Sepp, KalevNei, L., Lõhmus, R., Nei, L., 2009. Simultaneous determination of fluoroquinolones, sulfonamides and tetracyclines in sewage sludge by pressurized liquid extraction and liquid chromatography electrospray ionization-mass spectrometry. J. Chromatogr. A 1216, 5949–5954. https://doi.org/10.1016/j.chroma.2009.06.029

Lim, M.H., Snyder, S.A., Sedlak, D.L., 2008. Use of biodegradable dissolved organic carbon (BDOC) to assess the potential for transformation of wastewater-derived contaminants in surface waters. Water Res. 42, 2943–2952. https://doi.org/10.1016/j.watres.2008.03.008

Lin, A.Y.C., Lin, C.A., Tung, H.H., Chary, N.S., 2010. Potential for biodegradation and sorption of acetaminophen, caffeine, propranolol and acebutolol in lab-scale aqueous environments. J.

Hazard. Mater. 183, 242–250. https://doi.org/10.1016/j.jhazmat.2010.07.017

Lin, K., Gan, J., 2011. Sorption and degradation of wastewater-associated non-steroidal anti-inflammatory drugs and antibiotics in soils. Chemosphere 83, 240–246. https://doi.org/10.1016/j.chemosphere.2010.12.083

Lingle, D.A., Kehew, A.E., Krishnamurthy, R. V, 2017. Use of nitrogen isotopes and other geochemical tools to evaluate the source of ammonium in a confined glacial drift aquifer, Ottawa County, Michigan, USA. Appl. Geochemistry 78, 334–342. https://doi.org/10.1016/j.apgeochem.2017.01.004

Liu, F., Ying, G.-G., Tao, R., Zhao, J.-L., Yang, J.-F., Zhao, L.-F., 2009. Effects of six selected antibiotics on plant growth and soil microbial and enzymatic activities. Environ. Pollut. 157, 1636–42. https://doi.org/10.1016/j.envpol.2008.12.021

Maeng, S.K., Sharma, S.K., Abel, C.D.T., Magic-Knezev, A., Amy, G.L., 2011a. Role of biodegradation in the removal of pharmaceutically active compounds with different bulk organic matter characteristics through managed aquifer recharge: Batch and column studies. Water Res. 45, 4722–4736. https://doi.org/10.1016/j.watres.2011.05.043

Maeng, S.K., Sharma, S.K., Abel, C.D.T., Magic-Knezev, A., Song, K.G., Amy, G.L., 2012. Effects of effluent organic matter characteristics on the removal of bulk organic matter and selected pharmaceutically active compounds during managed aquifer recharge: Column study. J. Contam. Hydrol. 140–141, 139–149. https://doi.org/10.1016/j.jconhyd.2012.08.005

Maeng, S.K., Sharma, S.K., Lekkerkerker-Teunissen, K., Amy, G.L., 2011b. Occurrence and fate of bulk organic matter and pharmaceutically active compounds in managed aquifer recharge: A review. Water Res. 45, 3015–3033. https://doi.org/10.1016/j.watres.2011.02.017

Mania, D., Heylen, K., van Spanning, R.J.M., Frostegård, A., 2014. The nitrate-ammonifying and nosZ-carrying bacterium Bacillus vireti is a potent source and sink for nitric and nitrous oxide under high nitrate conditions. Environ. Microbiol. 16, 3196–3210. https://doi.org/10.1111/1462-2920.12478

Mariotti, A., Germon, J.C., Hubert, P., Kaiser, P., Letolle, R., Tardieux, A., Tardieux, P., 1981. Experimental determination of nitrogen kinetic isotope fractionation: Some principles; illustration for the denitrification and nitrification processes. Plant Soil 62, 413–430. https://doi.org/10.1007/BF02374138

Martínez-Hernández, V., Meffe, R., Herrera, S., Arranz, E., de Bustamante, I., 2015.

Sorption/desorption of non-hydrophobic and ionisable pharmaceutical and personal care products from reclaimed water onto/from a natural sediment. Sci. Total Environ. 505, 1232–1233. https://doi.org/10.1016/j.scitotenv.2014.10.104

Massmann, G., Greskowiak, J., Dünnbier, U., Zuehlke, S., Knappe, A., Pekdeger, A., 2006. The impact of variable temperatures on the redox conditions and the behaviour of pharmaceutical residues during artificial recharge. J. Hydrol. 328, 141–156. https://doi.org/10.1016/j.jhydrol.2005.12.009

Matamoros, V., Caselles-Osorio, A., García, J., Bayona, J.M., 2008. Behaviour of pharmaceutical products and biodegradation intermediates in horizontal subsurface flow constructed wetland. A microcosm experiment. Sci. Total Environ. 394, 171–176. https://doi.org/10.1016/j.scitotenv.2008.01.029

McIlvin, M.R., Casciotti, K.L., 2011. Technical updates to the bacterial method for nitrate isotopic analyses. Anal. Chem. 83, 1850–1856. https://doi.org/10.1021/ac1028984

Mengis, M., Schiff, S.L., Harris, M., English, M.C., Aravena, R., Elgood, R.J., MacLean, A., 1999. Multiple geochemical and isotopic approaches for assessing ground water NO3- Elimination in a riparian zone. Ground Water. https://doi.org/10.1111/j.1745-6584.1999.tb01124.x

Miller, J.H., Ela, W.P., Lansey, K.E., Chipello, P.L., Arnold, R.G., 2006. Nitrogen Transformations during Soil–Aquifer Treatment of Wastewater Effluent—Oxygen Effects in Field Studies. J. Environ. Eng. 132, 1298–1306. https://doi.org/10.1061/(ASCE)0733-9372(2006)132:10(1298)

Miotlinski, K., Barry, K., Dillon, P., Breton, M., 2010. Alice Springs SAT Project Hydrological and Water Quality Monitoring Report 2008-2009.

Monteiro, S.C., Boxall, A.B. a, 2009. Factors affecting the degradation of pharmaceuticals in agricultural soils. Environ. Toxicol. Chem. 28, 2546–2554. https://doi.org/10.1897/08-657.1

Müller, J., Drewes, J.E., Hübner, U., 2017. Sequential biofiltration – A novel approach for enhanced biological removal of trace organic chemicals from wastewater treatment plant effluent. Water Res. 127, 127–138. https://doi.org/10.1016/j.watres.2017.10.009

Murphy, D.V., Recous, S., Stockdale, E.A., Fillery, I.R.P., Jensen, L.S., Hatch, D.J., Goulding, K.W.T., 2003. Gross Nitrogen Fluxes in Soil: Theory, Measurement and Application of 15Npool Dilution Techniques. Adv. Agron. 79, 69–118. https://doi.org/10.1016/S0065-2113(02)79002-0

Nham, H.T.T., Greskowiak, J., Nödler, K., Rahman, M.A., Spachos, T., Rusteberg, B., Massmann, G., Sauter, M., Licha, T., 2015. Modeling the transport behavior of 16 emerging organic contaminants during soil aquifer treatment. Sci. Total Environ. 514, 450–458.

https://doi.org/10.1016/j.scitotenv.2015.01.096

Nieto, A., Borrull, F., Pocurull, E., Marcé, R.M., 2010. Pressurized liquid extraction: A useful technique to extract pharmaceuticals and personal-care products from sewage sludge. TrAC - Trends Anal. Chem. 29, 752–764. https://doi.org/10.1016/j.trac.2010.03.014

Nieto, A., Borrull, F., Pocurull, E., Marcé, R.M., 2007. Pressurized liquid extraction of pharmaceuticals from sewage-sludge. J. Sep. Sci. 30, 979–984. https://doi.org/10.1002/jssc.200600360

Nikolaou, A., Meric, S., Fatta, D., 2007. Occurrence patterns of pharmaceuticals in water and wastewater environments. Anal. Bioanal. Chem. 387, 1225–1234. https://doi.org/10.1007/s00216-006-1035-8

Okamura, Y., Wada, K., 1984. Ammonium-calcium exchange equilibria in soils and weathered pumices that differ in cationexchange materials. J. Soil Sci. 35, 387–396. https://doi.org/10.1111/j.1365-2389.1984.tb00295.x

Parkhurst, D.L., Appelo, C.A.J., 1999. User'S Guide To Phreeqc (Version 2)— a Computer Program for Speciation, Batch-Reaction, One-Dimensional Transport, and Inverse Geochemical Calculations M a R C H 3 1 8 4 9. Denver, Colorado, USA.

Parkin, G.F., McCarty, P.L., 1981. A comparison of the characteristics of soluble organic nitrogen in untreated and activated sludge treated wastewaters. Water Res. 15, 139–149. https://doi.org/10.1016/0043-1354(81)90194-9

Patterson, B.M., Shackleton, M., Furness, A.J., Bekele, E., Pearce, J., Linge, K.L., Busetti, F., Spadek, T., Toze, S., 2011. Behaviour and fate of nine recycled water trace organics during managed aquifer recharge in an aerobic aquifer. J. Contam. Hydrol. 122, 53–62. https://doi.org/10.1016/j.jconhyd.2010.11.003

Pavelic, P., Dillon, P.J., Mucha, M., Nakai, T., Barry, K.E., Bestland, E., 2011. Laboratory assessment of factors affecting soil clogging of soil aquifer treatment systems. Water Res. 45, 3153–3163. https://doi.org/10.1016/j.watres.2011.03.027

Pérez, S., Eichhorn, P., Aga, D.S., 2005. Evaluating the biodegradability of sulfamethazine, sulfamethoxazole, sulfathiazole, and trimethoprim at different stages of sewage treatment. Environ. Toxicol. Chem. 24, 1361–7. https://doi.org/10.1897/04-211R.1

Postigo, C., Barceló, D., 2015. Synthetic organic compounds and their transformation products in groundwater: Occurrence, fate and mitigation. Sci. Total Environ. 503–504, 32–47. https://doi.org/10.1016/j.scitotenv.2014.06.019

Powelson, D.K., Gerba, C.P., Yahya, M.T., 1993. Virus transport and removal in wastewater during aquifer recharge. Water Res. 27, 583–590. https://doi.org/10.1016/0043-1354(93)90167-G

Radjenović, J., Jelić, A., Petrović, M., Barceló, D., 2009. Determination of pharmaceuticals in sewage sludge by pressurized liquid extraction (PLE) coupled to liquid chromatography-tandem mass spectrometry (LC-MS/MS). Anal. Bioanal. Chem. 393, 1685–1695. https://doi.org/10.1007/s00216-009-2604-4

Rauch-Williams, T., Drewes, J.E., 2006. Using soil biomass as an indicator for the biological removal of effluent-derived organic carbon during soil infiltration. Water Res. 40, 961–968. https://doi.org/10.1016/j.watres.2006.01.007

Rauch-Williams, T., Hoppe-Jones, C., Drewes, J.E., 2010. The role of organic matter in the removal of emerging trace organic chemicals during managed aquifer recharge. Water Res. 44, 449–460. https://doi.org/10.1016/j.watres.2009.08.027

Regnery, J., Wing, A.D., Kautz, J., Drewes, J.E., 2016. Introducing sequential managed aquifer recharge technology (SMART) - From laboratory to full-scale application. Chemosphere 154, 8–16. https://doi.org/10.1016/j.chemosphere.2016.03.097

Rodriguez-Escales, P., Sanchez-Vila, X., 2016. Fate of sulfamethoxazole in groundwater: Conceptualizing and modeling metabolite formation under different redox conditions. Water Res. 105, 540–550. https://doi.org/10.1016/j.watres.2016.09.034

Runnqvist, H., Bak, S.A., Hansen, M., Styrishave, B., Halling-Sørensen, B., Björklund, E., 2010. Determination of pharmaceuticals in environmental and biological matrices using pressurised liquid extraction-Are we developing sound extraction methods? J. Chromatogr. A 1217, 2447–2470. https://doi.org/10.1016/j.chroma.2010.02.046

Schaffer, M., Kröger, K.F., Nödler, K., Ayora, C., Carrera, J., Hernández, M., Licha, T., 2015. Influence of a compost layer on the attenuation of 28 selected organic micropollutants under realistic soil aquifer treatment conditions: Insights from a large scale column experiment. Water Res. 74, 110–212. https://doi.org/10.1016/j.watres.2015.02.010

Scheytt, T.J., Mersmann, P., Heberer, T., 2006. Mobility of pharmaceuticals carbamazepine, diclofenac, ibuprofen, and propyphenazone in miscible-displacement experiments. J. Contam. Hydrol. 83, 53–69. https://doi.org/10.1016/j.jconhyd.2005.11.002

Schlögl, J., 2016. Investigation of the origin of ammonium in column experiments with treated wastewater by stable isotope methods. M.Sc. Thesis, Technische Universität Darmstadt.

Darmstadt, Germany.

Schmidt, C.M., Fisher, A.T., Racz, A., Wheat, C.G., Los Huertos, M., Lockwood, B., 2012. Rapid nutrient load reduction during infiltration of managed aquifer recharge in an agricultural groundwater basin: Pajaro Valley, California. Hydrol. Process. 26, 2235–2247. https://doi.org/10.1002/hyp.8320

Sigman, D.M., Casciotti, K.L., Andreani, M., Barford, C., Galanter, M., Böhlke, J.K., 2001. A bacterial method for the nitrogen isotopic analysis of nitrate in seawater and freshwater. Anal. Chem. 73, 4145–4153. https://doi.org/10.1021/ac010088e

Stanford, G., Smith, S.J., 1972. Nitrogen Mineralization Potentials of Soils. Soil Sci. Soc. Am. J. 36, 465–472. https://doi.org/10.2136/sssaj1972.03615995003600030029x

Storck, F.R., Schmidt, C.K., Lange, F.T., Henson, J.W., Hahn, K., 2010. Removal and Fate of EDCs and PPCPs in Bank Filtration Systems. Project report 3136. Denver, Colorado, USA.

The Council of the European Union, 2000. Directive 2000/60/EC of the European Parliament and of the Council of 23 October 2000 establishing a framework for Community action in the field of water policy, Official Journal of the European Parliament. https://doi.org/10.1039/ap9842100196

The Council of the European Union, 1998. Council Directive 98/83/EC of 3 November 1998 on the quality of water intended for human consumption, Official Journal of the European Communities. https://doi.org/2004R0726 - v.7 of 05.06.2013

Tufenkji, N., Ryan, J.N., Elimelech, M., 2002. The promise of bank filtration: a simple technology may inexpensively clean up poor-quality raw surface water. Environ. Sci. Technol. 36, 422A-428A. https://doi.org/10.1021/es022441j

US EPA, 2012. Estimation Programs Interface Suite™ for Microsoft® Windows, v4.11.

Valhondo, C., Carrera, J., Ayora, C., Barbieri, M., Nödler, K., Licha, T., Huerta, M., 2014. Behavior of nine selected emerging trace organic contaminants in an artificial recharge system supplemented with a reactive barrier. Environ. Sci. Pollut. Res. 21, 11832–11843. https://doi.org/10.1007/s11356-014-2834-7

Valhondo, C., Carrera, J., Ayora, C., Tubau, I., Martinez-Landa, L., Nödler, K., Licha, T., 2015. Characterizing redox conditions and monitoring attenuation of selected pharmaceuticals during artificial recharge through a reactive layer. Sci. Total Environ. 512–513, 240–250. https://doi.org/10.1016/j.scitotenv.2015.01.030

Valhondo, C., Martinez-Landa, L., Carrera, J., Ayora, C., Nödler, K., Licha, T., 2018. Evaluation of EOC

removal processes during artificial recharge through a reactive barrier. Sci. Total Environ. 612, 985–994. https://doi.org/10.1016/j.scitotenv.2017.08.054

van den Berg, E.M., Boleij, M., Kuenen, J.G., Kleerebezem, R., van Loosdrecht, M.C.M., 2016. DNRA and denitrification coexist over a broad range of acetate/N-NO3- ratios, in a chemostat enrichment culture. Front. Microbiol. 7, 1–12. https://doi.org/10.3389/fmicb.2016.01842

Verlicchi, P., Al Aukidy, M., Zambello, E., 2012. Occurrence of pharmaceutical compounds in urban wastewater: Removal, mass load and environmental risk after a secondary treatment-A review. Sci. Total Environ. 429, 123–155. https://doi.org/10.1016/j.scitotenv.2012.04.028

Vidal-Gavilan, G., Carrey, R., Solanas, A., Soler, A., 2014. Feeding strategies for groundwater enhanced biodenitrification in an alluvial aquifer: Chemical, microbial and isotope assessment of a 1D flow-through experiment. Sci. Total Environ. 494–495, 241–251. https://doi.org/10.1016/j.scitotenv.2014.06.100

Vorenhout, M., van der Geest, H.G., van Marum, D., Wattel, K., Eijsackers, H.J.P., 2004. Automated and continuous redox potential measurements in soil. J. Environ. Qual. 33, 1562–1567. https://doi.org/10.2134/jeq2004.1562

Walker, C.W., Watson, J.E., Williams, C., 2012. Occurrence of Carbamazepine in Soils under Different Land Uses Receiving Wastewater. J. Environ. Qual. 41, 2012. https://doi.org/10.2134/jeq2011.0193

Wegst-Uhrich, S.R., Navarro, D.A.G., Zimmerman, L., Aga, D.S., 2014. Assessing antibiotic sorption in soil: A literature review and new case studies on sulfonamides and macrolides. Chem. Cent. J. 8, 1–12. https://doi.org/10.1186/1752-153X-8-5

Wilkinson, J., Boxall, A., Kolpin, D., 2019. A Novel Method to Characterise Levels of Pharmaceutical Pollution in Large-Scale Aquatic Monitoring Campaigns. Appl. Sci. 9, 1368. https://doi.org/10.3390/app9071368

Yoon, S., Cruz-García, C., Sanford, R., Ritalahti, K.M., Löffler, F.E., 2015. Denitrification versus respiratory ammonification: environmental controls of two competing dissimilatory NO3(-)/NO2(-) reduction pathways in Shewanella loihica strain PV-4. ISME J. 9, 1093–104. https://doi.org/10.1038/ismej.2014.201

Zaranyika, M.F., Dzomba, P., Kugara, J., 2015. Speciation and persistence of doxycycline in the aquatic environment: Characterization in terms of steady state kinetics. J. Environ. Sci. Heal. Part B 0, 1–11. https://doi.org/10.1080/03601234.2015.1067101

Zemann, M., Majewsky, M., Wolf, L., 2016. Accumulation of pharmaceuticals in groundwater under arid climate conditions - Results from unsaturated column experiments. Chemosphere 154, 463–471. https://doi.org/10.1016/j.chemosphere.2016.03.136

Zhao, L., Zhu, W., Tong, W., 2009. Clogging processes caused by biofilm growth and organic particle accumulation in lab-scale vertical flow constructed wetlands. J. Environ. Sci. 21, 750–757. https://doi.org/10.1016/S1001-0742(08)62336-0

Zvorykin, I.A., Saul, P.J., 1948. Soil map of Attica [WWW Document]. Inst. Ximeias kai Georg. Nikolaos Kanellopoulos. https://esdac.jrc.ec.europa.eu/content/soil-map-attica-edafologikos-xartis-attikis

Zwiener, C., Frimmel, F.H., 2003. Short-term tests with a pilot sewage plant and biofilm reactors for the biological degradation of the pharmaceutical compounds clofibric acid, ibuprofen, and diclofenac. Sci. Total Environ. 309, 201–211. https://doi.org/10.1016/S0048-9697(03)00002-0

Appendix A

Figures A-1 through A-19 show stable isotopes in nitrate from the individual sampling events. Three graphs are shown for each: a) stable isotopes in nitrate, b) concentration dependency of ^{15}N and c) enrichment (ε) of ^{15}N. On graphs (a) and (b), where no data point appears for a specific depth graphs, nitrate concentration was too low for detection of stable isotopes. On graph (c), only data points indicating enrichment of ^{15}N relative to the inflow water are shown. For sampling events in which no samples were measured for stable isotopes, the figure number is skipped so that all figure numbers correspond directly to the sampling event number.

a) Stable isotopes in nitrate

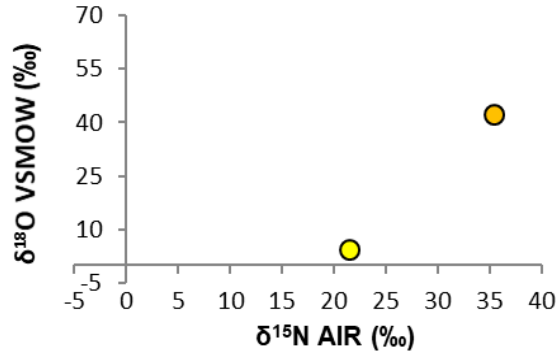

b) Concentration dependency of ^{15}N

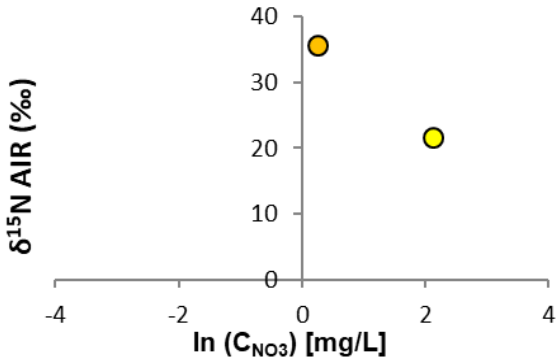

c) Enrichment of ^{15}N

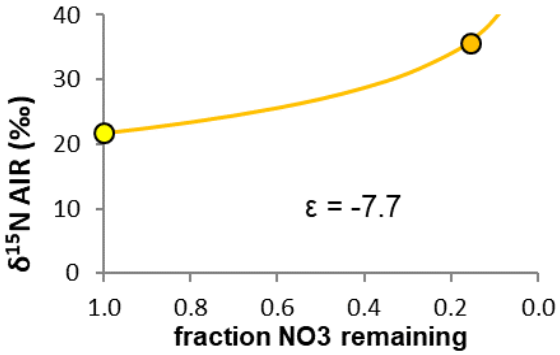

Sample depth (cm)

0 5 15 30 45 60 75

Figure A-1. Stable isotopes in nitrate, first sampling event

a) Stable isotopes in nitrate

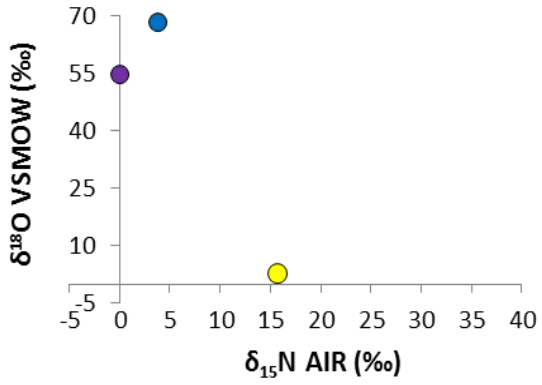

b) Concentration dependency of ^{15}N

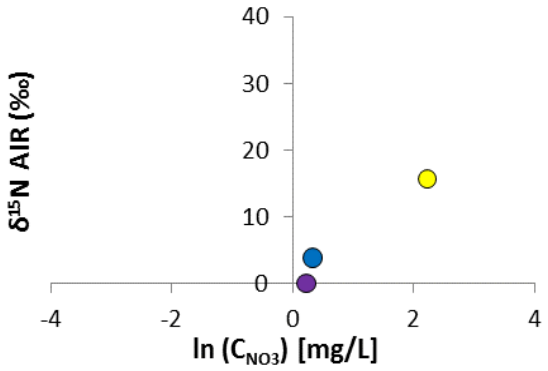

c) Enrichment of ^{15}N No data showing enrichment

Sample depth (cm)

0 5 15 30 45 60 75

Figure A-2. Stable isotopes in nitrate, second sampling event

a) Stable isotopes in nitrate

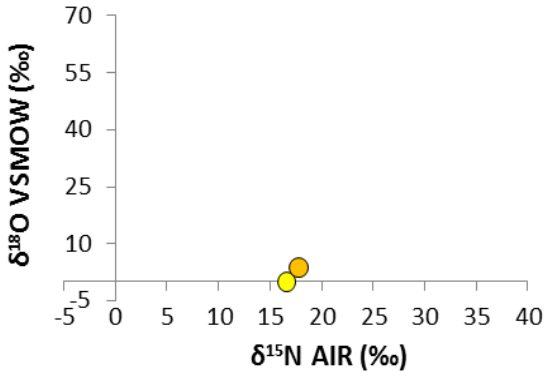

b) Concentration dependency of ^{15}N

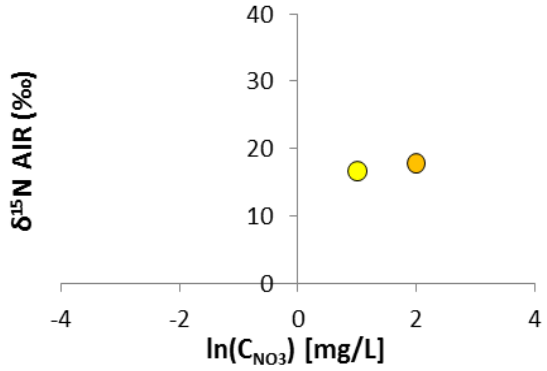

c) Enrichment of ^{15}N

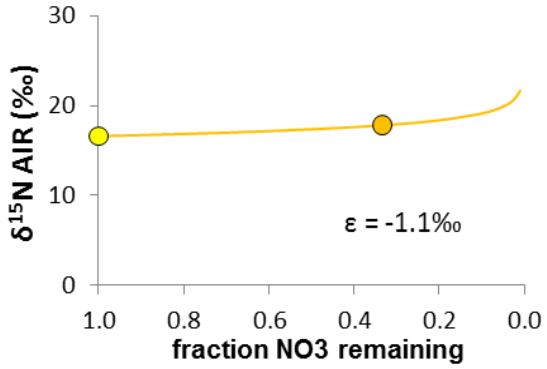

Figure A-3. Stable isotopes in nitrate, third sampling event

a) Stable isotopes in nitrate

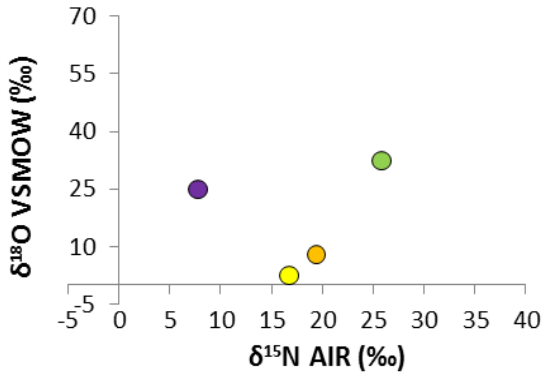

b) Concentration dependency of ^{15}N

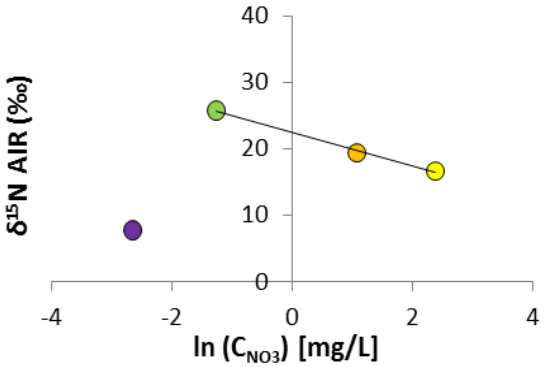

c) Enrichment of ^{15}N

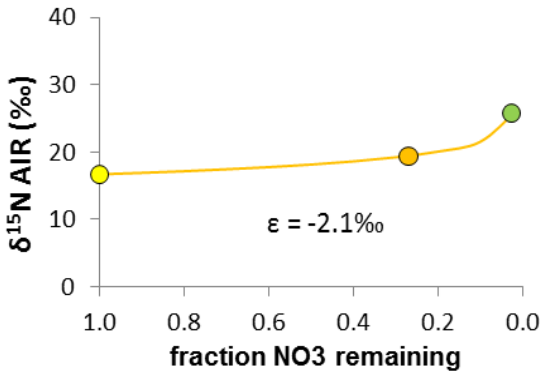

Sample depth (cm)

0 5 15 30 45 60 75

Figure A-4. Stable isotopes in nitrate, fourth sampling event

a) Stable isotopes in nitrate

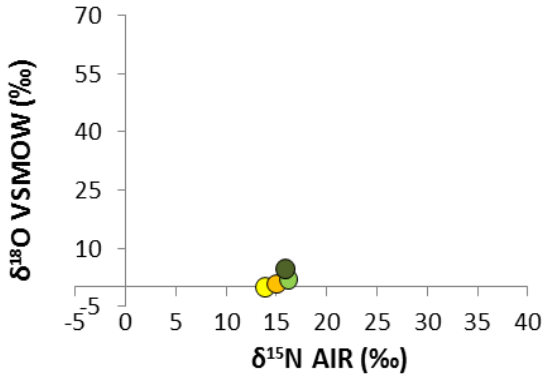

b) Concentration dependency of ^{15}N

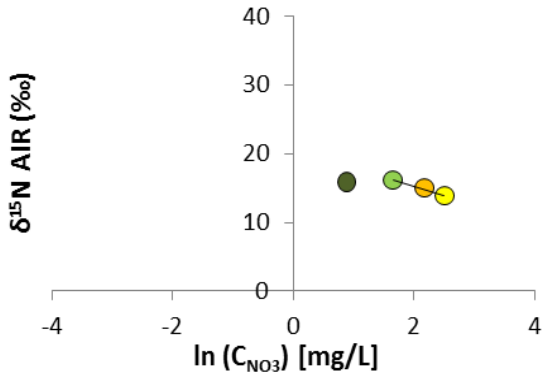

c) Enrichment of ^{15}N

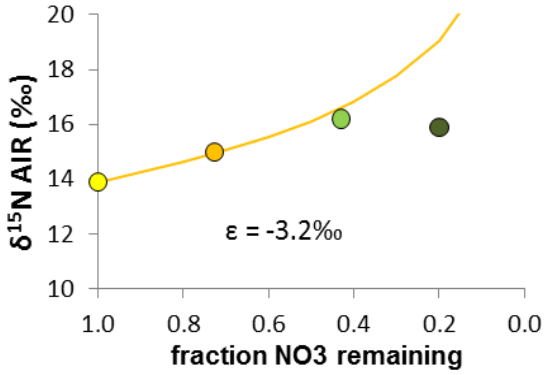

Sample depth (cm)

0 5 15 30 45 60 75

Figure A-5. Stable isotopes in nitrate, fifth sampling event

a) Stable isotopes in nitrate

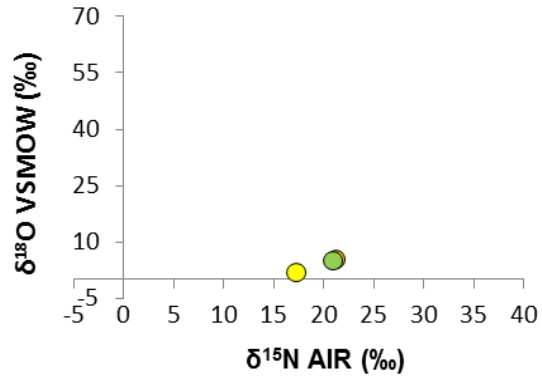

b) Concentration dependency of ^{15}N

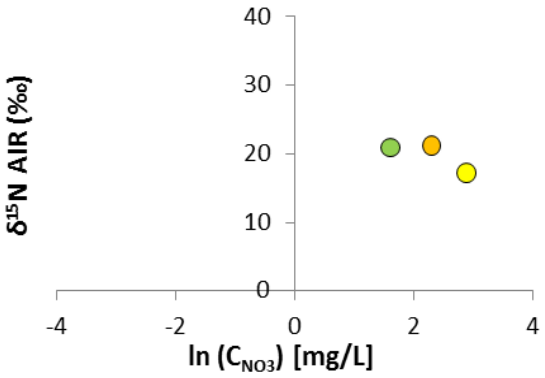

c) Enrichment of ^{15}N

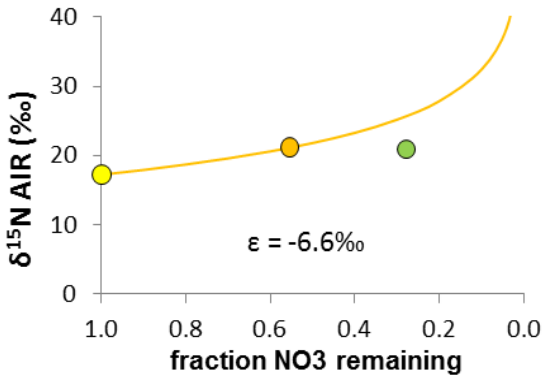

Sample depth (cm)

0 5 15 30 45 60 75

Figure A-6. Stable isotopes in nitrate, sixth sampling event

a) Stable isotopes in nitrate

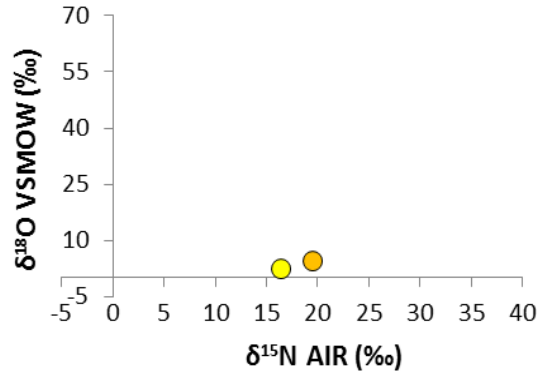

b) Concentration dependency of ^{15}N

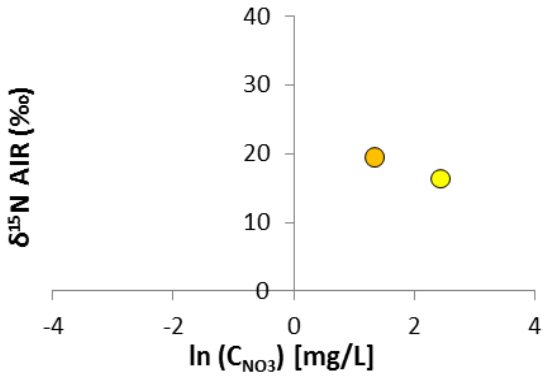

c) Enrichment of ^{15}N

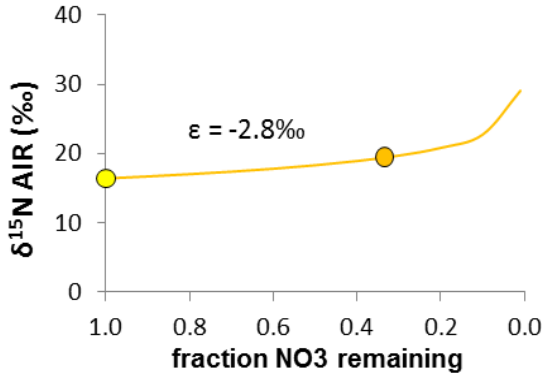

Sample depth (cm)

0 5 15 30 45 60 75

Figure A-7. Stable isotopes in nitrate, seventh sampling event

a) Stable isotopes in nitrate

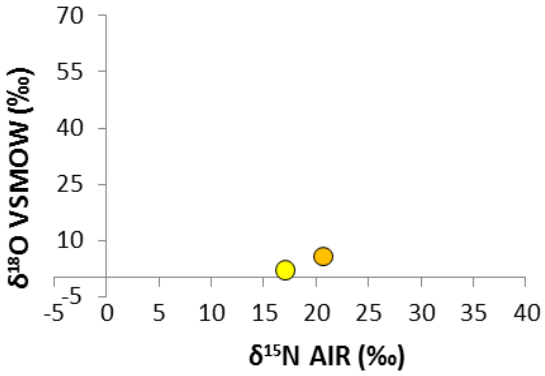

b) Concentration dependency of ^{15}N

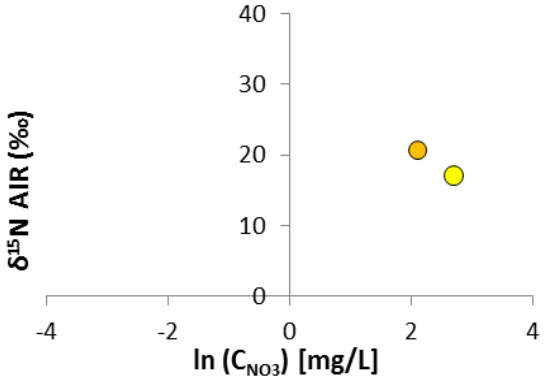

c) Enrichment of ^{15}N

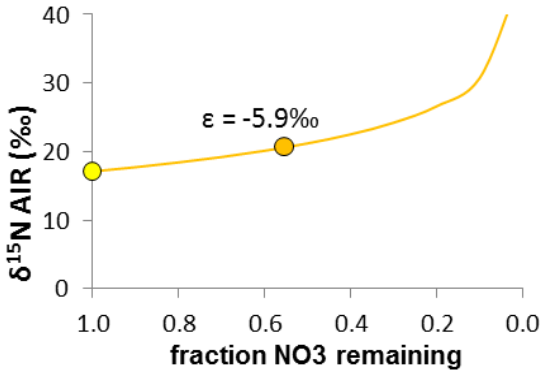

Sample depth (cm)

0 5 15 30 45 60 75

Figure A-8. Stable isotopes in nitrate, eight sampling event

a) Stable isotopes in nitrate

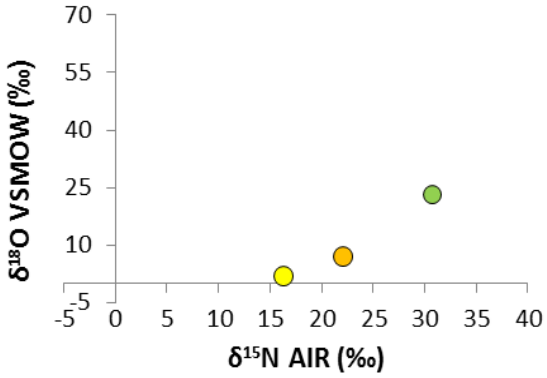

b) Concentration dependency of ^{15}N

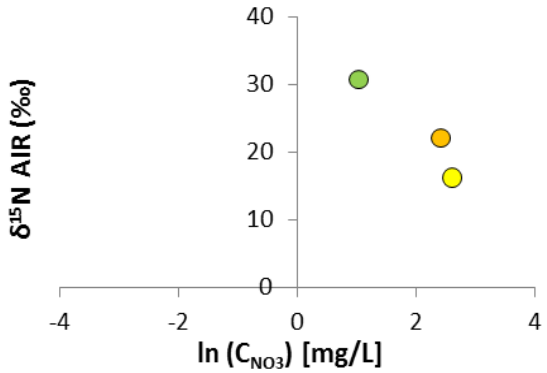

c) Enrichment of ^{15}N

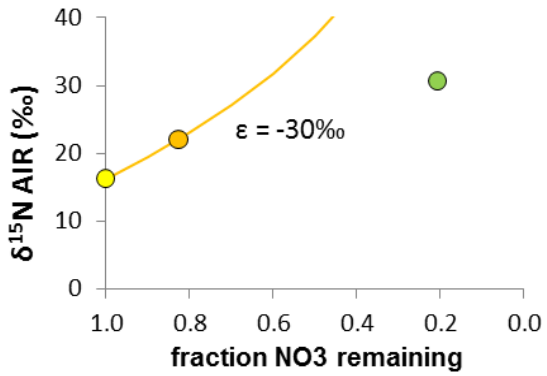

Sample depth (cm)

0 5 15 30 45 60 75

Figure A-9. Stable isotopes in nitrate, ninth sampling event

a) Stable isotopes in nitrate

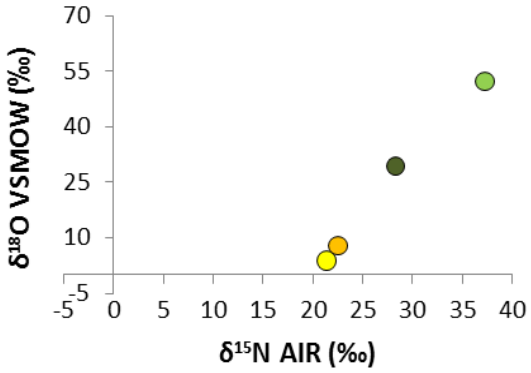

b) Concentration dependency of ^{15}N

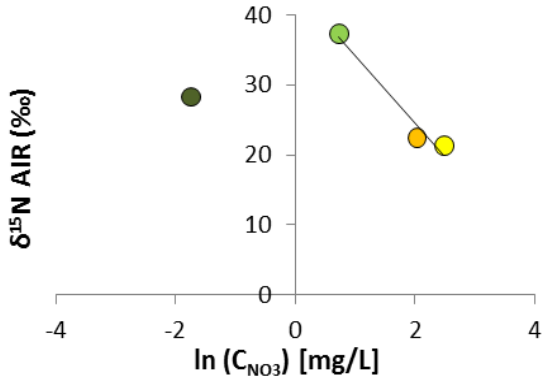

c) Enrichment of ^{15}N

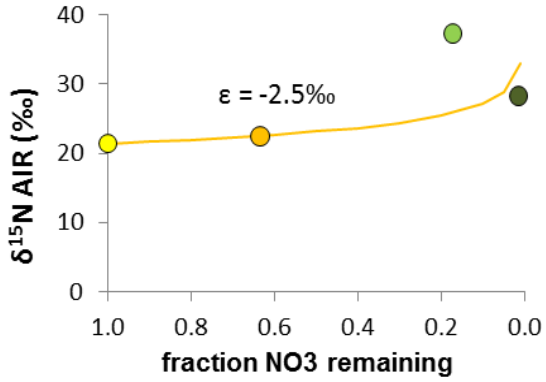

Figure A-10. Stable isotopes in nitrate, tenth sampling event

a) Stable isotopes in nitrate

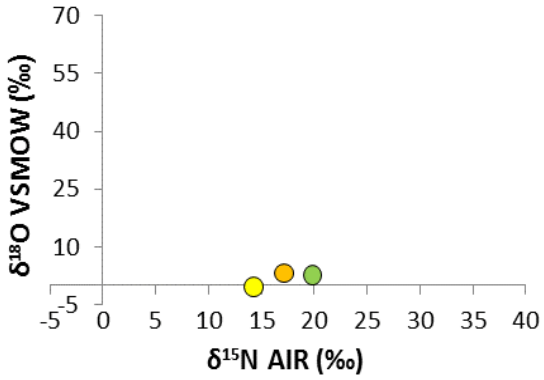

b) Concentration dependency of ^{15}N

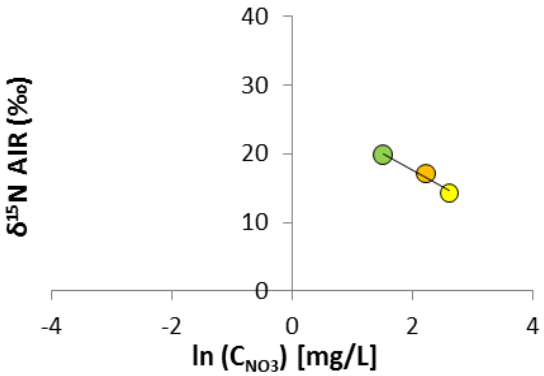

c) Enrichment of ^{15}N

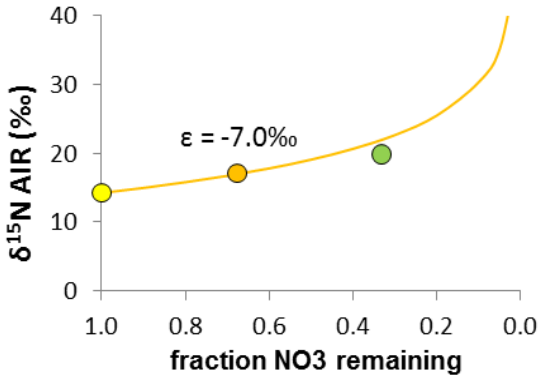

Sample depth (cm)

0 5 15 30 45 60 75

Figure A-12. Stable isotopes in nitrate, twelfth sampling event

a) Stable isotopes in nitrate

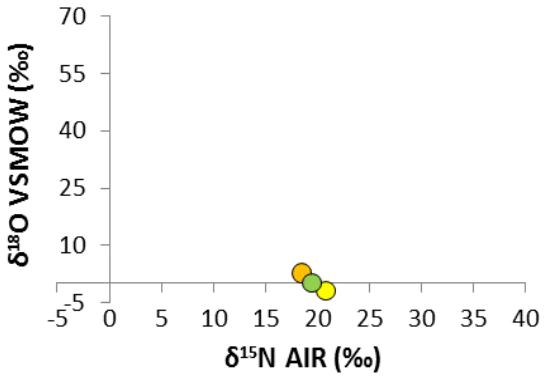

b) Concentration dependency of ^{15}N

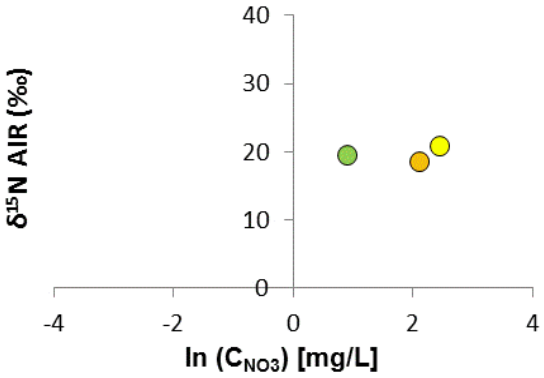

c) Enrichment of ^{15}N No data showing enrichment

Sample depth (cm)

0 5 15 30 45 60 75

Figure A-13. Stable isotopes in nitrate, thirteenth sampling event

a) Stable isotopes in nitrate

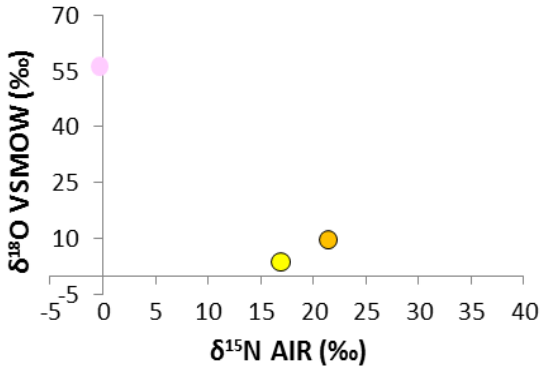

b) Concentration dependency of ^{15}N

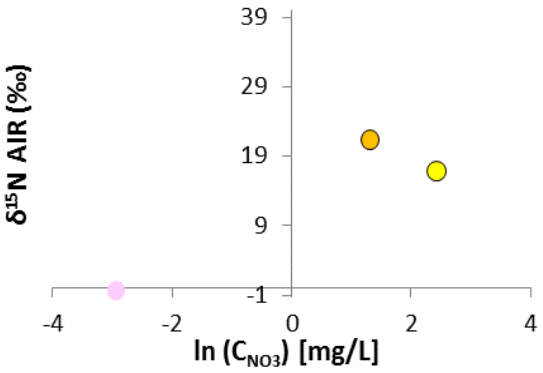

c) Enrichment of ^{15}N

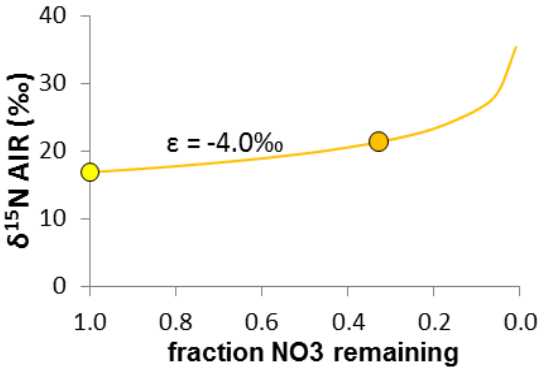

Sample depth (cm)

0 5 15 30 45 60 75

Figure A-14. Stable isotopes in nitrate, fourteenth sampling event

a) Stable isotopes in nitrate

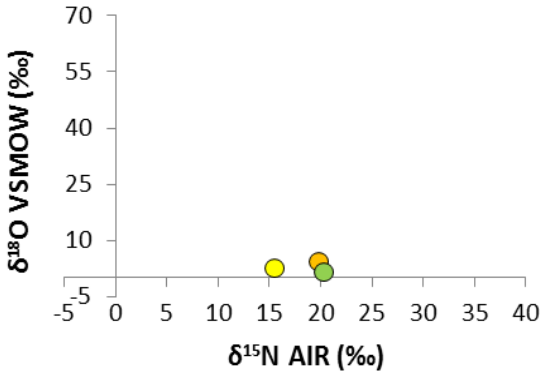

b) Concentration dependency of ^{15}N

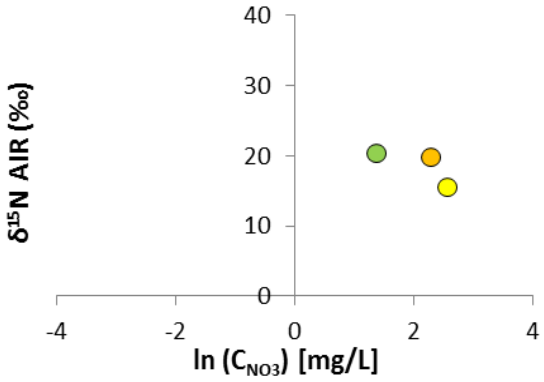

c) Enrichment of ^{15}N

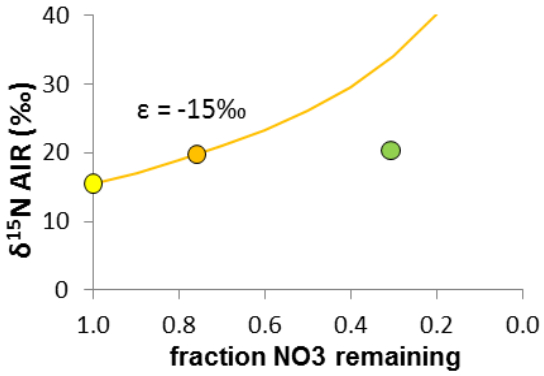

Sample depth (cm)

0 5 15 30 45 60 75

Figure A-15. Stable isotopes in nitrate, fifteenth sampling event

a) Stable isotopes in nitrate

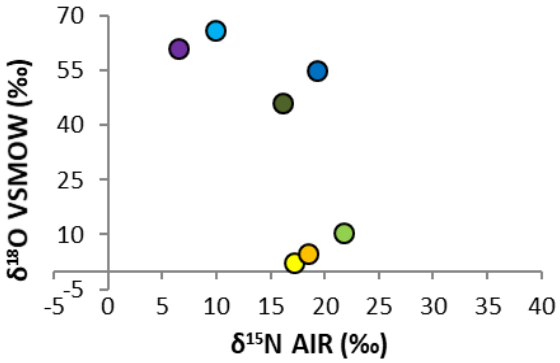

b) Concentration dependency of ^{15}N

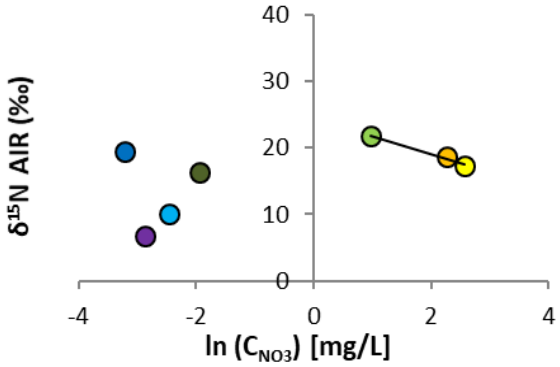

c) Enrichment of ^{15}N

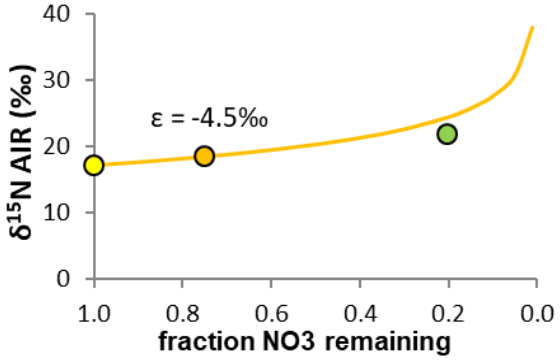

Sample depth (cm)

0 5 15 30 45 60 75

Figure A-19. Stable isotopes in nitrate, nineteenth sampling event

Appendix B

Sorbed concentrations found from all replicates of the extraction samples are shown in Table B-1. The spiked mass added per spiked sample (4 g milled soil) was as follows: carbamazepine 832 ng, diclofenac 766 ng, fenoprofen 797 ng, gemfibrozil 800 ng, naproxen 819 ng.

Table B-1. Results of extraction samples including all replicates

			CMP	**DCF**	**FEN**	**GMB**	**NX**
Sample		Replicate	ng / g	ng / g	ng / g	ng / g	ng / g
A12		1	531	195	20	56	10
A12		2	430	184	18	51	8
A12		3	505	205	18	53	8
		Average	*489*	*195*	*19*	*53*	*8*
A12	S	1	642	293	153	173	153
A12	S	2	602	293	141	161	141
A12	S	3	723	265	133	161	128
		Average	*656*	*284*	*142*	*165*	*141*
A27		1	303	134	18	45	5
A27		2	430	136	15	43	5
A27		3	243	124	15	38	3
		Average	*325*	*131*	*16*	*42*	*4*
A72		1	207	121	15	43	3
A72		2	227	121	20	40	5
A72		3	187	121	15	43	3
		Average	*207*	*121*	*17*	*42*	*3*
B12		1	379	33	10	30	5
B12		2	329	35	10	33	5
		Average	*354*	*34*	*10*	*32*	*5*
B27		1	169	63	15	43	1
B27		2	278	33	13	38	5
		Average	*224*	*48*	*14*	*40*	*3*
B72		1	202	63	15	43	nd
B72		2	167	58	15	40	nd
B72		3	162	58	15	40	nd
		Average	*177*	*60*	*15*	*41*	
C12		1	379	51	13	38	5

			CMP	**DCF**	**FEN**	**GMB**	**NX**
Sample		Replicate	ng / g	ng / g	ng / g	ng / g	ng / g
C12		2	404	53	15	40	5
C12		3	238	56	15	40	8
		Average	*340*	*53*	*14*	*40*	*6*
C12	S	1	522	193	149	177	141
C12	S	2	482	205	157	193	149
C12	S	3	562	205	153	185	141
		Average	*522*	*201*	*153*	*185*	*143*
C27		1	278	20	10	28	3
C27		2	278	25	10	30	3
C27		*Average*	*278*	*23*	*10*	*29*	*3*
C72		1	217	91	18	40	3
C72		2	212	93	18	40	3
C72		3	na	99	18	43	1
		Average	*215*	*94*	*18*	*41*	*2*
C72	S	1	357	241	145	169	133
C72	S	2	337	237	145	165	137
C72	S	3	442	241	149	181	141
		Average	*379*	*240*	*146*	*171*	*137*

Notes:
Sample ID is comprised of the column letter followed by sample depth in cm
CMP = carbamazepine, DCF = diclofenac, FEN = fenoprofen, GMB = gemfibrozil, NX = naproxen
S = spiked
na = not analyzed
nd = not detected
gray font = nd, half the detection limit used for averaging

Table B-2 displays the infiltrated (a), attenuated (b), sorbed (c), and degraded (d) mass over the duration of the experiments, along with cumulative error and the fate of mass as a percentage of total mass infiltrated. For carbamazepine and diclofenac, the calculated mass value includes the average of the two possible scenarios for the pre-spiking mass (scenario 1, all pre-spiking mass passing the sampling ports in the water phase; scenario 2, only a minimum amount of pre-spiking mass, based on the pre-spiking outflow concentration, passing in the water phase). The cumulative error displayed in the "±" column is one propagated standard deviation of measurement errors plus (for attenuated and degraded mass only) half of the difference between the calculated values for the two pre-spiking mass scenarios. Although these uncertainties are of a different nature, they are added together for convenience in viewing the overall results. For fenoprofen, gemfibrozil and naproxen, pre-spiking mass

is included in the infiltrated (a) total but any pre-spiking mass is neglected in the attenuated and degraded calculations as well as the uncertainty analysis, i.e. the “±” entry is one propagated standard deviation.

Table B-2. Mass Balance

	Carbamazepine			Diclofenac			Fenoprofen			Gemfibrozil			Naproxen		
a) Infiltrated mass															
		±	p_i		±	p_i		±	p_i		±	p_i		±	p_i
	mg	mg	%	mg	mg	%	mg	mg	%	mg	mg	%	mg	mg	%
A	15.5	0.7	100	21.4	1.3	100	9.2	0.5	100	18.3	1.2	100	9.3	0.9	100
B	12.4	0.6	100	16.0	1.0	100	7.1	0.5	100	15.0	1.1	100	6.5	0.8	100
C	11.1	0.4	100	12.7	0.7	100	6.5	0.4	100	12.0	0.5	100	6.8	0.7	100
b) Attenuated mass															
A 12	3.4	1.1	22	4.1	2.5	19	5.3	0.8	57	7.4	1.4	41	7.3	1.2	79
A 27	4.6	1.1	30	5.8	2.3	27	5.9	0.6	64	9.7	1.4	53	8.7	0.9	94
A 72	9.8	1.0	64	8.7	2.3	41	5.4	0.6	59	12.1	1.3	66	9.0	0.9	97
B 12	2.9	0.6	24	5.4	1.6	34	3.4	0.6	47	5.1	1.3	34	3.6	0.8	55
B 27	5.2	0.6	42	9.5	1.5	59	4.3	0.6	60	8.1	1.2	54	4.9	0.8	75
B 72	9.8	0.5	79	11.7	1.5	73	4.3	0.5	61	11.1	1.1	74	6.1	0.8	94
C 12	2.3	0.5	21	4.1	1.4	32	1.3	0.6	19	2.7	0.7	22	2.5	0.9	37
C 27	6.1	0.4	55	7.9	1.2	62	3.2	0.6	49	6.9	0.7	58	5.8	0.7	85
C 72	8.3	0.4	75	8.4	1.2	66	3.6	0.6	56	7.8	0.6	65	6.4	0.7	93
c) Sorbed mass															
A 12	3.0	0.9	19	1.5	0.1	7	0.14	0.01	2	0.41	0.02	2	0.06	0.01	1
A 27	6.3	1.5	41	3.1	0.2	15	0.32	0.02	3	0.91	0.04	5	0.13	0.01	1
A 72	12.8	2.5	83	6.9	0.3	32	0.82	0.04	9	2.22	0.07	12	0.24	0.03	3
B 12	2.2	0.6	18	0.26	0.02	2	0.078	0.002	1	0.25	0.01	2	0.039	0.001	1
B 27	4.4	1.1	35	0.65	0.07	4	0.19	0.01	3	0.60	0.02	4	0.08	0.01	1
B 72	9.0	1.8	73	2.2	0.3	14	0.62	0.02	9	1.80	0.06	12	0.14	0.04	2
C 12	2.1	0.7	19	0.41	0.03	3	0.11	0.01	2	0.31	0.01	3	0.05	0.01	1
C 27	4.5	1.2	41	0.77	0.04	6	0.23	0.01	4	0.65	0.02	5	0.09	0.01	1
C 72	10.2	1.8	92	2.5	0.1	19	0.64	0.02	10	1.70	0.05	14	0.15	0.01	2
d) Degraded mass															
A 12	0.4	1.4	3	2.7	2.5	12	5.1	0.8	56	7.0	1.4	38	7.3	1.2	78
A 27	-1.7	2.0	--	2.6	2.4	12	5.5	0.6	60	8.8	1.4	48	8.6	0.9	93
A 72	-2.9	2.8	--	1.8	2.3	9	4.6	0.6	50	9.9	1.3	54	8.7	0.9	94
B 12	0.8	0.8	6	5.1	1.6	32	3.3	0.6	46	4.8	1.3	32	3.6	0.8	55

	Carbamazepine			Diclofenac			Fenoprofen			Gemfibrozil			Naproxen		
B 27	0.8	1.2	7	8.9	1.5	55	4.1	0.6	57	7.5	1.2	50	4.8	0.8	74
B 72	0.8	1.8	6	9.5	1.5	59	3.7	0.5	52	9.3	1.1	62	6.0	0.8	92
C 12	0.2	0.8	2	3.7	1.4	29	1.1	0.6	18	2.4	0.7	20	2.5	0.9	36
C 27	1.6	1.2	14	7.1	1.3	56	2.9	0.6	45	6.3	0.7	52	5.7	0.7	84
C 72	-1.9	1.8	--	5.9	1.2	46	3.0	0.6	46	6.1	0.6	51	6.2	0.7	91

p_i = portion of infiltrated mass

± = cumulative error

Negative values are a result of calculations and values lie within or close to the cumulative error (propagated standard deviation plus uncertainty due to unmeasured pre-spiking mass) range shown.